Characterising the role of murine gammaherpesvirus-68 host shutoff protein in mediating cellular mRNA degradation

Thesis submitted in accordance with the requirements of the University of Liverpool for the degree of Doctor in Philosophy

by

Victoria Helen Sheridan

September 2012

Abstract

During lytic infection with a number of pathogenic viruses, host cells have been found to exhibit loss of mRNA culminating in loss of cellular proteins, a phenomenon termed host shutoff. In γ-herpesviruses, the precise mechanism by which host shutoff takes place is yet to be fully determined. Initially, host shutoff in Kaposi's sarcoma-associated herpesvirus (KSHV) was associated with the viral DNA exonuclease SOX (shutoff and exonuclease), which was followed by the identification of host shutoff in Epstein Barr virus (EBV) linked to the SOX homologue BGLF5. Murine γ-herpesvirus-68 (MHV-68) is a γ-herpesvirus that infects murid rodents including laboratory mice, with extensive viral genome homology to KSHV and EBV. MHV-68 was also found to induce host shutoff via the SOX homologue ORF37. The similarities between MHV-68 and the human γ-herpesviruses make the mouse virus an ideal model for studying host shutoff and consequences of host shutoff in disease pathogenesis. In this study, MHV-68 was used to investigate the role of ORF37 in MHV-68 infection *in vitro* and *in vivo* and to examine possible mechanisms of mRNA degradation mediated by ORF37. A stop codon mutant of MHV-68 (ORF37Stop) and its corresponding revertant (ORF37StopRev) were engineered. ORF37Stop virus exhibited highly restrictive phenotype in immunocompetent cells. In contrast, lack of ORF37 was tolerated in cells lacking a functional intereferon- α/β receptor (IFNαβRKO). These *in vitro* observations were replicated, to some extent, *in vivo* with the mutant virus establishing lytic infection in the lungs of IFNαβRKO mice. Interestingly, host shutoff was found to proceed even in the absence of ORF37, but only where functional type I IFN-mediated responses were lacking. A poly(A) tail assay was used to investigate the possibility of mRNA degradation at the 3' mRNA. In contrast

to a previously published study, the results suggest that cellular poly(A) tails do not appear to be elongated as a result of MHV-68 lytic infection.

Data generated during this project have identified a novel function by which ORF37-mediated host shutoff causes mRNA degradation and that a primary role of this viral protein is to overcome the type I interferon-receptor-mediated responses. The observation that host shutoff can proceed in the absence of ORF37 in cells unable to respond to type I IFNs highlight two important possibilities: other viral proteins may mediate host shutoff; and type I IFN effector mechanisms are a key player in host shutoff. These novel observations together with lack of a mechanism by which ORF37 mediates mRNA degradation warrant further studies in this field.

Table of contents

List of figures

List of tables

Abbreviations

S.I. (Systeme International d'Unites) abbreviations for units are used in this thesis. Other abbreviations are listed below.

α	Alpha
β	Beta
γ	Gamma
AE	Alkaline exonuclease
AIDS	Autoimmune deficiency syndrome
AMP	Adenosine monophosphate
Amp	Ampicillin
ARE	AU-rich element
ATCC	American type culture collection
BAC	Bacterial artificial chromosome
bp	Base pairs
CPE	Cytopathic effect
Ct	Cycle threshold
DNA	Unmethylated DNA
DMEM	Dulbecco's Modified Eagle's Medium
DNA	Deoxyribonucleic acid
dpi	Days post-infection
dsRNA	Double stranded RNA
DTT	Dithiothreotol
EBER	EBV-encoded RNA
EBV	Epstein Barr virus
ECL	Enhanced chemiluminescence
E.coli	*Escherichia coli*
EDTA	Ethylenediaminetetraacetic acid
eEF	Eukaryotic elongation factor
EHV	Equine herpesvirus
eIF	Eukaryotic initiation factor
EMCV	Encephalomyocarditis virus
eRF	Eukaryotic release factor
HCMV	Human cytomegalovirus
HHV	Human herpesvirus
HIV-1	Human immunodeficiency virus type 1
hpi	Hours post-infection
HSPG	Heparan sulphate peptidoglycan
HSV-1	Herpes virus simplex-1
HSV-2	Herpes virus simplex-2
HVS	Herpes virus Saimiri
IE	Immediate early
IFN	Interferon

IFNAR	Interferon alpha receptor
IL	Interleukin
IM	Infectious mononucleosis
IPTG	Isopropyl-D-1-thiogalactopyranoside
IRAK	Interleukin-1 receptor-associated kinase
IRF	Interferon regulatory factor
IFN	Interferon
ISG	Interferon stimulated gene
ISRE	Interferon stimulated response element
JAK	Janus activated kinase
Kan	Kanamycin
Kbp	Kilo base pairs
K-bZIP	K8 basic region-leucine zipper
KS	Kaposi's sarcoma
KSHV	Kaposi´s sarcoma associated herpesvirus
LA	Luria Bertani agar
LB	Luria Bertani broth
LMP-1	Latent membrane protein-1
M^7G	7-methylguanosine residue
MCD	Multicentric Castleman's disease
MDL	mediastinal lymph node
MEF	Mouse embryonic fibroblasts
Mg^{2+}	Magnesium ion
MHC	Major histocompatibility complex
MHV-68	Murine gammaherpesvirus 68
miRNA	microRNA
MLN	Mediastinal lymph node
Mn^{2+}	Manganese ion
mRNA	Messenger ribonucleic acid
mRNP	Messenger ribonucloprotein
Mta	mRNA transcript accumulation
Mut	Mutant
MyD88	Myeloid differentiation primary response gene 88
ND10	Nuclear domain 10
NF-κB	Nuclear factor kappa B
NK	Natural Killers
NMD	Nonsense mediated decay
NPC	Nuclear pore complex
nt	Nucleotide
OAS	Oligoadenylate synthetase
ORF	Open reading frame
PABP	Poly(A) binding protein
PAGE	Polyacrylamide gel electrophoresis
PAMP	Pathogen associated molecular pattern

PBMC	Peripheral mononuclear blood cells
P-body	Processing body
PBS	Phosphate buffer saline
PCR	Polymerase chain reaction
pDC	Plasmacytoid dendritic cells
PEL	Primary efusion lymphoma
PKR	Protein kinase R
PLB	Passive lysis buffer
PML	Promyeolytic leukaemia nucleur bodies
PMSF	phenylmethanesulfonylfluoride
Pol II	RNA polymerase II
PRR	Pattern recognition receptor
Rev	Revertant
RISC	RNA-induced silencing complex
RNA	Ribonucleic acid
RPM	Revolutions per minute
rRNA	Ribossomal ribonucleic acid
Rta	Replication and transcriptor activator
SDS	Sodium dodecyl sulfate
siRNA	Small interfering RNA
snRNA	Small nuclear RNA
SOX	Shutoff and exonuclease
ssRNA	Single strand RNA
STAT	Signal transduction and activator of transcription
SV40	Simian virus 40
TAE	Tris/Acetate/EDTA
TBE	Tris/Borate/EDTA
TBP	TATA binding protein
TBK-1	TANK-binding kinase 1
TFIIB	Transcription factor II B
TIR	toll/IL-1R
TLR	Toll-like receptor
TRAF-6	tumor necrosis factor (TNF) receptor associated factor 6
TREX	Transcription export complex
TRIF	TIR-domain-containing adapter-inducing interferon-β
Tris	Tris(hydroxymethyl)methylamine
U	Units
vhs	Virion host shutoff
vIL	viral interleukin
VP	Virion protein
VSV	Vesicular stomatitis virus
VZV	Varicella zoster virus
WT	Wild type

Acknowledgements

I would like to thank my supervisor, Dr Bahram Ebrahimi, for his help and support during my PhD studies. I am also grateful to my second supervisor, Professor James Stewart, for his help and guidance. I am indebted to the CIMB (BBSRC) for funding both my MRes and PhD, which allowed me to fulfil my aspirations of going into post-graduate education and completing my PhD.

I have to give special thanks to my favourite Portuguese person, Bruno, I couldn't have asked for a better lab mate and friend, thank you. Also all of my friends from the Duncan Building days, the office may have been damp, but that didn't dampen our spirits. In particular, thank you to Christina and Jo for your friendship and copious amounts of tea and cake! I would also like to thank everyone in lab H for making me feel welcome and showing me where everything was in the lab.

I also have to thank my husband, Johnny, without whom I could not have done any of this; he has given up a lot to allow me to follow my dream. He has always believed in me, even when I didn't believe in myself. Finally, a massive thank you to my family; especially my mum, dad and my brother Antony who have always supported me and pushed me to achieve my goals. I would also like to mention my nan and grandad, who I wish were still here to see me complete my PhD, I hope they would be proud.

Chapter One

Introduction

1.1 Herpesviruses

Herpesviruses are enveloped double-stranded DNA viruses of eukaryotes. They are highly disseminated in nature, having been isolated from a diverse range of species, from mammals to oysters (Knipe 2007). Most animal species will yield at least one herpesvirus, however, the most studied group includes viruses which infect amniotes, such as mammals, birds and reptiles (Knipe 2007; Wang 2007). One of the key features of infection with these viruses is their ability to remain latent within certain cell types in their hosts. During this time the viral genome forms closed circular molecules, termed episomes, with only a small subset of viral genes being expressed (Knipe 2007).

1.1.1 Classification of herpesviruses

In recent years the International Committee on Taxonomy of Viruses (ICTV) has carried out a major review of how herpesviruses are classified. These changes have come in the form of the introduction of the *Herpesvirales* order which encompasses three herpesvirus families, namely the *Herpesviridae*, *Alloherpesviridae* and the *Malacoherpesviridae*. These three families cover a diverse range of host species: the *Herpesviridae* include mammal, bird and reptile hosts; the *Alloherpesviridae* are associated with fish and amphibians and; the *Malacoherpesviridae* have been found to infect bivalves (Davison *et al.* 2009). This thesis will focus on *Herpesviridae*, which contain three subfamilies namely the *Alphaherpesvirinae*, the *Betaherpesvirinae* and the *Gammaherpesvirinae* (Figure 1.1). Historically,

membership of these three subfamilies was based on biological properties of these viruses, such as tissue tropism; however, more recently genome sequence information has been used in their classification. Nevertheless, the initial classification (based on cell tropism/disease) has proved relatively consistent with more recent genomic profiling (McGeoch *et al.* 2006).

Alphaherpesvirinae: The alpha-herpesvirus (α-herpesvirus) subfamily contains neurotropic viruses, with the majority of latent infections found in sensory ganglia. The prototypic human α-herpesvirus is herpes simplex virus (HSV1), however this group also contains the human viruses herpes simplex virus 2 (HSV2) and Varicella zoster virus (VZV) (Knipe 2007; Liu 2007).

Betaherpesvirinae: Members of the beta-herpesvirus (β-herpesvirus) subfamily have been found in a number of cell and tissue types, such as secretory glands and lymphoreticular cells. Human viruses in this group include human cytomegalovirus (HCMV) and human herpesviruses 6 and 7 (HHV6 and HHV7 respectively) (Knipe 2007; Liu 2007).

Gammaherpesvirinae: Gammaherpesvirus (γ-herpesvirus) subfamily consists of lymphotropic viruses, infecting mainly B and T lymphocytes. The γ-herpesvirus subfamily can be further divided into two genera: *Lymphocryptoviruses;* and *Rhadinoviruses*. The two human viruses of medical importance within this subfamily include the Epstein Barr virus (EBV or HHV4) a lymphocryptovirus, and Kaposi's sarcoma-associated herpesvirus (referred to as KSHV or HHV-8), which is a rhadinovirus, (Knipe 2007; Liu 2007). A hallmark of γ-herpesviruses is that infection

with these viruses is highly species-specific therefore limiting their study to their natural hosts. Due to this species-specificity, the murine gammaherpesvirus 68 (MHV-68 also referred to as MHV4, MuHV-4 and γHV-68) has often been used to study γ-herpesviruses pathobiology (reviewed by Nash *et al.* 2001; Blackman and Flano 2002).

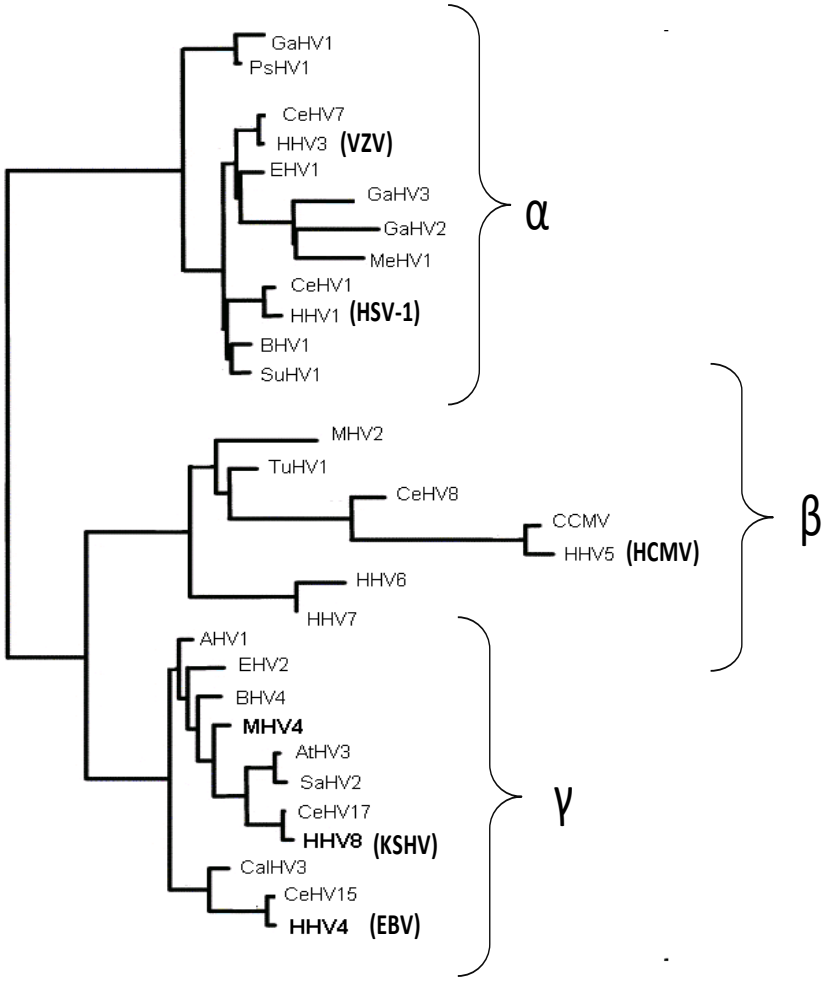

Figure 1.1 Phylogenetic tree showing the evolutionary relationships within the herpesvirus family. The herpesvirus family can be divided into three subfamilies; α, β- and γ-herpesviruses. In the figure some known human herpesviruses are highlighted within each subfamily: HSV-1 and VZV are α-herpesviruses, HCMV belongs to the β-herpesvirus subfamily, while EBV and KSHV have been assigned into the γ-herpesvirus subfamily (Wang 2007).

1.1.2 Herpesvirus virion structure

Membership of order *Herpesvirales* is classically based on virion architecture (Figure 1.2). The basic herpesvirus structure consists of a core containing linear double-stranded (ds) DNA in the form of a torus, between 124-230 kilo base pairs (kbp). This is surrounded by an icosahedral capsid of approximately 125nm in diameter, containing 162 capsomeres (Knipe 2007). Surrounding the capsid is the tegument, a proteinaceous compartment unique to herpesviruses. The tegument proteins have multiple roles in the viral life cycle, such as assembly and egress of herpesvirus particles (reviewed by Guo *et al.* 2010). Furthermore tegument proteins can stimulate expression of viral immediate early (IE) genes and can also modulate the host cellular environment during initial infection through inhibition of host signalling pathways and host shutoff of cellular protein synthesis (Knipe 2007; Guo *et al.* 2010). Although originally believed to be an amorphous structure, the tegument has now been found to be built up through protein-protein interactions that form an organised structure (reviewed by Sathish *et al.* 2012). The use of electron cryomicroscopy has led to further insights into virion structure as 3D images have been produced for members of the α-, β- and γ-herpesviruses, which have highlighted both similarities and differences between tegument structures (Chen *et al.* 1999; Zhou *et al.* 1999; Dai *et al.* 2008). Dai *et al.* also used a process of cryo-electron tomography, which identified two tegument layers; one (inner) attached to the capsid and the other (outer) tegument layer, which is flexible and conforms to the shape of the envelope (Dai *et al.* 2008). Although the presence of inner and outer tegument layers appears to be conserved across the herpesvirus family the pattern of tegument proteins which interact with the capsid is different for different members of this family (Chen *et al.* 1999; Zhou *et al.* 1999; Dai *et al.* 2008). Encapsulating the

tegument is a cell-derived lipid bilayer envelope, which has a number of viral-encoded glycoprotein spikes on its surface (Knipe 2007). Upon infection of the cell the capsid uncoats in the cell cytoplasm and the viral DNA enters the host nucleus where viral genes are transcribed and translated (Liu 2007). The process of virion assembly is highly conserved within the herpesvirus family. Initially a procapsid is formed, which contains internal scaffolding proteins. Upon maturation into a nucleocapsid, the internal scaffolding is replaced with the viral genomic DNA (Liu 2007). During the assembly process viral proteins are present which recognise and cleave at conserved sequences on the DNA, which signal the genomic termini allowing the correct packaging of the DNA into the capsid (Knipe 2007).

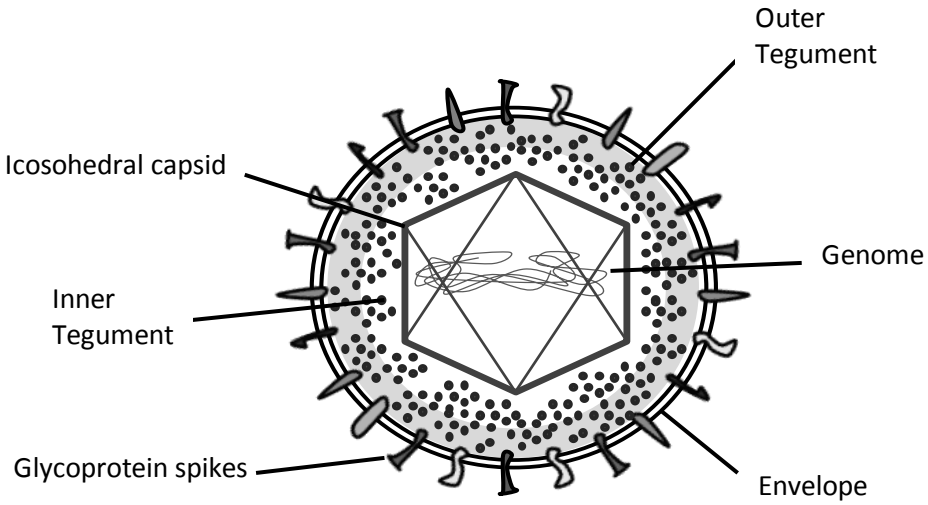

Figure 1.2 Herpesvirus structure. Diagram depicting herpesvirion structure, which comprises; the viral genome, capsid, inner and outer tegument and the envelope. Information from (Knipe 2007; Dai *et al.* 2008).

1.1.3 Virus entry and traffic to the nucleus

Herpesvirus entry into cells is a complex process that requires the interactions of viral glycoproteins with cell surface receptors. A combination of different viral glycoproteins and cellular receptors more than likely determines the virus tropism. There are two main stages of entry: first is attachment, during which the virus is tethered to the cell; second is fusion, which can occur either via direct fusion of the plasma membrane or endocytosis (Figure 1.3A) (reviewed by Krummenacher *et al*. 2007; Connolly *et al.* 2011).

The entry of EBV into B cells is via endocytosis, however, entry into epithelial cells does not require endocytosis, occurring instead via fusion at the cell surface, both of which occur in a pH-independant manner (Miller and Hutt-Fletcher 1992). In contrast, KSHV enters both fibroblasts and endothelial cells via endocytosis, both of which occur in a low pH-dependant manner (Akula *et al.* 2003; Greene and Gao 2009). Similar to KSHV, MHV-68 also uses the process of endocytosis to enter cells (Gill *et al.* 2006). Although a variety of herpesvirus glycoproteins are involved in virion entry, there are three fusion glycoproteins (gB and the heterodimer gH/gL), which are conserved and are often referred to as the core fusion machinery (Table 1.1). Initial contact between herpesvirus glycoproteins and the cell surface is usually via heparan sulphate (Table 1.1). However this association is not essential for virus infection and viral glycoproteins are also not essential for viral entry, but the association does increase the efficacy of viral entry by allowing viral glycoproteins to locate the correct entry receptor. One notable exception is EBV, which does not bind heparan sulphate, but instead uses binding and entry receptors found on very few cell types and mainly B cells. These findings are consistent with the fact that

KSHV for example can infect a number of different cell types, whereas EBV has a much more limited host range (specifically in relation to B-cell targets) (reviewed by Spear and Longnecker 2003).

Once the fusion glycoproteins have attached to cell receptors this triggers a rearrangement of the host cytoskeleton. One of the components of the cytoskeleton are microtubules, comprising of α and β-tubulin heterodimers. The stiff, cylindrical microtubules are polar, allowing the positive (plus) end to grow and shrink rapidly while the negative (minus) end is tethered to the organising centre. Directional transport along the microtubules is governed by two motors; the plus-end kinesin motors involved in transport to the cell periphery and the minus-end dynein motor involved in movement from the periphery to the cell centre (reviewed by Lyman and Enquist 2009). After attachment and fusion have taken place the capsid is released into the cytosol leaving behind the glycoproteins and the outer tegument at the plasma membrane (Maurer *et al.* 2008). The partially tegumented capsid is then transported to the nucleus via the interaction of both capsid and inner tegument proteins with the minus-end directed dynein motor and dynactin protein complex (Sodeik *et al.* 1997; Dohner *et al.* 2002). During infection with KSHV the dynein motor is also used to transport the viral DNA to the nucleus. Furthermore KSHV has also been found to induce Rho GTPases, which lead to stabilisation of microtubules thus promoting delivery of viral capsids to the nucleus (Naranatt *et al.* 2005). The capsid then docks at the nuclear pore where the viral DNA is released into the nucleoplasm hence completing the process of uncoating (reviewed by (Mettenleiter *et al.* 2009).

1.1.4 Trafficking of viral genomic DNA and replication in the nucleus

During herpesvirus infection, the processes of transcription, DNA replication, assembly of new capsids, and viral DNA packaging take place in the nucleus (reviewed by Mettenleiter 2002). Once inside the nucleus, the parental viral genomes become associated with nuclear domain 10; ND10 (also known as PML-nuclear bodies) and the initial site of transcription is usually adjacent to these domains. ND10 is associated mainly with three cellular proteins; PML, Sp100 and hDaxx, which form a subnuclear structure that acts as a cellular organising centre. A number of roles for ND10 have been suggested one of which is antiviral defence, as PML and Sp100 are interferon (IFN)- inducible. Members of the herpesvirus family have evolved different mechanisms to overcome the antiviral effect of ND10. The first to be discovered was in infection with HSV-1, which triggers proteosomal degradation of PML causing rapid destruction of the subnuclear structure. Similarly, MHV-68 induces proteosomal degradation leading to disassembly of the subnuclear structure reducing the antiviral activity of ND10 (reviewed by Tavalai and Stamminger 2009). It has also been suggested that apart from diminishing the antiviral activity of ND10, herpesviruses may localise at sites close to ND10 as it may be beneficial to viral replication due to cellular proteins involved in cell growth, gene expression, and DNA recombination being within this location (Wilkinson and Weller 2003). The viral linear DNA then becomes circularised (episome) and is replicated via a rolling circle mechanism producing linear concatemers of tandemly repeated viral genomes. The newly replicated viral DNA is then cleaved at conservered sequences, that define genomic termini, into monomeric molecules that are then packaged into capsids (encapsidation) (Figure 1.3B) (Knipe 2007).

Table 1.1 Interaction between human herpesvirus and MHV-68 glycoproteins and cellular receptors.

Herpesvirus	Glycoprotein	Function	Cellular receptors
HSV-1	gB	Fusion	HSPG, CD209, MAG, PILRα
	gC	Attachment	HSPG
	gD	Attachment/fusion	Nectin 1 & 2, HVEM, 3-O-S-HS
	gH/gL	Fusion	Integrins
HSV-2	gB	Fusion	HSPG, PILRα
	gC	Attachment	HSPG
	gD	Attachment/fusion	Nectin 1
VZV	gB	Fusion	HSPG
	gC	Attachment	HSPG
CMV	gB	Attachment/fusion	HSPG, TLR, EGFR, Integrins
	gH/gL/gO	Fusion	Integrins
HHV-6	gH/gL/gQ1/gQ2	Attachment/fusion	CD46
HHV-7	gB	Attachment/fusion	HSPG, CD4
EBV	BMRF2	Attachment	Integrins
	gp42	Attachment/fusion	MHC-II
	gp350/220	Attachment	CD21
	gB	Fusion	Unknown
	gH/gL	Attachment/fusion	Integrins
KSHV	gB	Attachment/fusion	HSPG, Integrins
	K8.1	Attachment/fusion	HSPG
	gH/gL	Attachment/fusion	Integrins, HSPG, EphA2
MHV-68	gH/gL	Attachment/fusion	HSPG
	gB	Attachment/fusion	HSPG
	gp150	Attachment/fusion	HSPG

*HSPG -heparan sulphate peptidoglycans, HVEM – Herpesvirus entry mediator**,** 3-OS-HS – 3-O-sulfated heparan sulphate**,** TLR – Toll like receptor**,** EGFR – Epidermal growth factor receptor, MHC-II – Major histocompatibility complex II, MAG- myelin associated glycoprotein, EphA2 – ephrin receptor tyrosine kinase A2. (Stevenson and Efstathiou 2005; Gillet *et al.* 2006; Krummenacher *et al.* 2007; Gillet *et al.* 2008; Connolly *et al*. 2011; Hahn *et al.* 2012).

1.1.5 Virus assembly and egress from the cytoplasm

The next stage is the export of the virus from the nucleus into the cytoplasm and then egress out of the cell. There are three possible pathways to explain how the herpesvirus particles move through the cell and become enveloped (Figure 1.3C). The first is the single envelopment pathway. After accumulation of tegument proteins in the nucleus and an envelope from the inner nuclear membrane, the virion travels along secretory pathways leading to interactions with membranes such as the Golgi apparatus. In this pathway the virion maintains its original tegument and envelope and has its glycoproteins matured by the Golgi apparatus. The virions are then released out of the cell via fusion of the vesicle to the cell plasma membrane (reviewed by Campadelli-Fiume 2007). The second pathway and the one that has gained the most support in recent years is the de-envelopment-re-envelopment pathway (reviewed by Campadelli-Fiume 2007; Guo *et al.* 2010; Johnson and Baines 2011). In this pathway the first stage is envelopment, which is the same as the first pathway, with the virion gaining an envelope from the inner nuclear membrane, however in this pathway de-envelopment takes place at the outer nuclear membrane, releasing the nucleocapsid into the cytoplasm. These nucleocapsids then gain their tegument in the cytoplasm and are re-enveloped by the Golgi apparatus. This gives rise to an enveloped virion encased in a cytoplasmic vesicle. The key difference is that the virion acquires its tegument in the cytoplasm rather than the nucleus. The virions are then released in the same manner as described in pathway

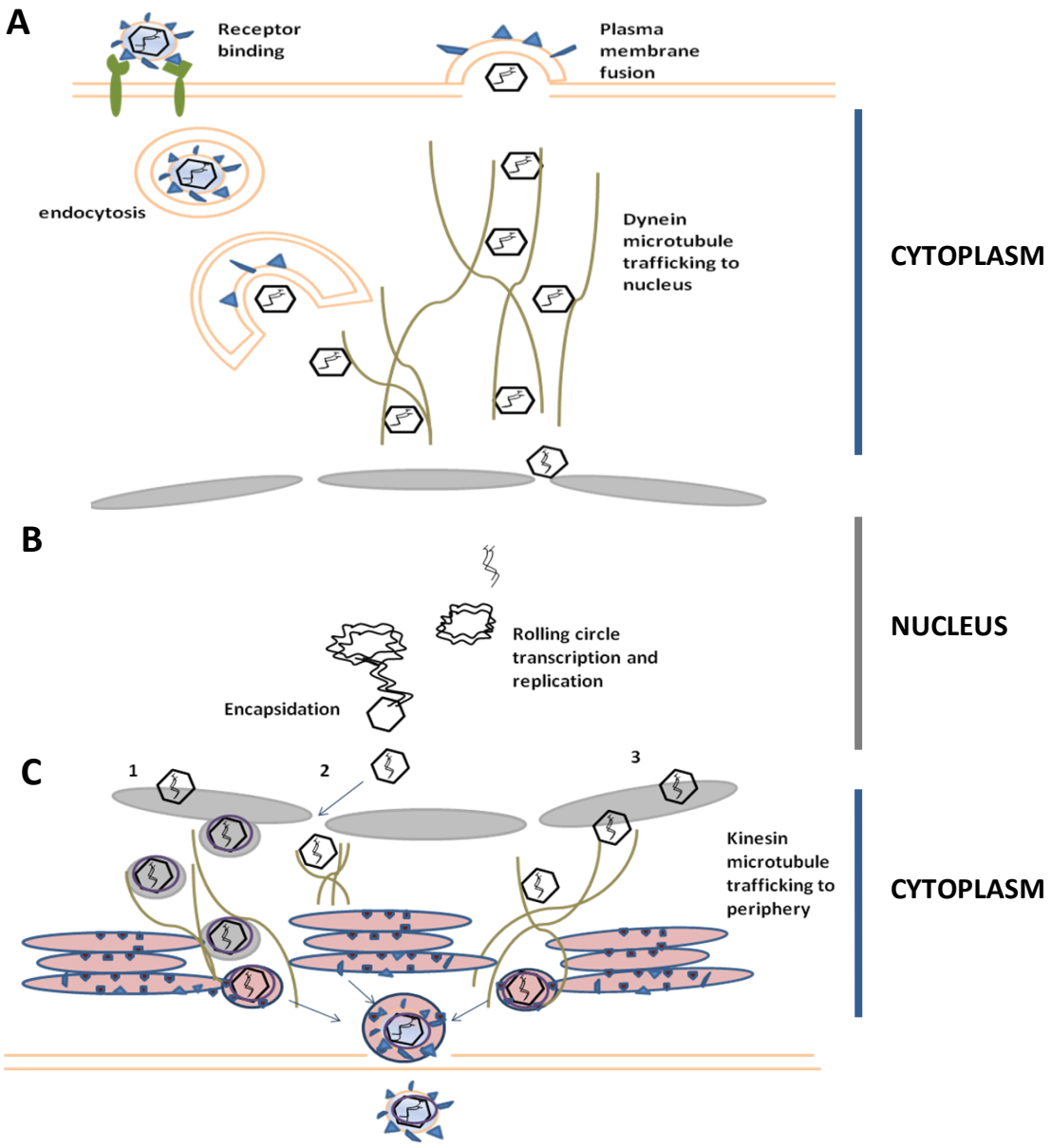

Figure 1.3 Herpesvirus entry, genome replication and virion egress from cells. **A)** Herpesvirus particles enter into cells via fusion with the plasma membrane or endocytosis, which in turn causes remodeling of the cytoskeleton. Viral capsids are then transported to the nucleus along microtubules using dynein motors. **B)** In the nucleus, linear viral DNA is circularized and replicates via a rolling circle mechanism followed by packaging into capsids. **C)** Virion egress from cell which may happen using one of three possible pathways: **1.** Single-envelopment pathway; **2.** Nuclear pore pathway; or **3.** De-envelopment-re-envelopment pathway. Information compiled from (Campadelli-Fiume 2007; Knipe 2007; Lyman and Enquist 2009; Connolly *et al.* 2011).

one (reviewed by Campadelli-Fiume 2007). The third possible pathway involves the transport of non-enveloped capsids to the cytoplasm via enlarged nuclear pores, which are subsequently modified into a mature form in the Golgi or early endosomes (Knipe 2007).

The viral envelope is believed to originate from the trans-Golgi network (reviewed by Mettenleiter *et al.* 2009), although fluorescence immunolabelling has suggested that endosomes may also play a role in envelope supply (Turcotte *et al.* 2005; Das *et al.* 2007). During the processes of nuclear egress and viral envelopment the virion must also acquire its tegument, a process which has proved difficult to characterise, although interactions between viral capsid, tegument and glycoproteins have been described (reviewed by Mettenleiter *et al.* 2009). One example of this is the interaction between the HSV-1 tegument protein VP22 and the envelope glycoproteins gM and gE (Stylianou *et al.* 2009).

The last stage in the lytic replication cycle is the release of virions, which involves the transport of vesicles containing enveloped virions to the plasma membrane and the subsequent exocytosis by fusion of vesicles to the plasma membrane. The proteins involved in herpesvirus egress are yet to be deciphered (reviewed by Mettenleiter *et al.* 2009). However the cellular endosomal sorting complexes required for transport (ESCRT) complexes may be involved as they have been found to play an important role in the viral budding of several enveloped viruses (reviewed by Bieniasz 2006) and in particular HIV-1 (von Schwedler *et al.* 2003). Work carried out on HSV-1 has found a possible link to ESCRT pathways and cytoplasmic

envelopment, as inhibition of the activity of the Vps4 enzyme required for ESCRT function caused a reduction in infectious HSV-1 (Crump *et al.* 2007).

1.1.6 Herpesvirus lytic and latent infection cycles

A key feature of herpesvirus infections is that the infection invariably leads to two outcomes with respect to the virus life cycle: lytic and latent replication. During a herpesvirus infection amplification of the virus is achieved during the lytic stage, when virus genome is replicated to high levels and infectious progeny virions are released from infected cells. The virus may then enter into a latent (persistent) stage during which time a smaller subset of viral genes are expressed, however the virus retains the ability to lytically reactivate and produce progeny virions (reviewed by Penkert and Kalejta 2011). During *in vitro* α- and β-herpesvirus infections the majority of cells infected contain lytic virus particles, with only a small group of cells supporting the latent infection. This differs in γ-herpesvirus infection, as these viruses favour latent infection, with only a small subset of cells being lytically infected at any given time (reviewed by Ackermann 2006). The cell type in which different herpesviruses can become latent is highly specific, with α-herpesviruses favouring neurons, the β-herpesviruses different subsets of hematopoietic cells and the γ-herpeviruses establishing latency predominantly in B lymphocytes. The ability of herpesviruses to enter into a latent cycle during infection allows them to persist for the lifetime of host organisms whilst retaining the capability to re-activate (reviewed by Penkert and Kalejta 2011).

1.2 Gammaherpesviruses

1.2.1 Kaposi's sarcoma-associated herpesvirus

Kaposi's sarcoma-associated herpesvirus (KSHV), also referred to as HHV8 was first described by Chang *et al* in 1994, after they identified γ-herpesvirus-like DNA sequences in tissues from Kaposi's sarcoma neoplasms (Chang *et al*. 1994). However the classic or endemic Kaposi's disease was first described back in 1872 by Moritz Kaposi (Hungarian dermatologist b. 1837) (Sternbach and Varon 1995). Endemic KS is found mostly in elderly Mediterranean or African men and generally affects the skin. In later years two more forms of KS were discovered: one was a variant of the endemic disease identified in young children; the second form was AIDs-related KS, seen in immunodeficient HIV sufferers. KS differs from classic forms of cancer, as lesions comprise of multifocal elongated (spindle) endothelial cells. The different forms of KS share similar histology; however the AIDS-related form is the most aggressive and can also cause lesions in the lungs and gastrointestinal tract, which can then lead to further complications (reviewed by Ganem 2006). A year after the link between KS and KSHV had been established, KSHV was also linked to two more lymphoproliferative diseases: primary effusion lymphoma (PEL); and multicentric Castleman's disease (MCD) (reviewed by Viejo-Borbolla and Schulz 2003).

1.2.2 Epstein Barr virus

Epstein Barr virus (EBV), also referred to as HHV4, was the first human tumor virus to be discovered and since then has been implicated in a number of B-cell lymphoproliferative disorders, such as Burkitt's lymphoma, Hodgkin's lymphoma, nasopharyngeal carcinoma, and lymphomas in immunocompromised individuals

(reviewed by Carbone *et al.* 2008). Infection of immunocompetent hosts with EBV via an oral transmission route is generally asymptomatic, however if infection occurs during adolescence it can cause infectious mononucleosis (IM). It is thought that IM infection involves mucosal B cells, but there is evidence that it is also associated with the oropharyngeal epithelium (reviewed by Thorley-Lawson 2001; Young and Rickinson 2004).

1.2.3 Murine gammaherpesvirus-68

Due to the high species-specificity of the human gammaherpesviruses (Knipe 2007), murine gammaherpesvirus -68 (γ-herpesvirus-68, MHV-68, also referred to as γHV68, MuHV4, and MHV4) is often used as an amenable mouse model to study γ-herpesvirus pathobiology. MHV68 was originally isolated from bank voles (*Myodes glareolus*) and yellow-necked field mice (*Apodemus flavicollis*) captured in Slovakia (Blaskovic *et al.* 1980; Nash *et al.* 2001) and have been found to be endemic in wood mice (*Apodemus sylvaticus*) in some parts of the UK (Blasdell *et al.* 2003). Sequencing of the MHV-68 genome has revealed that it encodes for approximately 80 gene products, at least 63 of which are homologous to KSHV genes. Comparison of the MHV-68 genome with other γ-herpesviruses has indicated that it is arranged into large co-linear gene blocks interspersed with virus–specific Open Reading Frames (ORFs) (Virgin *et al.* 1997). It is believed that virus-specific ORFs provide an advantage for virus infection in each respective host. For example MHV-68 encodes for the unique gene M2, which through M2-null virus infections in mice, has been found to play an important role in establishment and reactivation from latency (Jacoby *et al.* 2002; Herskowitz *et al.* 2005). With extensive genome homology to KSHV and EBV (Virgin *et al.* 1997), along with the relative ease of constructing

MHV-68 gene deletion mutants (Adler *et al.* 2000; Adler *et al.* 2003; Song *et al.* 2005) MHV68 has proved an important experimental model to study aspects of γ-herpesvirus pathobiology, not readily feasible in their respective hosts, for example, *de novo* infections and use of host knockouts.

The route of MHV-68 infection is not clear, although *in vivo* imaging of mice infected either orally, intranasally or intraperitoneally has suggested that the most likely route of infection is the intranasal route (Milho *et al.* 2009). Interestingly, in contrast to EBV which is transmitted via saliva (reviewed by Thorley-Lawson 2001) oral MHV-68 was very poorly infectious and so it may be that in mice MHV-68 favours a nasal entry route as sense of smell is an important part of a murine social life (Milho *et al.* 2009). After intranasal infection of mice, replication of MHV-68 occurs mainly in the lung epithelium, where the primary pathology observed is pneumonia with a proportion of mice developing clinical disease. This acute infection is then followed by life-long latent virus persistence in lymphoid tissues. Intranasal MHV-68 infection also leads to a disease state similar to infectious mononucleosis seen in human γ-herpesvirus infections. Moreover, similar to human infections, MHV-68 causes lymphoma formation during persistent infection *in vivo* (Figure 1.4) (Sunil-Chandra *et al.* 1992). The biological similarities, such as tropism of MHV-68 for predominantly splenic B lymphocytes (other cells may also become infected e.g. cells of the monocyte/macrophage lineage) and lymphoproliferative disease, together with a mouse being an easily manipulated small animal make, MHV-68 a powerful experimental system for the study of human γ-herpesviruses (reviewed by Blackman and Flano 2002).

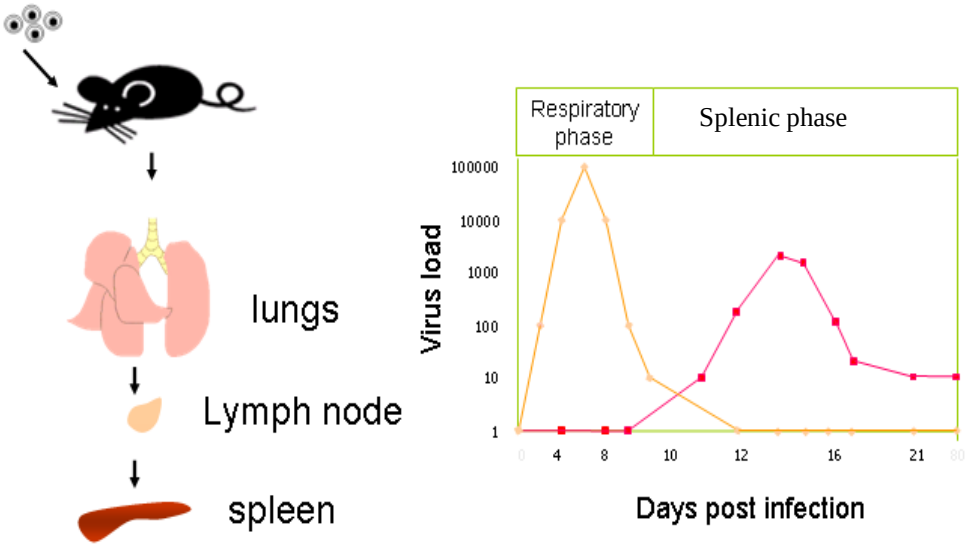

Figure 1.4 Infection path of MHV-68 in mice via the respiratory route. After primary lytic infection in the lungs, the virus traffics to the lymphoid tissues including the spleen where MHV-68 then establishes latency mainly in B cells. The productive infection lasts for around 10 days in the lung tissues before it is cleared by the immune system. Just before the productive infection is resolved in the lungs, MHV-68 moves to the spleen where it enters its latent phase in B lymphocytes. Infective center assays are used to detect latent infection, the results of which have shown that MHV-68 reaches a peak in spleens two to three days post-infection before declining and reaching a stable level. Latency can then be maintained indefinitely in the mouse (Information from Sunil-Chandra *et al.* 1992; Stewart *et al.* 1998a; Stewart *et al.* 1998b; Nash *et al.* 2001).

1.2.4 Gammaherpesvirus lytic and latent infection cycles

The site of latency for EBV is in memory B cells. Three viral lytic proteins have been found to be important in establishment of EBV latency: BALF1; BHRF1 and BZLF1. Once latency has been established, EBV expresses nine latency-associated proteins, six nuclear proteins (EBNA 1, 2, 3A, 3B, 3C and LP) and three latency-associated membrane proteins (LMP 1, 2A and 2B). There are also three different states of latency in EBV infection based on the subset of viral proteins being synthesised. In all three latency states, EBNA-1 plays a key role in viral genome maintenance, DNA replication and cell division, while the other viral proteins contribute to the transformation and immortalisation of infected B cells. In addition to these viral proteins, non-coding viral RNAs are also detected in infected cells during latency, known as EBERs (EBV-encoded RNAs) and BARTs (BAMH1-A rightward transcripts). EBERs and BARTs are involved in PKR-associated apoptosis and LMP modulation, respectively. One of the key EBV proteins is the Z protein; bZip transactivator (Zta) encoded by BZLF1. Zta, plays a part in establishment of latency and in reactivation of the virus (reviewed by Ackermann 2006; Penkert and Kalejta 2011).

Similar to EBV infection, latency in KSHV appears to be the default pathway established in the B cell compartment. In immunocompromised individuals, KSHV DNA is found in a variety of cell types e.g. T cells, monocytes, and endothelial cells, although viral genomes are most frequently harboured by peripheral B lymphocytes (Longnecker and Neipel 2007). *In vitro*, KSHV can infect a variety of adherent cells and readily establishes latency. However, unlike EBV, KSHV does not trigger B cell transformation *in vitro* (reviewed by Speck and Ganem 2010). During latency only a

few viral genes are expressed. A major latency locus encodes for latency associated nuclear antigen (LANA), v-cyclin, v-FLIP and kaposins A, B and C (reviewed by Speck and Ganem 2010). However, differences in latency-associated gene expression patterns have been observed in other diseases caused by KSHV; as a second locus vIRF3 (LANA-2) is expressed in PEL and MCD, but not in KS (Rivas *et al.* 2001). Recently a third latency-associated locus has been identified: K1, which mimics B-cell receptor signalling similar to the effect of LMP2 during EBV latency (Lee *et al.* 2005; Chandriani and Ganem 2010). The viral protein, vFLIP is a potent activator of cellular NF-κB, which leads to stabilisation of latency (reviewed by Speck and Ganem 2010). Interestingly, NF-κB activation is also prominent in EBV latency in which LMP1 has been shown to be a strong constitutive activator of NF-κB (Adler *et al.* 2002). As well as encoding the Kaposin proteins the Kaposin locus also encodes for a series of viral microRNAs (miRNAs), which may play an important role in latency (reviewed by Speck and Ganem 2010). For example the miRNA miRK9* appears to regulate the stability of latency by preventing the triggering of inappropriate lytic reactivation (Bellare and Ganem 2009). LANA has been found to have a number of activities one of which is regulation of transcription, which may lead to negative regulation of lytic gene transcription. The other gene encoded by the major latency locus is v-cyclin, which appears to induce replicative stress, although much is still to be learnt about this gene (reviewed by Speck and Ganem 2010).

Induction of the lytic cycle is linked to one viral gene that encodes a key transcription factor, known as the Replication and Transcription Activator (RTA). Although RTA is the key lytic switch other viral proteins, such as K-bZIP help to

regulate the switch from latent into lytic cycle. Induction of the lytic cycle leads to the temporal expression of virtually the entire viral genome, DNA replication and production of progeny virions (reviewed by Viejo-Borbolla and Schulz 2003; Ganem 2006).

In contrast to KSHV and EBV, the default pathway for MHV-68 infection *in vitro* is lytic replication. This has meant that it has been harder to study the genes involved in MHV-68 latency, however a number of genes have been linked to latency in particular LANA and v-cyclin. The murine homologue of LANA (mLANA) appears to share a great deal of biochemical functionality with the KSHV LANA gene. However, in contrast, work on the v-cyclin gene has highlighted some biochemical differences between KSHV and MHV-68, as they appear to bind different factors (reviewed by Speck and Ganem 2010). One key similarity between the two human γ-herpesviruses and MHV-68 is the importance of NF-κB in stabilising latency (Krug *et al.* 2007). MHV-68 also encodes for a number of unique genes not conserved in the other γ-herpesviruses that can have effects on latency and reactivation (e.g. M1 and M2) (reviewed in Speck and Ganem 2010). Similarly to KSHV and EBV, MHV-68 reactivation is controlled by RTA (encoded for by ORF50), which can disrupt latency and activate lytic replication (Wu *et al*. 2000).

1.3. Innate immune responses to viruses

The innate immune responses are the first line of defence against viral infections, which lead to the cell entering an antiviral state. The first stage is the recognition of virus-associated molecules, such as genomic DNA, RNA or outer structural proteins,

which are recognised by host pattern recognition receptors (PRRs). Viral recognition by PRRs leads to the induction of a variety of cellular proteins, in particular type I interferons (IFNs). The most common types of PRRs are Toll-like receptors (TLRs), which recognise pathogen-associated molecular patterns (PAMPs) such as viral or bacterial components. So far 13 human TLRs have been identified, six of which have been linked to viral recognitions; TLR2 and TLR4 recognise viral structural proteins or glycoproteins, TLR3 recognises dsRNA, TLR7 and TLR8 recognise ssRNA and TLR9 senses cytidine-phosphate-guanosine (CpG) DNA motifs during viral replication (reviewed by Kawai and Akira 2006).

TLRs are composed of a leucine-rich extracellular domain involved in PAMP recognition, a transmembrane domain and a cytoplasmic tail which contains a Toll-interleukin-1 receptor (TIR) homology domain, required for signalling (reviewed by Kawai and Akira 2006; Boo and Yang 2010). Upon recognition of PAMPs, TLRs recruit a set of TIR containing adaptors including MyD88, TIRAP, TRIF and TRAM. Most TLR signalling pathways are MyD88-dependant, with the exception of TLR3. MyD88 forms a complex with members of the IL-1 receptor-kinase (IRAK) family and TRAF6. In contrast TLR3 signals via its interaction with TRIF. The signalling pathways that the TLRs induce lead to the activation of a number of cellular transcription factors, including interferon regulatory factor 3 (IRF3), IRF7, NF-κB and ATF2-c-jun. In turn, these lead to the induction of type I IFNs and whilst IRF3 and IRF7 play a key role in this induction, NF-κB and ATF2-c-jun regulate genes involved in inflammation and interact with IRF3 and IRF7 to enhance type I IFN induction (reviewed by Kawai and Akira 2006). In more recent years work has been carried out to identify other DNA sensors apart from TLR9 that can trigger innate

immune responses. As a result, a number of DNA sensors have been identified some of which have been linked to recognition of DNA viruses (reviewed by Sharma and Fitzgerald 2011). In particular the DExD/H box helicases (DHX36 and DHX9) bind to CpG-DNA in plasmacytoid dendritic cells (pDCs), which in turn binds to the Toll-interleukin receptor domain on MyD88, leading to activation of IRF7 and NF-κB (Kim *et al.* 2010). Another receptor which acts as an important part of the immune response to DNA viruses is IFI16, which upon binding DNA activates IFN-β production (Unterholzner *et al*. 2010).

1.3.1 Interferon response to viral infections

The IFN family encompasses three groups, namely Type I, II and III. Type I IFNs encompass a large group of molecules, classified into IFNs-α, -β, -δ, -κ, -ε, -τ, -ω, however only IFN-α and -β are involved in control of viral infection. Type II IFNs produce IFN-γ in response to recognition of viral infection by T-lymphocytes and natural killer (NK) cells. Type III IFNs produce a number of cytokines in direct response to viral infection following similar pathways to type I IFNs and elicit similar responses, however type III receptor exhibits limited tissue distribution and so appears not to play an essential role in host survival (reviewed by Goodbourn *et al.* 2000; Randall and Goodbourn 2008). Once the type I IFNs (α/β) have been induced they both bind to a common receptor, IFNAR, composed of two subunits IFNAR1 and IFNAR2. The cytoplasmic domains of IFNAR1 and IFNAR2 are associated with the Janus tyrosine kinases; Tyk2 and Jak1, respectively; IFNAR2 is also associated with the Signal Transducer and Activator of transcription (STAT) molecule (STAT2). Binding of the type I IFNs with the IFNAR leads to a cascade of phophorylation events that result in a STAT1/STAT2 heterodimer translocating to

the nucleus where it associates with a monomer of IRF9 to form the Interferon-stimulated gene factor 3 ISGF3 heterotrimer. ISGF3 then binds to an IFN-stimulated response element (ISRE), which is present in the promoters of most IFN-responsive genes, which in turn leads to up-regulation of genes involved in creating the antiviral state. Activation of the type I IFN pathway upregulates a number of genes involved in the antiviral state, several of which have been extensively studied (Table 1.2). The antiviral state induce by type I IFNs is effective against a number of viral infections, however, viruses have evolved mechanisms to circumvent the IFN system (reviewed by Brierley and Fish 2002; Randall and Goodbourn 2008; Boo and Yang 2010).

1.3.2 Innate immune avoidance by herpesviruses

In order to successfully infect their host, viruses must first overcome the host innate immune responses and different viruses have evolved different mechanisms to do so (reviewed by Randall and Goodbourn 2008). In herpesvirus infections, the most effective evasion strategy is the ability of these viruses to enter a latent state where only a minimal number of viral genes are expressed. This in turn reduces the number of antigens presented to the host immune surveillance system for example cytotoxic T cells. However during lytic infection or re-activation, the majority of viral genes are expressed and the virus becomes vulnerable to innate immune responses and it is during this time that the virus will employ active evasion strategies (reviewed by Rezaee *et al.* 2006).

Herpesviruses use different mechanisms to interrupt the antiviral state (reviewed by Randall and Goodbourn 2008). In particular HSV-1 can disrupt protein kinase R (PKR) activity through two mechanisms; through the direct binding of HSV-1 Us11

to PKR, which blocks the phosphorylation of the α subunit of the eukaryotic translational initiation factor 2 (eIF2α) (Cassady *et al.* 1998); and via the indirect binding of HSV-1 ICP34.5 with the cellular protein phosphatase 1α, which in turn dephosphorylates eIF2α (He *et al.* 1997). PKR targets eIF2α, as eIF2-GTP forms a complex with initiator $tRNA^{met}$, which scans mRNA for AUG codons, hence phosphorylation of eIF2α prevents eIF2-GDP being recycled to eIF2-GTP by the GDP-GTP exchange factor eIF2B. The consequence of this is a decrease in $tRNA^{met}$/eIF2-GTP, which in turn decreases translation initiation of viral and cellular mRNA (reviewed by Thompson and Sarnow 2000). Other HSV-1 proteins have dual mechanisms for innate immune avoidance, such as ICP0, which can induce degradation of PML and Sp100 via its E3 ligase activity (reviewed by Randall and Goodbourn 2008). Secondly, ICP0 recruits IRF3 and its transcriptional co-activators; CBP and p300 to nuclear foci, which lead to inactivation and accelerated degradation of IRF3, a key component of type I IFN system (Melroe *et al.* 2007).

Table 1.2 Type I IFN induced genes and their role in activating the antiviral state of an infected cell.

Gene	Mode of action
Protein kinase R (PKR)	PKR is an enzyme that upon activation phosphorylates eukaryotic initiation factor 2α (eIF2α). This prevents recycling of translation initiation factors, which in turn blocks protein synthesis and can lead to autophagy. PKR has also been linked to apoptosis.
2'-5' Oligoadenylate synthetase (OAS)	Activation of OAS causes polymerisation of ATP into 2'-5' oligoadenylates, which bind and activate RNase L. RNase L degrades cellular and viral RNA inhibiting protein synthesis. OAS/RNase L has also been associated with apoptosis.
Mx proteins	Mx proteins belong to a family of GTPases, related to dynamin. They recognise nucleocapsid structures and stop them from entering the nucleus. This control viral replication by inhibiting nuclear export and hence blocks further assembly.
Interferon-stimulated genes (ISGs)	A number of genes become upregulated in response to interferon and these have been named ISGs along with their molecular mass e.g. ISG54 is a 54kDa protein. Much is still to be learnt about this family, although ISG15 has been reported to inhibit degradation of IRF3 by viral components.
p200 family	The p200 proteins affect cell cycle progression, the best characterised is p202. This protein binds to members of the E2F transcription family stopping DNA binding leading to loss of transcription of genes important for cell cycle progression.
Promyelocytic leukaemia (PML) nuclear bodies	Contain IFN-inducible proteins such as PML and Sp100, which appear to play a role in restricting viral replication by regulating chromatin structure and promoter accessibility.
Viperin (cig5)	Disrupts lipid rafts on plasma membranes, which are important in budding of some viruses. It achieves this through binding and inhibiting an enzyme involved in lipid biosynthesis.

Information compiled from (Brierley and Fish 2002; Randall and Goodbourn 2008; Boo and Yang 2010).

1.3.3 Immune evasion strategies employed by γ-herpesviruses

The γ-herpesviruses have evolved a number of mechanisms to evade both the innate and adaptive host immune responses. The main adaptive immune evasion strategy seen in KSHV, EBV and MHV-68 is the avoidance of the T cell response. MHV-68 achieves this through the down-regulation of MHC class I molecules via the viral K3 gene, a mechanism that is also seen with KSHV homologues K3 and K5 (Stevenson *et al.* 2000). In contrast EBV produces an IL10 homologue (vIL10), which down-regulates MHC class II molecules suppressing the Th1 immune response (reviewed by Goodbourn *et al.* 2000).

1.3.3.1 Innate immune evasion strategies employed by γ-herpesviruses

Type I IFNs are the first antiviral defence mechanisms against most viruses including herpesviruses. As a result, herpesviruses have evolved a number of immune evasion strategies against type I IFN effector mechanisms (Table 1.3). As table 1.3 highlights, the complexity of the host innate immune response is equalled by a range of immune evasion strategies employed by γ-herpesviruses.

One interesting group of immunomodulatory proteins expressed in KSHV are the four vIRFs (vIRF1-4), which share some homology with the cellular IRFs (reviewed by Areste and Blackbourn 2009). Of the four proteins only vIRF1-3 have been functionally characterised with little known about vIRF4, however vIRF1-3 have been implicated in immune evasion strategies (reviewed by Lee *et al.* 2009). vIRF1 was the first member of the viral IRF family to be described (Moore *et al.* 1996) and has since been found to negatively regulate IFN signalling (reviewed by Rezaee *et al.* 2006). vIRF1 achieves this through an association with the cellular p300 protein,

which in turn prevents IRF3-mediated activation of IFN-α (reviewed by Lee *et al.* 2009). Similar to vIRF1, vIRF2 has been found to inhibit expression of the IFN-inducible genes; IRF3 and IRF1, but not IRF7, however vIRF2 probably does it through a different mechanism than the one employed by vIRF1 (Fuld *et al.* 2006). In contrast to vIRF1 and vIRF2 that mostly target IRF3-mediated signalling, vIRF3 interacts with IRF7, which leads to inhibition of IRF7's DNA-binding activity, which in turn inhibits IFN-α production (reviewed by Lee *et al.* 2009). Taken together the vIRF proteins play an important role in down-regulation of the IFN pathway.

In MHV-68, ORF36, a protein kinase, was found to also play a role in IFN immune evasion during screening of mutant viruses. MHV-68 ORF36 was shown to bind to activated IRF3, blocking IRF3's interaction with co-transcriptional activators, which in turn inhibited the recruitment of RNA polymerase II to the IFN-β promoter. This anti-IFN function was found to be conserved in the ORF36 homologues in EBV (BGLF4) and in KSHV (ORF36). The results from the *in vivo* study using mutant ORF36 virus found that a much greater IFN response was seen during infection with the mutant virus, which lead to a compromised infection in the lungs and spleens of mice (Hwang *et al.* 2009). The highly complex nature of the host immune response and the γ-herpesvirus evasion strategies means that there is still much to learn in this area, however the use of MHV-68 as a model may help to gain insights into key evasion strategies *in vivo*.

Table 1.3 Immunomodulatory proteins involved in evasion of type I IFN immune response to human γ-herpesviruses and MHV-68.

Herpesvirus	Immunomodulatory protein	Function
EBV	BARF1	BARF1 is a soluble receptor for colony stimulating factor 1 (CSF1), which can block function of CSF1, which in turn interferes with secretion of antiviral factors like IFN-α.
	EBNA-2	Blocks IFN signal transduction although the mechanism is unknown.
	EBER-1 and 2	EBER RNA binds to dsRNA binding site on PKR acts as an inhibitor and so fails to activate PKR.
	BS-MLF1	Acts as a dsRNA-binding protein to sequester any dsRNA produced as a viral by-product and reducing PAMPs.
	BGLF4	Inhibits activation of IFN-β in a dose-dependent manner.
KSHV	Viral IRFs	Four protein (vIRFs 1-4) function as cellular IRF homologues interfering with their functions, especially IRF3 and 7.
	ORF45	Is an IE protein that binds to inhibitory domain of IRF7, blocking its function.
	RTA	Binds to IRF7 inducing proteosomal degradation and also mediates the degradation of TRIF via the ubiquitin-proteosome pathway.
	ORF36	Inhibits activation of IFN-β in a dose-dependent manner.
	K-bZIP	Targets IRF3 binds to IFN-β promoter, resulting in defective transcription of IFN-β.
	RIF	Targets multiple components of IFN signalling pathway, which inhibits generation and accumulation of ISGF3 impeding transcription of ISGs.
	vIL6	vIL6 inhibits binding of the ISRE promoter to ISGF3, suppressing the IFN response.

MHV-68	ORF36	Binds to IRF3 inhibiting its interaction with CBP, which suppresses the recruitment of Pol II to the IFN-β promoter.
	ORF45	Represses activation of IRF7 and IFN-αβ ISG transcription.
	ORF54	Degrades IFNAR1 protein, which interferes with type I IFN response.

Information compiled from (Goodbourn *et al.* 2000; Snow and Martinez 2007; Randall and Goodbourn 2008; Barton *et al*. 2011; Leang *et al.* 2011; Sathish and Yuan 2011)

Another immune evasion strategy that can be employed by viruses is the interference of viral proteins with cellular gene transcription, mRNA processing, export or protein synthesis within the cell. This process, known as host shutoff, can be linked to a number of cellular processes although it is believed that one of the main reasons for the virus to cause global inhibition of cellular gene expression is to avert the IFN response (reviewed by Randall and Goodbourn 2008).

1.4 Eukaryotic RNA synthesis

In eukaryotic cells, mRNA biosynthesis is a multistage process that begins with transcription in the nucleus, the product of which is then transported to the cytoplasm for translation to take place. Transcription is a process by which DNA is copied into RNA with the potential to be translated into protein (Lewin 2004). Biochemical and genetic analysis of various model organisms has identified eukaryotic gene transcription as an intricate biochemical process that is tightly regulated at many levels with a number of protein factors responsible for its control (Lemon 2000) (Figures 1.5 &1.6).

The complexity of the gene expression process means that it must be tightly regulated. The first problem that the transcription machinery encounters is that the DNA template is embedded in the chromatin structure. The chromatin structure consists of histone and non-histone proteins that compact the large genome allowing it to fit into confines of the nucleus. However, a number of chromatin-remodelling complexes, such as ATP-dependant remodelers and histone modifying enzymes are recruited which in turn facilitate gene expression (reviewed by Svejstrup 2004; Shandilya and Roberts 2012). Transcription of genes is performed by three main enzymes associated with different sets of genes: RNA polymerase I (Pol I) which transcribes ribosomal RNA (rRNA); RNA Pol II which transcribes protein-coding genes from messenger RNA (mRNA) and RNA Pol III which transcribes transfer RNA (tRNA) genes (reviewed by Engelhardt 2006). The transcription of mRNA requires Pol II to bind to promoters of genes, via transcription factors forming a transcription complex (reviewed by Deng 2007). Eukaryotic promoters generally contain either a sequence called the TATA box around 25-35 bp upstream from the start site of transcription or an initiator element located around the transcription start site. Lack of such elements within a sequence will result in reduced transcription efficiency (Turner 2000). Transcription may also be increased by the presence of an enhancer element, a sequence linked to a promoter independent of orientation and position (reviewed by Szutorisz 2005). The TATA sequence is recognised by the TATA-binding protein (TBP), which binds to the DNA along with its associated factors, for example, TFIID. Binding of the TBP to the promoter distorts the TATA sequence recruiting other general transcription factors (e.g. TFIIA), these factors along with RNA Pol II form a complex that is competent for transcription. Once the

RNA Pol II has cleared the promoter sequence it begins the process of transcription of pre-mRNA (reviewed by Svejstrup 2004; Shandilya and Roberts 2012).

Once RNA Pol II has started making the transcript, before the chain is 20-30 nt long, the 5' end is capped by the enzyme mRNA guanyltransferase, which adds a 7-methylguanosine residue (m^7G). The addition of the cap stabilises the transcript by forming a barrier to 5'-exonucleases and also plays a role in splicing, nuclear transport and translation. As well as a cap a poly(A) tail is added at the 3' end of the pre-mRNA. The addition of the poly(A) tail is dependent on sequences in the DNA, which make up the polyadenylation site. A number of protein factors recognise the sequence elements and form a complex on the pre-mRNA, one of these factor, poly(A) polymerase (PAP) adds A residues to the 3' end of the pre-mRNA forming the tail. Similarly to the cap, the poly(A) tail is thought to stabilise the mRNA as it binds poly(A)-binding protein, preventing 3' exonucleases from removing the tail (Turner 2000). Once the pre-mRNA has been transcribed it undergoes a process known as splicing (directed by uracil rich small nuclear RNAs or snRNAs) to remove non-coding regions (introns) to produce continuous protein-coding regions comprising of exons (Turner 2000) (Figure 1.5). The reliance of eukaryotic mRNA processing on splicing may seem a disadvantage. However, splicing leads to proteomic complexity, as sequences can be interpreted as intronic or exonic depending on cell type or environmental conditions and it allows the generation of multiple mRNAs from a single transcript (reviewed by Mendes Soares and Valcarcel 2006).

During mRNA synthesis, proteins associate with the RNA molecules, forming complexes known as messenger ribonucleoproteins (mRNPs). The composition of these mRNPs is dynamic, allowing different proteins that are required for different steps of gene expression to bind to the mRNA facilitating its progression through to translation. One of the key functions of these proteins is to facilitate the transport of the mRNA through nuclear pore complexes (NPCs) into the cytoplasm (reviewed by Folkmann *et al.* 2011). Initially movement of the mRNPs occurs via diffusion through areas of the nucleus not occupied by chromatin to the nuclear surface (Zachar *et al.* 1993). Export of tRNA, rRNA, miRNA and small nuclear RNA (snRNA) rely on a family of nuclear transport receptors known as importin-β or karyopherins and are regulated by Ran GTPase. These receptors recognise nuclear localisation and nuclear export signals on RNA, which signal the export and transport of the RNA either into the nucleus or out of the nucleus into the cytoplasm. In contrast, mRNA export uses a transport receptor that is not related to the karyopherins and does not require Ran GTPase (reviewed by Kohler and Hurt 2007).

A number of proteins are linked to export of mRNA; one of the main protein complexes is THO, which is involved in transcription elongation and also associates with REF and UAP56 proteins, which together form the transcription-export complex (TREX). The REF export adaptor then recruits the TAP-p15 mRNA export factor. The TAP-p15 complexes have the ability to associate with nuclear mRNA, shuttle and interact with NPC components (reviewed by Erkmann and Kutay 2004). Work carried out in yeast has suggested that the carrier complex Mex67:Mtr2 (TAP-p15 in metazoans) interacts with FG-nucleoporins that line the NPC, which in turn moves the mRNP through the NPC via Brownian motion (Stewart 2007). The mRNP

is remodelled by the DEAD box protein Dbp5 (DDX19 in vertebrates), which is activated by Gle1 and IP_6 at the cytoplasmic face of the NPC. This process releases transport factors and nuclear mRNA binding proteins allowing them to be recycled and it also stops the mRNP from re-entering the nucleus (reviewed by Folkmann *et al.* 2011). The complexity of mRNA export means that surveillance can take place which ensures that only export-competent mRNPs are transported. In contrast to tRNA, which is transported to the cytoplasm via the exportin-t pathway, which does not discriminate between intron-containing and spliced tRNAs (Arts *et al.* 1998). Studies in yeast examining mRNA export have identified myosin-like Mlp1 and Mlp2 proteins as key components of the surveillance process at the NPCs. The Mlps have been found to interact with mRNPs and retain improperly assembled mRNPs in the nucleus (reviewed by Cole and Scarcelli 2006)

Once the mRNA has entered the cytoplasm translation can occur. This process involves the sequence being read in triplets to give a series of amino acids that make the corresponding protein (Lewin 2004) (Figure 1.6). Translation can be broken down into three stages; initiation, elongation and termination. The first stage of initiation refers to the assembly of a ribosome at the AUG start codon on the mRNA. The next stage of elongation is the codon-dependent assembly of the polypeptide. The final stage is termination and this is the release of the protein when the ribosome has reached the termination codon. All three stages rely on a number of proteins referred to as eukaryotic

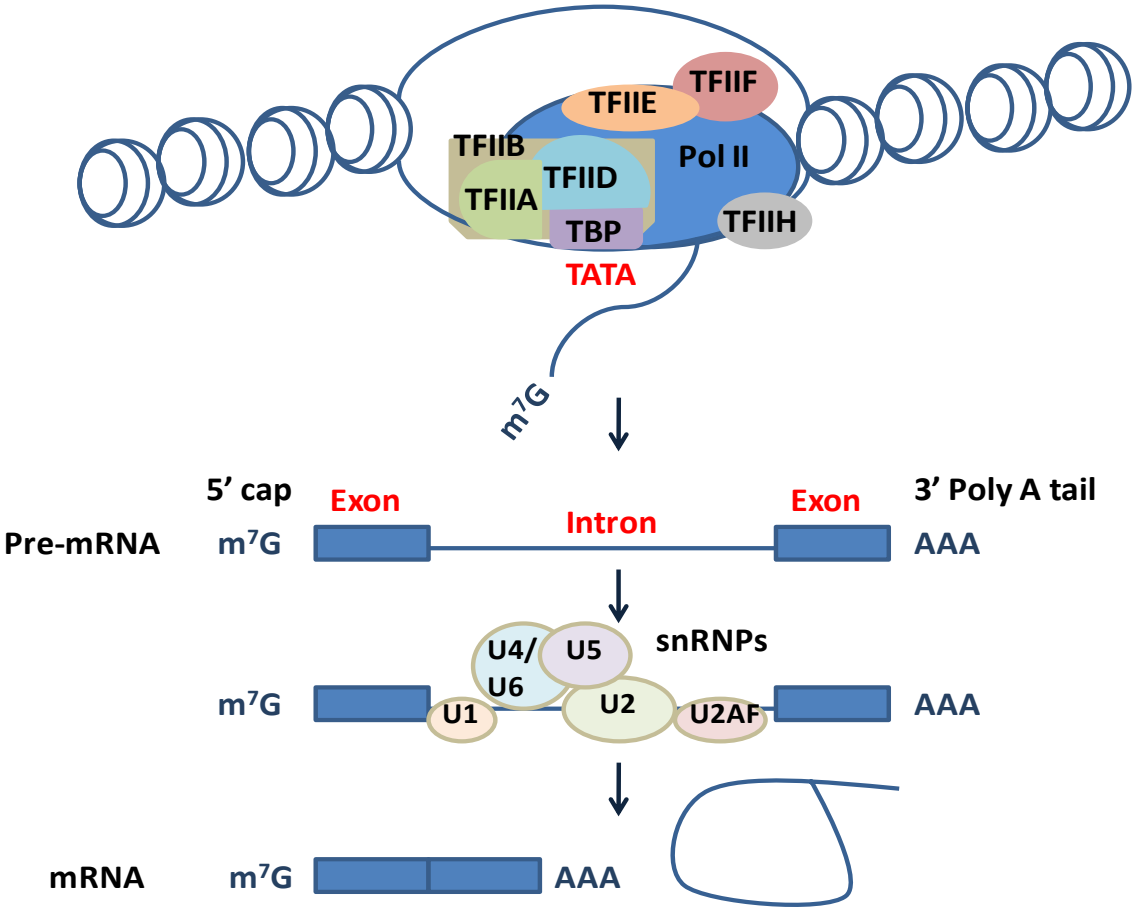

Figure 1.5 Eukaryotic transcription of mRNA from a DNA template. Chromatin remodeling enzymes open up the chromatin structure allowing transcription to take place. The first step of transcription is the recognition of the TATA sequence by the TBP, which in turn recruits transcription factors along with RNA Pol II. Pol II starts making the pre-mRNA transcript and a 5' cap is added. Once the mRNA has been transcribed a poly(A) tail is added to the 3' end. A number of snRNPs then bind to the pre-mRNA forming a spliceosome, which remove intron sequences. The introns are removed in a lariat configuration leaving just the coding exons forming the mRNA (Information from Svejstrup 2004; Mendes Soares and Valcarcel 2006; Shandilya and Roberts 2012).

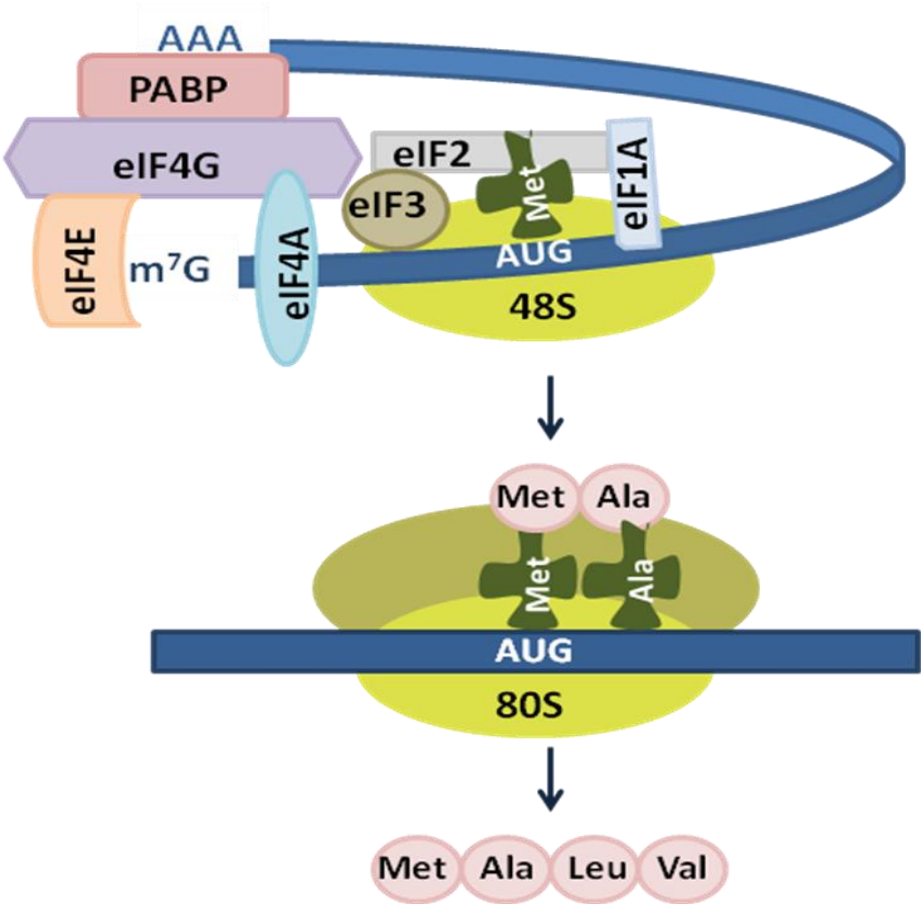

Figure 1.6 Translation of eukaryotic mRNA into a protein. A number of eukaryotic initiation factors (eIFs) along with methionyl-transfer RNA (Met-tRNA) bind to the 40S ribosomal subunit forming a 43S pre-initiation complex. A cap-binding complex, which consists of eIF4G, 4E and 4A bind to the 5' cap structure, eIF4G also binds to poly(A) binding protein (PABP), which bridges the 5' and 3' ends of the mRNA. It is thought that the circularisation of mRNA promote the binding of the 43S complex to the mRNA, which then scans the mRNA for the AUG start codon. The eIFs then dissociate and the 60S ribosomal subunit is recruited forming an 80S ribosome, which activates translation elongation. The ribosome moves along the mRNA with each coded tRNA binding to the mRNA forming a protein sequence attached by peptide bonds. This process continues until a stop codon is reached leaving the newly synthesized protein (Information from Klann and Dever 2004).

initiation factors (eIF), elongation factors (eEF) and release factors (eRF) (reviewed by (Klann and Dever 2004).

1.4.1 mRNA turnover in eukaryotic cells

An important part of gene expression is mRNA turnover, as it sets the basal level of gene expression, is a site of regulatory response, and plays an important role in antiviral defenses (reviewed by Coller and Parker 2004; Lewin 2004). Once the mRNA has been transcribed it is transported to the cytoplasm for translation to occur and it is here that the mRNA is subject to regulatory processes that may lead to repression of translation or mRNA degradation. The factors required for mRNA surveillance and degradation co-localise in cytoplasmic processing bodies known as P bodies. It is in the P bodies that most of the mRNA decay takes place (reviewed by Newbury 2006; Eulalio *et al.* 2007). A significant body of the work on mRNA degradation pathways has been carried out in model organisms such as yeast and fungi. There are two general mechanisms for degradation of mRNA: (i) deadenylation dependant pathways (either 5'-3' or 3'-5'); and (ii) endonucleolytic digestion (reviewed by Coller 2004) (Figure 1.7).

Degradation of the bulk of mRNA takes place under the control of deadenylation-dependant pathways, which begin with the shortening of poly(A) tails at the 3' end of the mRNA via deadenylases (reviewed by Eulalio *et al.* 2007). Deadenylases are Mg^{2+}-dependant exoribonucleases that hydrolyse RNA in a 3'-5' direction, resulting in the release of 5'-AMP. Poly(A) tails are the main substrate for deadenylases and once the tail is removed other degradative enzymes initiate degradation of the mRNA (reviewed by Goldstrohm and Wickens 2008). Following deadenylation the complete

degradation of mRNA by the 5'-3' RNA decay pathway requires the removal of the cap structure by decapping enzymes. A decapping complex known as Dcp1-Dcp2 has been identified in yeast to catalyse mRNA cap hydrolysis, which releases m^7GDP and monophosphated mRNA (Gu and Lima 2005). This Dcp1-Dcp2 decapping complex is thought to play a similar role in decay mechanisms in all eukaryotes (reviewed by Coller and Parker 2004). However, there are some differences. In yeast Dcp1 has been found to associate directly with Dcp2, whereas in mammalian cells it is thought Dcp1 forms a larger complex including EDC3 and Ge-1 (reviewed by Eulalio *et al.* 2007). Removal of the cap structure opens up the mRNA to degradation by Xrn1, a 5'-3' exoribonuclease, which preferentially degrades substrates containing a 5' monophosphated end (reviewed by Coller and Parker 2004; Eulalio *et al.* 2007).

The 3'-5' mRNA decay pathway is reliant on an exoribonuclease complex known as the exosome. The exosome is a large protein complex consisting of multiple 3'-5' exonucleases, which form a ring structure that can encircle RNA. This structure gives the exosome flexibility, as different exonucleases may be specific for different RNA sequences. The ability of the exosome to degrade RNA is reliant on a helicase complex Ski2p-Ski3p-Ski8p, which unwinds the RNA structure helping RNA entry into the exosome for digestion (reviewed by Newbury 2006). Following the exosome-mediated 3'-5' mRNA decay the scavenger decapping enzyme, DcpS catalyses residual cap hydrolysis (Gu and Lima 2005).

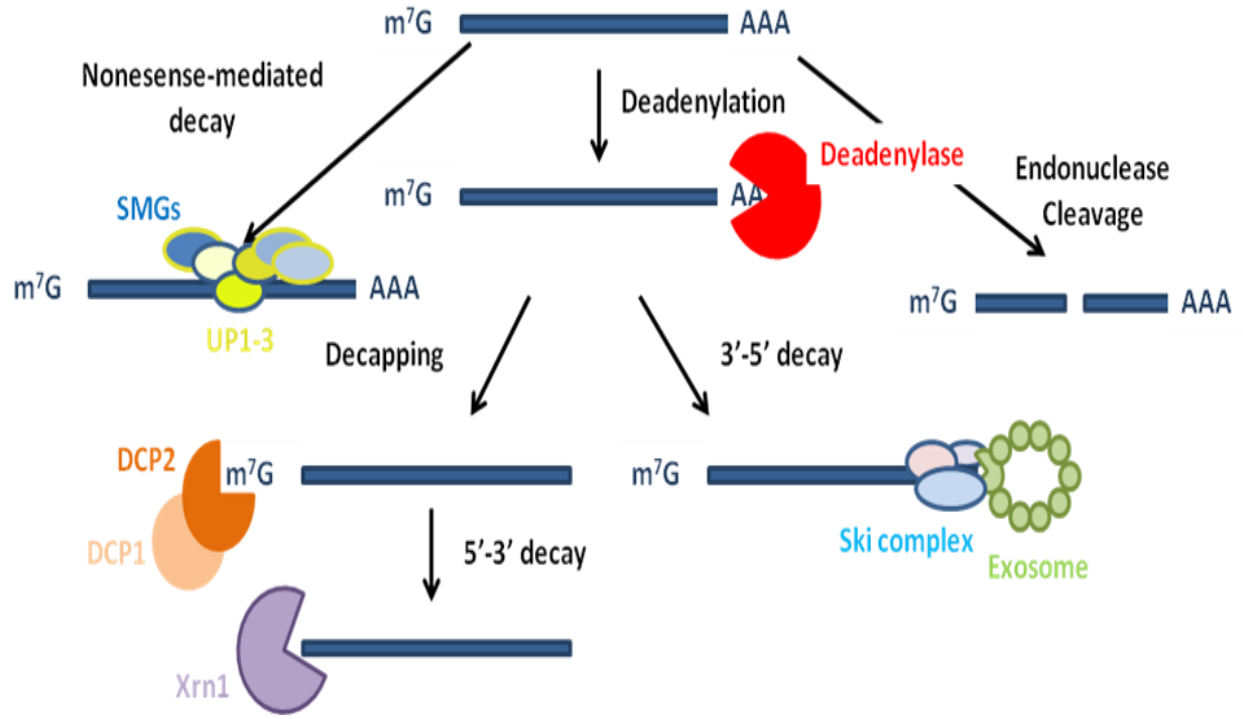

Figure 1.7 Eukaryotic mRNA decay pathways. The two main mRNA decay pathways first require that the 3' poly(A) tail is removed via deadenylases. Once this has occurred the mRNA is either decapped by DCP1 and 2 enzymes before 5'-3' degradation takes place via Xrn1 or the mRNA is degraded by the exosome in conjunction with the Ski complex. Alternative pathways include cleavage of the mRNA by endonucleases, which then allow the mRNA to be degraded by the mRNA machinery and nonsense-mediated decay (NMD). The NMD pathway is initiated by the premature termination of the ribosome due to a nonsense codon, which recruits the surveillance complex (UP1-3 and SMGs) to the mRNA. The surveillance complex then recruits the general mRNA decay machinery for degradation (Information from Coller and Parker 2004; Eulalio *et al.* 2007; Goldstrohm and Wickens 2008).

Decay of mRNA can also take place prior to deadenylation with endonucleolytic cleavage and there appears to be a variety of different endonucleases that have different cleavage specificities (reviewed by Coller and Parker 2004). One example of endonucleolytic cleavage is RNA mediated gene silencing (RNAi), which functions to protect the genome from viruses and transposons as well as controlling gene expression of some mRNAs. The process of RNAi involves the recognition of a dsRNA sequence by an endonuclease known as Dicer, which cleaves dsRNA into 21-22 nt siRNAs (small interfering RNAs). The siRNAs are incorporated into a complex called the RNA-induced silencing complex (RISC), which will also contain at least one Argonaute protein. Argonaute proteins adopt an RNase H-like fold that cleaves the mRNA at sites complementary to the siRNAs. Following endonucleolytic cleavage the mRNA fragments are degraded by the general mRNA decay machinery (reviewed by Coller and Parker 2004; Newbury 2006; Eulalio *et al*. 2007).

Eukaryotes have also evolved specialised quality control mechanisms to ensure that only fully processed error free mRNA is translated. Nonsense-mediated decay (NMD) is a crucial mRNA quality control mechanism which includes pathways that degrade transcripts with premature translation termination codons known as nonsense codons (reviewed by Coller and Parker 2004; Eulalio *et al.* 2007). The premature termination of translation triggers the NMD pathway, which leads to the formation of UPF1-3 complex on the mRNA along with NMD effectors SMG1 and SMG5-7. The UPF1 protein is an RNA helicase, which is regulated by phosphorylation and dephosphorylation events, which in turn requires additional complex factors. Once the complex has assembled on the mRNA it recruits enzymes from the normal mRNA decay machinery to degrade it (reviewed by Eulalio *et al.*

2007). Another specialised pathway referred to as nonstop decay degrades mRNA which does not have a stop codon; the mRNA is targeted to the cytoplasmic exosome by a specific adapter protein, Ski7p, which is thought to interact with the stalled ribosome (reviewed by Coller 2004).

1.5. Viral manipulation of host transcription machinery

Different viruses are able to down-regulate or inhibit cellular gene expression within their host with a subsequent reduction in cellular protein pool, a phenomena which is known as host shutoff. The mechanism causing this host shutoff can be virus-specific, with different viruses targeting different stages in mRNA biosynthesis (reviewed by Aranda and Maule 1998) (Table 1.4). The mechanisms employed by different viruses can be very similar or vary greatly, as viruses may only produce one protein linked to host shutoff, that can have multiple effects, whereas other viruses appear to target one key area of the host transcription or translation machinery (Table 1.4). The host shutoff identified during viral infections allows the virus to usurp the cellular machinery, which in turn enhances viral replication and may also compromise the synthesis of proteins required for the host to mount its antiviral defence (reviewed in Pe'ery and Mathews 2000).

1.5.1 Host shutoff identified in RNA viruses

The inhibition of host gene expression in RNA viruses has been well studied (reviewed by Lyles 2000; Bushell and Sarnow 2002). One of the most studied families of RNA viruses that has been found to cause host shutoff is the *Picornaviridae* and in particular the prototype picornavirus; poliovirus (reviewed by Lyles 2000). Polioviruses have been found to employ two mechanisms of host

shutoff: disruption of transcription; or disruption of translation using two viral proteases; $3C^{PRO}$ and $2A^{PRO}$ (reviewed by Aranda and Maule 1998; Lyles 2000). The two proteases share some functional similarity as they can both cleave Poly(A) binding protein (PABP) (Joachims *et al.* 1999) and can also both cleave the TBP (Yalamanchili *et al.* 1996; Yalamanchili *et al.* 1997). However they cleave TBP at different sites and only $3C^{PRO}$ is able to inhibit Pol II transcription (Yalamanchili *et al.* 1997). These findings indicate that the main role of $2A^{PRO}$ in host shutoff is not to interfere with transcription, but to inhibit translation. As well as its ability to cleave PABP, $2A^{PRO}$ has been found to cleave the translation initiation factors eIF4G inhibiting translation of capped mRNAs (Krausslich *et al.* 1987).

Poliovirus is an RNA virus that replicates in the cytoplasm and does not require the host transcription machinery meaning that the action of $3C^{PRO}$ hinders the host, but not the viral replication. This is also true of the mechanism of $2A^{PRO}$ as cleavage of eIF4G separates the domain responsible for association with the cap-binding subunit eIF4E inhibiting the translation of capped mRNAs, but as poliovirus mRNAs are uncapped this does not affect viral mRNA translation (reviewed by Lyles 2000). The obvious benefits of host shutoff in poliovirus infection can be seen throughout the *Picornoviridae* family as similar mechanisms are employed to inhibit host gene expression. Examples of this include the cleavage of eIF4G seen in coxsackievirus and rhinovirus (Lamphear *et al.* 1993) and the cleavage of PABP by coxsackievirus B3 2A protease (Joachims *et al.* 1999). However, some differences are seen in the Picornaviridae family, such as in encephalomyocarditis virus (EMCV), which does not cleave eIF4G, but instead activates eIF4E binding proteins (4E-BPs) that sequester eIF4E from the eIF4F complex. This process is also seen in poliovirus, but

takes place following other shutoff mechanisms, whereas it coincides with EMCV shutoff (Gingras *et al.* 1996; Bushell and Sarnow 2002).

1.5.2 Host shutoff identified in DNA viruses

Adenovirus C is a DNA virus which, like poliovirus, employs two modes of action to mediate host shutoff. However, unlike poliovirus, adenovirus c produces proteins that block nuclear transport of cellular mRNA (Pilder *et al.* 1986), whilst the other protein causes displacement of a MAPK kinase from eIF4G impairing eIF4F activity (Cuesta *et al.* 2000). The advantage of a transport block during adenovirus infection is that E1B-55K and E4 proteins produce a selective block to nucleocytoplasmic transport so that cellular mRNAs do not enter the cytoplasm, but viral mRNAs do (reviewed by Aranda and Maule 1998). The advantage to adenovirus in impairing cap-dependant translation is less obvious since adenovirus mRNAs are capped, like cellular mRNAs. However a process known as ribosome shunting has been identified in adenovirus infections (Yueh and Schneider 1996). All adenovirus mRNAs derived from the major late promoter contain a 5' non-coding region known as the tripartite leader. The tripartite leader promotes export of mRNAs to the cytoplasm and also directs ribosome shunting. The process of ribosome shunting involves the loading of 40S subunits to the 5' end of mRNA, the 40S subunit is then translocated to the downstream initiation codon via shunting elements. Ribosome shunting decreases the dependence of mRNA on eIF4F during initiation, which in turn facilitates the translation of adenovirus mRNA (reviewed by Schneider 2000).

Table 1.4 Viruses and host shutoff.

Virus	Protein	Mode of Action	Reference
Poliovirus	3C	Protease cleaves TBP stopping it from binding to the TATA box, inhibiting Pol II transcription. Also cleaves PABP removing the C-terminal domain (CTD) inhibiting poly(A)-dependant translation.	(Clark *et al.* 1993; Yalamanchili *et al.* 1996; Joachims *et al.* 1999; Kuyumcu-Martinez *et al.* 2004b)
	2A	Protease indirectly cleaves the eIF4G (p220) subunit of eIF4F inactivating cap-dependant translation. Also cleaves PABP.	(Etchison *et al.* 1982; Krausslich *et al.* 1987; Joachims *et al.* 1999)
Adenovirus C	E1B-55K & E4	Block transport and accumulation of cellular mRNA, but facilitate the same processes for viral mRNA.	(Halbert *et al.* 1985; Pilder *et al.* 1986)
	100K	Displaces MAPK kinase (Mnk1) from eIF4G, which leads to dephosphorylation of eIF4E, impairing eIF4F activity and inhibiting translation.	(Cuesta *et al.* 2000)
Influenza A	NS1A	Binds to the cleavage and polyadenylation specificity factor (CPSF), inhibiting 3' processing and export. Also binds to U6 snRNA, inhibiting splicing and spliceosome formation.	(Qiu *et al.* 1995; Nemeroff *et al.* 1998)
Calcivirus	3CL	3C-like protease cleaves PABP	(Kuyumcu-Martinez *et al.* 2004a)
Rotavirus	NSP3	Interacts with eIF4G, displacing PABP from eIF4F. Also NSP3 interaction with eIF4G along with rotavirus X protein associated with NSP3 (RoXaN) redirects cytoplasmic PABP to nucleus.	(Piron *et al.* 1998; Harb *et al.* 2008)

Vesicular Stomatitis Virus	M	Interferes with transport mechanisms dependant on Ran GTPase and its associated factors inhibiting transport. Also binds mRNA export factor Rae1 and targets nucleoporin Nup98 inhibiting nuclear export. M protein also inhibits transcription from Pol I and Pol II dependant promoters.	(Her *et al.* 1997; Ahmed and Lyles 1998; von Kobbe *et al.* 2000; Faria *et al.* 2005)
Mouse hepatitis corona virus	?	Increases phophorylation of eIF2α leads to formation of stress granules (P-bodies) causing mRNA decay.	(Raaben *et al.* 2007)
Rift valley fever virus	NSs	Interacts with p44 and XPB components of TFIIH sequestering them into nuclear filamentous structures preventing assembly of TFIIH subunits.	(Le May *et al.* 2004)
SARS corona virus	Nsp1	Binds to 40S ribosomal subunits inactivating translational activity and inducing modification of 5' capped mRNA leading to endonucleolytic cleavage.	(Kamitani *et al.* 2009; Huang *et al.* 2011)
HIV	PR	Protease cleaves eIF4G and PABP blocking cap-and poly(A)-dependant translation.	(Ventoso *et al.* 2001; Alvarez *et al.* 2006; Castello *et al.* 2009)
Sindbis virus	nsP2	Transcriptional shutoff.	(Garmashova *et al.* 2006)
Semliki Forest Virus	?	Increased phosphorylation of eIF2α leading to formation of stress granules.	(McInerney *et al.* 2005)
Encephalomyocarditis virus	4E-BPs	Sequesters eIF4E from eIF4F complex.	(Gingras *et al.* 1996)
Vaccinia virus	POLADs	Polyadenylated small non-translating RNA sequences (POLADS) sequester PABP.	(Su and Bablanian 1990)

1.5.3 Host shutoff mediated by herpesviruses

Host shutoff was first identified in α-herpesviruses HSV-1 and HSV-2 as far back as 1965 (Roizman *et al.* 1965) and since then much work has been carried out to understand the underlying mechanisms of HSV-mediated host shutoff. Much of this work has focused on herpes simplex virus type 1 (HSV-1) which causes host shutoff through two distinct inhibitory pathways (reviewed by Smiley 2004b). One pathway influences host mRNA maturation, through, the product of the viral *ICP27* gene, which causes the major components of the spliceosome, the snRNP's to be redistributed, inhibiting splicing of cellular mRNA (Phelan 1993; Hardwicke and Sandri-Goldin 1994). ICP27 achieves this through interaction with a group of proteins linked to the regulation of splicing known as SR proteins. In particular ICP27 interacts with SR protein kinase 1 (SRPK1), which triggers aberrant SR phosphorylation impairing their ability to function in spliceosome assembly (Sciabica *et al.* 2003). This action is beneficial to the virus as HSV-1 carries very few genes with introns, hence a disruption to the splicesome allows for preferential maturation of viral transcripts (reviewed by Aranda and Maule 1998). However ICP27 is a multifunctional protein linked to a number of processes during virus infection, including transcriptional activation and mRNA export (reviewed by Sandri-Goldin 2011). The role of ICP27 as a transcriptional activator is linked to Pol II, as ICP27 has been found to bind to the C-terminal domain of Pol II, which recruits Pol II to viral replication sites (Dai-Ju *et al.* 2006). In terms of mRNA export, ICP27 binds to intronless RNAs and facilitates their export via cellular export machinery (reviewed by Sandri-Goldin 2011). The functions of ICP27 allow for the preferential processing of viral mRNAs over the cellular mRNAs. In other herpesviruses, positional homologues of ICP27 have been found in all sequenced

mammalian herpesviruses and have been shown to play a role in the lytic cycle of these viruses, there is, however, some divergence between these viral proteins (reviewed by Sandri-Goldin 2011). For example ICP27 has been found to stimulate the transcription of viral genes through recruitment of cellular RNA Pol II, a phenotype which has not been identified in ICP27 homologues (reviewed by Sandri-Goldin 2011). However KSHV ICP27 homologue (ORF57) has been found to interact with the transcriptional activator ORF50 to promote vial lytic gene expression (Malik *et al*. 2004).

The other pathway associated with HSV-1-mediated host shutoff is linked to mRNA stability, as the product of gene *UL41* encodes a *bona fide* virion host shutoff (vhs) protein, which functions as an RNase (Zelus 1996; Everly *et al.* 2002). The action of vhs protein is not restricted to HSV-1 as it has also been found to cause host shutoff in other members of the α-herpesvirus family, such as pseudorabies and varicella-zoster virus, however the activity of vhs protein in these viruses is not as extensive as that seen in HSV-1 (Sato *et al.* 2002; Lin *et al.* 2004) (Table 1.5). Interestingly, in the case of equine herpesvirus (EHV) although in cotransfection reporter assays vhs activity is observed no vhs-induced cellular mRNA degradation can be detected during viral EHV-1 infection even though the vhs homologue is transcribed and translated in cells. This has led to the speculation that host shutoff may not be seen during infection due to the smaller amount of vhs associated with viral particles or modulation from another viral factor, which may mask vhs activity (Feng *et al.* 1996).

The vhs protein degrades only mRNA, leaving other cytoplasmic RNA intact and it appears to do this through an interaction with the translation initiation machinery. The vhs protein has been found to interact with components of the eIF4F translation complex; eIF4H, eIF4B and eIF4AII (an isoform of eIF4A) and has been linked to the 5' capped region of mRNA (Doepker *et al.* 2004; Feng *et al.* 2005). These results are in accordance with a previous study which used RNase protection assays to compare 5' and 3' decay rates of a selected mRNA. Their results indicated that in wild type HSV-1 infection, the 5' end of the transcript was degraded quicker than the 3' end. In contrast upon infection with a vhs mutant virus the 5' and 3' decay rates of the transcript were very similar (Karr and Read 1999). However, there is also evidence that 3'-5' decay is taking place in a vhs-dependent manner linked to cellular mRNA sequences in stress-inducible genes (Taddeo *et al.* 2003; Esclatine *et al.* 2004a). Esclatine *et al* used Northern blotting techniques along with RT-PCR, which used primers targeted to 5' and 3' sequences along either AU-rich element (ARE) or non-ARE-containing mRNAs. Using these techniques they discovered that certain cellular mRNAs containing AREs were deadenylated before endonucleolytic cleavage within the ARE occurred in a vhs-dependent process, deadenylation was not seen in mRNAs with no AREs. They also found that the 5' cleavage products remained in the cytoplasm for many hours in the infected cell (Esclatine *et al.* 2004a). Taken together, these results suggest that in the absence of AREs, vhs will bind to the cap-binding proteins and initiate degradation in a 5'-3' manner. However, in the presence of ARE-containing stress response mRNAs, vhs initiates deadenylation and cleavage of the transcripts. The lingering 5' cleavage products may then be accounted for by the limited number of 5' degradation enzymes, which are being utilised by vhs on non-ARE containing mRNAs.

Homologues of vhs have been identified in all of the α-herpesviruses, but not in β- nor in γ-herpesviruses, suggesting an important role for vhs in α-herpesvirus infections, which is also highlighted in its crucial role in virulence and pathogenicity (reviewed by Smiley 2004). The degradation of cellular mRNA by vhs leads to a downregulation of proteins required for the innate and adaptive immune responses. The use of mutant vhs viruses and immune knockout cell lines and mice has led to a greater understanding of the role of vhs in immune evasion and pathogenesis. For example, infection of IFNαβRKO mice with wild type HSV-2 and HSV-2 vhs mutant viruses has indicated that vhs interferes with the IFN-αβ response, as replication and virulence of the vhs-deficient virus was restored to wild type levels in IFNαβRKO mice (Murphy *et al.* 2003), a phenotype that has also been identified in fibroblast cell lines from these mice (Duerst and Morrison 2004). In addition HSV-1 vhs has been shown to suppress cytokine production and reduce IFN-αβ activity (Suzutani *et al.* 2000). In terms of adaptive immunity, vhs (in combination with ICP47) blocks antigen presentation by MHC class I (Tigges *et al.* 1996) and also reduces levels of MHC class II (Trgovcich *et al.* 2002). Furthermore the vhs protein has also been found to block the activation of dendritic cells, which in turn may reduce efficient antigen presentation and reduced/delayed induction of cellular immune responses (Samady *et al.* 2003).

The dual host shutoff mechanism employed by HSV-1 is complex, but is structured in this way to give the most benefit to the virus. The vhs protein is packaged within the virion and it is taken into the infected cell allowing host shutoff to take place during the first stages immediately post infection (reviewed by Aranda and Maule 1998). However, at later times after infection the virion transactivator VP16 along

with VP22 act to neutralise the effects of vhs (Lam *et al.* 1996; Taddeo *et al.* 2007). This is then followed by the second host shutoff pathway linked to the immediate early (IE) gene, ICP27. Therefore the disruption to splicing occurs after the expression of the IE genes, which include three of the four intron-containing genes encoded by HSV-1. This allows ICP27 to disrupt cellular but not viral mRNA splicing (reviewed by Aranda and Maule 1998). Interestingly a more recent study has found that ICP27 and vhs interact with each other. They suggest that this may occur when ICP27 is bound to PABP during shuttling of mRNA late in infection, which then binds vhs in the cap structure preventing it from cleaving transported mRNAs. This interaction may function to stop the RNase action of vhs protein not previously neutralised by VP16 and VP22 (Taddeo *et al.* 2010).

Table 1.5 Herpesviral proteins associated with host shutoff.

Herpesvirus	Gene	Protein	Function	Reference
HSV-1	ICP27	ICP27	Redistribution of snRNPs disrupts splicing machinery.	(Phelan *et al.* 1993)
	UL41	vhs	Acts as an RNase causing non-specific mRNA degradation.	(Read and Frenkel 1983; Zelus *et al.* 1996)
HSV-2	ICP27	ICP27	Redistribution of snRNPs disrupts splicing machinery.	(reviewed by (Sandri-Goldin 2011)
	UL41	vhs	Acts as an RNase causing non-specific mRNA degradation.	(Schek and Bachenheimer 1985; Zelus *et al.* 1996)
Pseudorabies	UL41	vhs	Acts as an RNase causing mRNA degradation.	(Lin *et al.* 2004)
Varicella-zoster virus	ORF17	ORF17	Homologue of vhs induces cleavage of mRNA similar to HSV vhs, but to a much lesser extent.	(Sato *et al.* 2002)
Bovine herpesvirus	UL41	vhs	Strong mRNA degrading activity.	(Hinkley *et al.* 2000)
KSHV	ORF37	SOX	mRNA degradation.	(Glaunsinger and Ganem 2004b)
EBV	BGLF5	BGLF5	mRNA degradation.	(Rowe *et al.* 2007b)
MHV-68	ORF37	mSOX	mRNA degradation.	(Covarrubias *et al.* 2009)

1.5.4 Host shutoff in γ-herpesviruses

Host shutoff in γ-herpesviruses was first documented in MHV68 using microarray technology (Ebrahimi *et al.* 2003). This observation was then followed by that of host shutoff in cells undergoing lytic KSHV infection (Glaunsinger and Ganem 2004b). The mediator of this shutoff was shown to be the product of viral gene *ORF37*, which encodes a viral DNA alkaline exonuclease (AE). Because of the dual exonuclease and host shutoff activities of ORF37, the protein was re-named SOX (ShutOff and Exonuclease) (Glaunsinger and Ganem 2004b). This discovery was followed by identification of host shutoff activity in EBV-infected cells mediated by the EBV gene *BGLF5* product with a high degree of homology to KSHV SOX (Rowe 2007). More recently the host shutoff in MHV-68 was also shown to be linked to the protein product of MHV-68 *ORF37* gene (Covarrubias *et al.* 2009). All three host shutoff proteins KSHV SOX, MHV-68 ORF37 and EBV BGLF5 are herpesvirus alkaline exonucleases (AE) (Glaunsinger and Ganem 2004b; Rowe 2007; Covarrubias *et al.* 2009), encoded by a gene conserved across the herpesvirus family (Sheaffer 1997) and in particular the γ-herpesvirus family (Figure 1.8). However, the product of this gene has so far only been linked to mRNA turnover within the γ-herpesvirus family (Glaunsinger and Ganem 2004b; Rowe 2007; Covarrubias *et al.* 2009). As mentioned earlier, host shutoff has been seen in members of the α-herpesvirus family through vhs protein, which is packaged into the virions (reviewed by Smiley 2004) (Table 1.5). However KSHV does not encode a homologue of vhs and it is also unlikely that there is an RNA degradative function brought in with the virion as RNA turnover does not begin until the lytic cycle is induced (Glaunsinger and Ganem 2004b). The homologue of SOX protein AE functions as a DNase and is

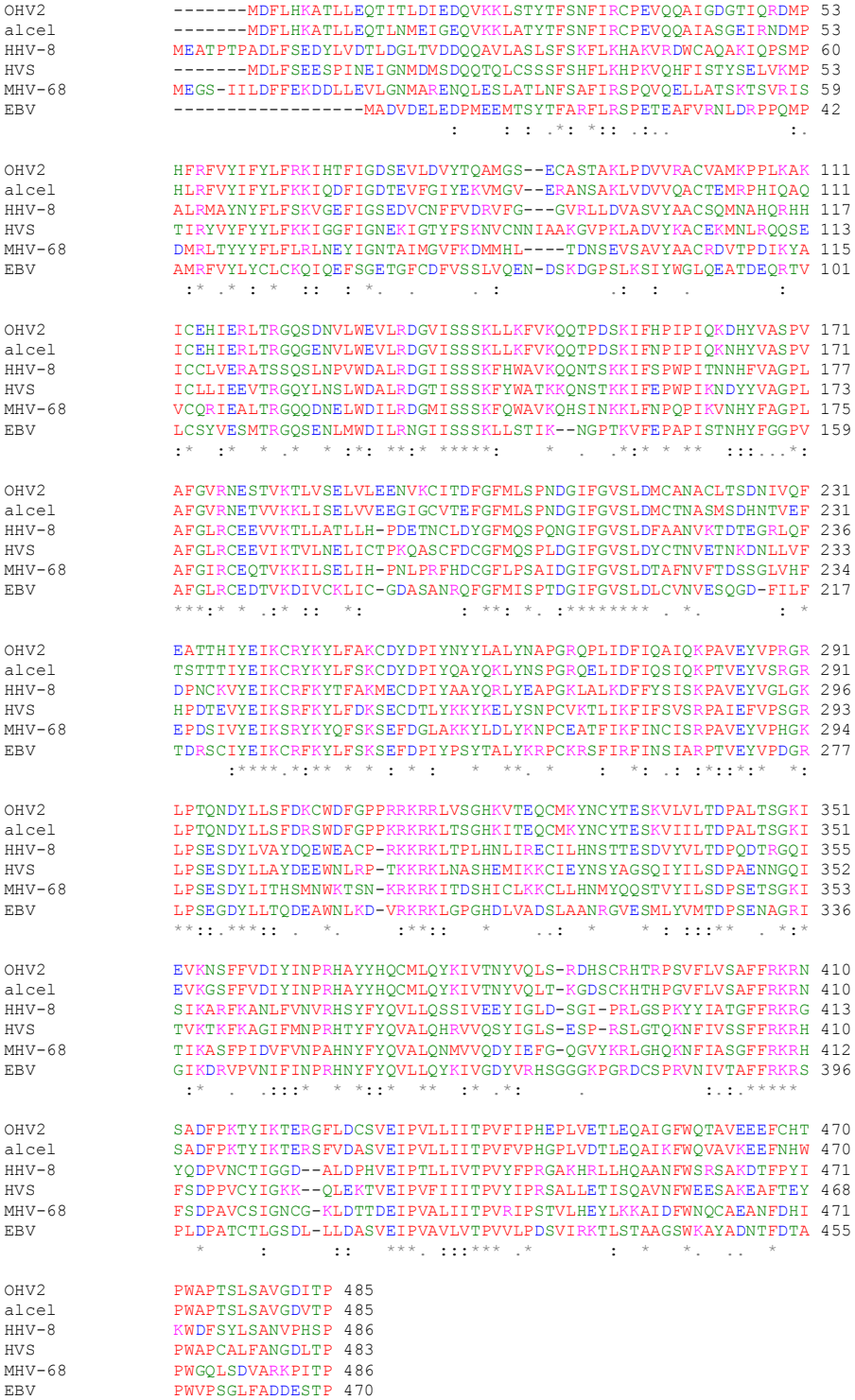

Figure 1.8 Highly conserved ORF37 homologues in γ-herpesviruses. Comparison of amino acid sequence of ORF37 protein from ovine herpesvirus, alcelaphine herpesvirus, KSHV, herpesvirus saimiri, MHV-68 and EBV.

normally involved in the packaging of the viral DNA (Martinez 1996; Goldstein and Weller 1998).

Based on sequence structures herpesvirus AE has been suggested to belong to the PD-(DE)XK deoxyribonuclease superfamily having a distant evolutionary relationship to the prokaryotic bacteriophage λ-exonuclease (Bujnicki and Rychlewski 2001). Herpesvirus AE exhibits 5'-3' exonuclease activity, which is dependent on the divalent cations Mg^{2+} or Mn^{2+}, although endonuclease activity has also been identified, but to a much lesser extent (Hoffmann and Cheng 1978; Hoffmann and Cheng 1979; Bronstein and Weber 1996; Sheaffer *et al.* 1997). Although SOX possesses *in vitro* DNase activity similar to that of HSV-1 AE, this does not explain its ability to influence host mRNA metabolism (Glaunsinger *et al.* 2005).

The obvious model for RNA turnover within cells would be that ORF37 and its homologues possess RNase as well as DNase activity. However, *in vitro* studies aimed at detecting direct RNase activity by ORF37 and its homologues have been unsuccessful (Glaunsinger and Ganem 2004b; Rowe *et al.* 2007). This has led to the hypothesis that SOX protein could possess latent or cryptic RNase activity requiring cellular cofactors for activation. Alternatively SOX protein may have no RNase activity at all and function instead to activate host mRNA degradation pathways (Figure 1.7), such as deadenylation or it may inactivate host factors that normally protect transcripts from degradation (Glaunsinger 2004). Recently the crystal structures of KSHV ORF37 and EBV BGLF5 have been elucidated, which confirmed that SOX and BGLF5 are members of the PD-(D/E)XK superfamily and

that they preferably act as 5'-3' exonucleases rather than 3'-5' exonucleases or endonucleases (Buisson *et al.* 2009; Dahlroth *et al.* 2009). Interestingly, both SOX and BGLF5 have also been found to possess RNase activity, but only in the presence of high levels of metal ions (Buisson *et al.* 2009; Bagneris *et al.* 2011). Taken together with the finding that SOX has a low affinity for binding RNA it appears that other factors may be involved in mRNA degradation. Furthermore, upon mutation of key residues that have been found to attenuate or abolish host shutoff, RNase activity was still seen suggesting that the RNase activity identified could not completely explain mRNA degradation (Bagneris *et al*. 2011). All of which points to ORF37 requiring other factors to cause mRNA degradation.

As previously discussed during HSV-1 infection, ICP27 plays an important role in host shutoff and working in conjunction with the viral vhs protein (reviewed by Smiley 2004). Similar to ICP27, the EBV homologue, SM plays a number of roles in regulating gene expression, such as acting as a nuclear export factor and facilitating export of intronless EBV mRNAs (reviewed by Swaminathan 2005). Similarly to ICP27, the SM protein may also play a role in host shutoff, as it has been found to inhibit expression of spliced mRNA transcripts (Ruvolo *et al.* 1998). Furthermore microarray analysis of the effect of SM in EBV-negative B lymphocytes has shown that the majority of cellular mRNAs were downregulated (Ruvolo *et al.* 2003). Taken together these results suggest a globally repressive effect on cellular splicing that is similar to ICP27. However how SM causes this repressive effect has not been elucidated and this along with the different roles that SM plays in gene expression means that no direct link has been made to host shutoff (reviewed by Swaminathan 2005). Alternatively it may be that SM is important for the switch from latency to

lytic infection, as EBV latent genes are spliced, hence its expression after reactivation may decrease latent gene mRNAs (Ruvolo *et al.* 1998). In contrast, the KSHV homologue of ICP27, ORF57, does not suppress the expression of most intron-containing genes and associates with components of the spliceosome to promote viral RNA splicing, which is beneficial to KSHV, as KSHV has over 30 intron-containing genes (reviewed by Majerciak and Zheng 2009).

A role of ORF37/BGLF5, would appear to be as an immune evasion mechanism. This link was first suggested for BGLF5, which was found to block synthesis of HLA class I and II molecules (Rowe *et al.* 2007). The effect of EBV BGLF5 and KSHV ORF37 on the down-regulation of HLA class I molecules was found to be enough to impair the recognition of lytic cycle antigens by virus-specific $CD8^+$ T cells (Zuo *et al.* 2008). There is a suggestion, however, that ORF37 host shutoff in KSHV is rather a blunt immune evasion strategy, as roughly one-quarter of KSHV genes encode cellular homologues or unique proteins with immunomodulatory roles. Lytic cycle immunomodulatory viral proteins, such as K15, K1 and vGPCR influence host cell survival through paracrine activity or through subversion of cell signalling pathways, which appear to be more sophisticated immune evasion strategies than host shutoff (reviewed by Rezaee *et al.* 2006). For example K15 has been found to block B- cell receptor signal transduction modulating lymphocyte signalling (Choi *et al.* 2000). Furthermore microarray experiments showed that K15 induces expression of multiple cytokines and chemokines, which play an important role in KSHV pathogenesis (Brinkmann *et al.* 2007).

Another interesting aspect of ORF37 host shutoff is cellular genes that escape shutoff. Much of the work looking at host shutoff escapees has focused on KSHV (Glaunsinger and Ganem 2004a; Chandriani and Ganem 2007; Clyde and Glaunsinger 2011) and more recently MHV-68 (Clyde and Glaunsinger 2011). Microarray experiments have indicated that over 75% of transcripts are significantly downregulated, approximately 20% decline less than two-fold, but 2% of cellular transcripts are significantly up-regulated, suggesting that there is a gradient of susceptibility (Chandriani and Ganem 2007). One of the most notable transcripts to be up-regulated is IL-6, a multi-functional cytokine which has effects on a wide range of cell types, particularly those involved in the innate and adaptive immunity. Over-expression of IL-6 has been identified in a number of proliferative diseases including MCD and PEL (Glaunsinger and Ganem 2004a; Rezaee *et al.* 2006). As previously discussed, although HSV mRNA degradation appears to be non-selective (reviewed by Smiley 2004), other studies have found evidence of selective degradation of mRNA during HSV infection based on the presence or absence of ARE sequences within the mRNA (Esclatine *et al.* 2004a). However, further studies found that vhs may induce rapid degradation of some mRNAs whilst stabilising or delaying degradation of other mRNAs and that this process is not completely reliant on the presence of AREs (Esclatine *et al.* 2004b). Interestingly, IL-6 has also found to be upregulated upon HSV-1 infection, which may highlight its importance in herpesvirus infection (Kanangat *et al.* 1996). In contrast to HSV-1 infection, Chandriani and Ganem suggested that AREs may be important for stabilisation of transcripts, as a statistically significant number of cellular mRNAs that did not succumb to virus-induced degradation contained two or more AREs in their 3' UTR. Conversely many escapees did not have AREs and some mRNAs that did have AREs

were downregulated (Chandriani and Ganem 2007). A later study that used next generation sequencing techniques did not find that the presence of an ARE sequence led to stabilisation of mRNA (Clyde and Glaunsinger 2011). It may be that the enrichment of mRNAs containing AREs is regulated by another viral protein such as kaposin B, which activates the MK2/p38 signalling pathway that inhibits ARE-mRNA decay (McCormick and Ganem 2005). One factor that did appear to determine which mRNAs were degraded was transcript abundance, as a strong correlation was seen between abundance and downregulation and furthermore overexpression of certain genes made them more susceptible to shutoff (Clyde and Glaunsinger 2011). However this theory is also imperfect as overexpression of some genes did not make them susceptible to SOX, including IL-6 (Chandriani and Ganem 2007; Clyde and Glaunsinger 2011). Taken together these results suggest that multiple mechanisms may influence SOX-mediated mRNA degradation and more work still needs to be executed to further elucidated how SOX is causing mRNA decay.

1.6 Aims

Host shutoff during lytic infection with γ-herpesviruses has been linked to the highly conserved herpesviral DNA exonucleases: ORF37/SOX in KSHV and MHV-68 and BGLF5 in EBV. The post-transcriptional loss of cellular mRNA may play an important role in modulating the host immune responses to these viruses, establishment of latency and disease progression. Thus, further understanding of how host shutoff is mediated in γ-herpesviruses undoubtedly will lead to insights into how these viruses evade immune responses, establish latency, and reactivate from latency as well as disease pathogenesis. To achieve these aims, an MHV-68 ORF37 mutant virus was constructed to study the role of ORF37 during virus lytic cycle and its role in host shutoff *in vitro* and in *vivo* and in different cellular environments. Attempts were also made to decipher how ORF37 actually mediates mRNA degradation by investigating bulk poly(A) tail length distribution.

Chapter Two

Materials and Methods

2.1 Molecular biology kits, reagents, chemicals and buffers

All molecular biology kits and reagents as well as chemicals used in this study are listed along with the manufacturer and catalogue number in Appendix B. The preparation of buffers and biological reagents are outlined in Appendix C.

2.2 Tissue Culture

2.2.1 Murine cell lines

Table 2.1 Cell lines utilized in this project

Cell line	Description
NIH3T3	Highly contact inhibited murine fibroblast cells developed from NIH Swiss embryo cultures, transformed with SV40 (Jainchill *et al.* 1969) – ATCC: CRL 1658
MEF IFNα/βRKO	Mouse embryonic fibroblasts derived from mice with an inactivated type I IFN receptor through homologous recombination (Muller *et al.* 1994).
MEF IFNαβR^{+}/$^{+}$	Mouse embryonic fibroblasts with an intact type I IFN receptor.

2.2.2 Growth and maintenance of cell lines

The mouse fibroblast cell lines NIH 3T3 and α/β-receptor knockout cells were grown in Dulbecco's Modified Eagle's Medium (DMEM) supplemented with 10% (w/w) bovine serum, 400µM L-Glutamine, 1U/ml penicillin, 2.5µg/ml Fungizone-amphotericin B and 1µg/ml streptomycin and incubated at 37ºC under a 5% CO_2 atmosphere. Cells were passaged using 0.05% trypsin along with the chelating agent

Versene-EDTA, cells were spun at 100 x *g* for 5 minutes before reconstitution in complete media.

2.3 Growth of viruses

2.3.1 MHV-68 viruses

Three viruses were used in the study namely MHV-68, ORF37Stop and ORF37StopRev. The stop mutants of MHV-68 *ORF37* were generated in collaboration with Dr Bernadette Dutia (Edinburgh University) by manipulating an MHV-68 genomic clone containing nucleotides (nt) 49951–59889 (Efstathiou *et al*. 1990). A 17 bp DNA sequence containing three stop codons and a diagnostic *Hpa*I site (DeLuca and Schaffer 1987) was inserted at nt 54157 into a PCR product spanning the Hpy99I site at nt 53949 and the SacI site at nt 54270. This product was cloned and sequenced and then inserted into the genomic clone. The mutated genomic clones were then ligated into the shuttle vector pST76_SR. The resultant plasmids were transformed into *Escherichia coli* DH10B containing the MHV-68 bacterial artificial chromosome (BAC) pHA3 (Adler *et al*. 2000). Recombinant BAC clones were produced as described (Figure 2.1) (Messerle *et al.* 1997; Adler *et al.* 2000), screened by PCR using primers spanning the region 53949-54270 followed by *Hpa*I digestion to identify mutated colonies. A revertant virus of MHV-68 ORF37Stop (termed ORF37StopRev) was made by transformation of bacteria containing mutant BAC with a shuttle vector containing the wild type genomic clone and selected by PCR in the same way. Virus stocks were produced by transfection of BAC DNA into mouse cells lacking type I interferon receptor and BAC sequences excised from the reconstituted virus by passage through cells expressing Cre recombinase (Stevenson *et al.* 2002).

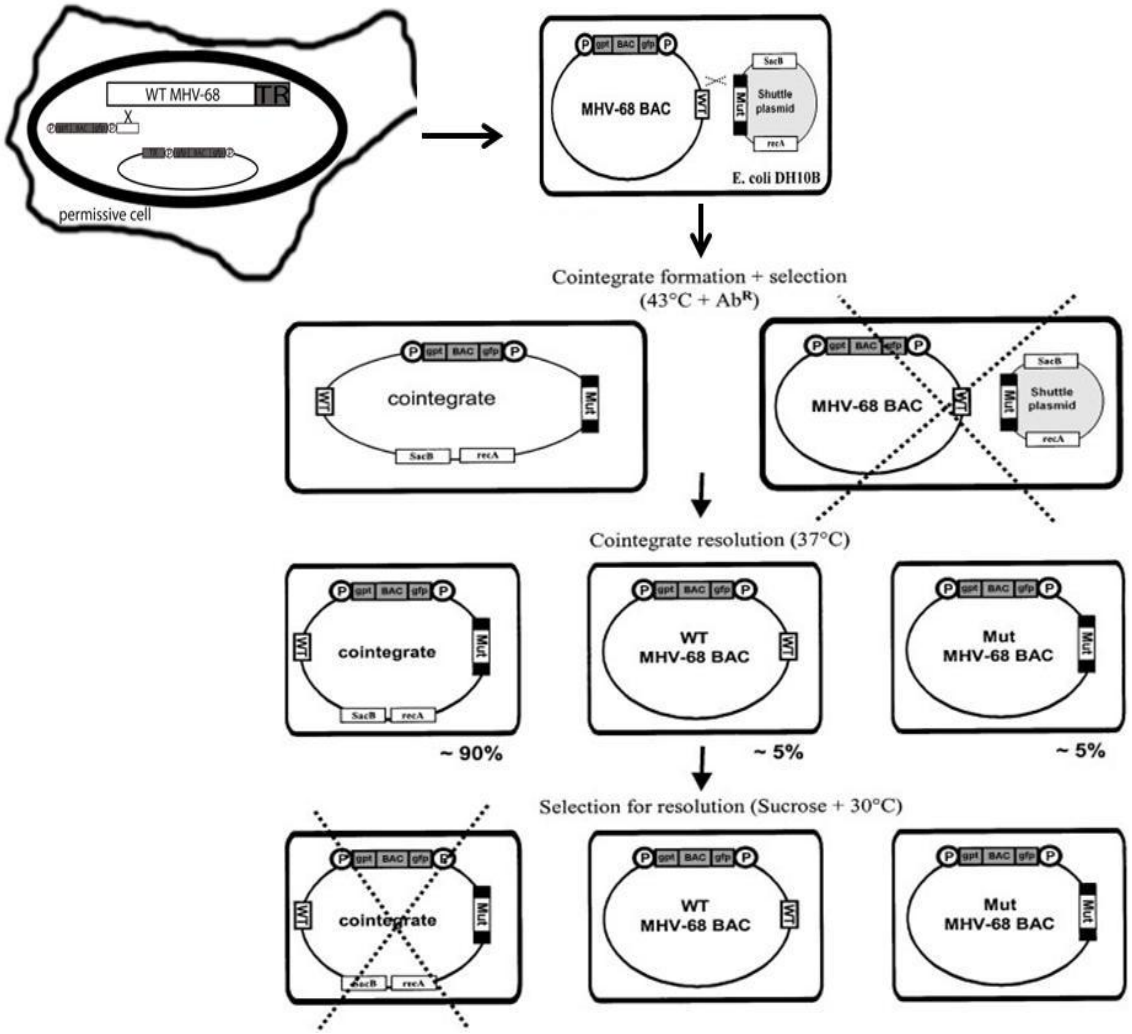

Figure 2.1 Construction of MHV-68 BAC viruses. The BAC cloned genome was generated in eukaryotic cells by homologous recombination of MHV-68 DNA with a recombination plasmid. Viral DNA and the linearised recombination plasmid were co-transfected into eukaryotic cells to generate a recombinant virus. Circular DNA of the recombinant virus genome was then isolated from cells and electroporated into the *E. coli* strain DH10B. In a first step, the shuttle plasmid carrying the desired mutation plus flanking homologies (black boxes) is transformed into DH10B. Through homologous recombination via one of the two homologies, the shuttle plasmid is completely integrated into the viral BAC genome, leading to a cointegrate. Bacteria containing the cointegrate were selected by incubation at 43°C plus both antibiotics. Bacteria harbouring a resolved cointegrate (either wildtype (WT) or mutant (Mut)) are selected at 30°C using the negative selection marker SacB together with the antibiotic whose resistance gene is encoded on the BAC (adapted from Adler *et al.* 2003).

2.3.2 Virus stock preparation

Virus was added to a 5ml volume of α/β-receptor knockout cells at a cell density of 10^7/ml to give an MOI of 0.001. Cells were then incubated at 37^{o}C with agitation for 1 hour. After the incubation period another 5ml of media was added to the cells. The infected cells were then split between 10x T175 flasks (1ml infected cells per flask) along with another of 50ml of fresh media per flask. The flasks were then incubated for 4-5 days and monitored for cytopathic effect (CPE). Cells were then harvested using a cell scraper and pipetted into 200ml centrifuge bottles and centrifuged at 3000rpm for 20 minutes at 4ºC. Supernate was discarded and the pellets were re-suspended in 3ml sterile PBS, and kept at -80ºC.

Prior to homogenization, virus stocks were thawed, poured into a 15ml dounce homogenizer and homogenized with 5x10 strokes with one minute to cool down in between each 10 strokes by placing the homogenizer on ice. The suspension was then poured into a 50ml tube and spun at 3000rpm, for 20 minutes at 4ºC. The supernate was then poured into a 50ml Falcon tube and kept on ice. Pellet was re-suspended in 1ml of sterile PBS and transferred back to homogenizer and homogenized pellet as before. Supernate was collected by spinning as before. The two supernates were then pooled into one tube, aliquoted into cryovials and kept at -80ºC.

2.3.3 Lytic virus titration

Dilutions of the virus prep were made by adding 100µl of virus prep to 0.9 ml media, which was subsequently mixed to give a 1/10 dilution. 100µl of the 1/10 dilution was then added to another bijoux containing 0.9 ml of medium, this process was repeated to give five serial dilutions. Then 4µl of each dilution was taken and placed into 4ml

media, to give final dilutions of 10^{-9}, 10^{-8}, 10^{-7}, 10^{-6}, and 10^{-5}. 200µl ($1x10^6$) of IFNα/βRKO cells were then added to each tube, mixed and placed in at 37ºC, with vigorous shaking for one hour. Two ml of each virus dilution was pipetted into tissue culture petri dishes containing 3ml media (so that each dilution was in duplicate), which were then left in a 37ºC incubator for approximately four days. The media was then removed and cells were covered with approximately 3ml formalin, which were the left for at least an hour to fix the cells. The formalin was then removed and cells were stained with 0.1% toluidine blue for roughly 40 minutes, washed and left to dry. Then the plaques were counted for each dilution using a microscope.

2.3.4 One-step growth curve

Six-well plates were seeded with $5x10^5$ cells and left to grow in 37ºC incubator overnight. Cells were then inoculated with either, mutant (ORF37Stop), revertant (ORF37StopRev) or WT (MHV68) virus at an MOI of 5. Cells were incubated for one hour to allow adsorption of virus into cells. Media containing the inocula were removed; cells were then rinsed three times with DMEM without bovine serum, followed by incubation in complete medium. At various time-points cells were removed using a cell scraper.

Viral particles were released from cells by three cycles of freeze-thaw (37ºC followed by incubation on dry ice for 30 minutes). Each virus sample was serially diluted, to give dilutions ranging from 10^{-1} to 10^{-5}. Virus titration was then carried out as described in section 2.3.3.

2.4 Isolation of protein and RNA from virus-infected cells

2.4.1 Virus infection for protein and RNA isolation

The correct amount of virus, to give an MOI of 5, was added to 3.8 ml of medium in bijoux. Into each bijou $1.5x10^6$ cells were added, they were then incubated at 37°C with constant agitation for one hour. The content of each bijou was then placed in a T25 flask and placed in 37ºC incubator until harvest time.

2.4.2 Protein isolation

To harvest total protein from cell cultures, growth medium was removed and replaced with one ml cold PBS to rinse cells. After two rinses, one ml cold PBS was added to cells and cells were scraped off the culture vessel using a disposable cell scraper. The cells were then transferred to a microfuge tube and spun at 6000rpm for 2 minutes. The supernate was removed and 50µl of cold lysis buffer (2.5ml cell extraction buffer (Invitrogen), 25µl phenylmethanesulfonylfluoride (PMSF) and 125µl protease inhibitor cocktail) was added to cell pellet. It was then placed on ice for 30 minutes, with vortexing every 10 minutes and stored at -20ºC.

2.4.3 RNA isolation

For intact monolayers the growth medium was removed and 700µl of lysis buffer (1ml RLT buffer (Qiagen) plus 10µl β-mercaptoethanol) was added. In the case where cell monolayers had become detached from the culture vessel due to virus infection, cells were harvested in growth medium in a universal tube and spun at 100x g for 5 minutes to collect the cells. The supernate was then removed. Cells were lysed by adding lysis buffer to the cell pellet. The lysates were then placed in Qiashredders and spun at 13,000rpm for 2 minutes. The samples were then transferred to microfuge tubes and stored at -70ºC.

2.5 Transient transfection assays

2.5.1 Bacterial growth cultures

Bacteria cultures were routinely plated in Luria Bertani agar (LA) and Luria Bertani broth (LB), supplemented with specific antibiotics. Agar plates were prepared with 1% LB (w/v) (Sigma-Aldrich), 1.5% agar (w/v) (Sigma-Aldrich) and 0.5% NaCl (w/v) in Millipore water. LB media was prepared with 2% LB (w/v) and 0.5% NaCl (w/v) in millipore water. The ingredients were mixed using a magnetic stirrer until dissolved and the liquid was clear and the broth/agar was divided into Duran glass bottles and autoclaved.

2.5.2 Reconstitution of plasmids from glycerol stocks

Previously constructed plasmids had been stored as glycerol stocks and kept at -80ºC. To grow up bacteria containing the plasmid of interest the tubes were removed from the freezer and placed on dry ice. Using a heated loop (allowed to cool slightly) the top of the glycerol stock was scraped off and streaked onto the first quadrant of an LB agar plate. The loop was re-heated and the following three quadrants were streaked to give single colonies. The plates were then placed in a 37ºC and left overnight.

2.5.3 Transformation of bacterial competent cells

The XL-10 Gold supercompetent cells (Agilent) were used in transformation reactions. One hundred microlitres of thawed competent cells were transferred to pre-chilled 50 ml falcon tubes and incubated on ice for 10 minutes. Fifty nanograms of plasmid DNA in a total volume of 10 µl was then added to competent cells, mixed gently and incubated on ice for a further 30 minutes. The cells were heat-shocked in

a water bath set at 42℃ for 45 seconds followed by immediate incubation on ice for 2 minutes. Pre-warmed LB (900 µl) with no antibiotics was added to the cells followed by incubation at 37 ℃, for one hour shaking at 220rpm. The mixture was then plated on LA, supplemented with the specific antibiotic. The plates were incubated overnight, at 37°C.

2.5.4 Bacterial growth for plasmid preparations

The media supplements ampicillin (100 mg/ml) and kanamycin (50 mg/ml) were stored as stock solutions. Starter cultures were prepared by inoculating 3ml LB in a universal containing 100 µg/ml of the appropriate antibiotic with a single colony from a freshly streaked selective plate. The starter cultures were then incubated at 37ºC for roughly 8 hours, shaking at 250rpm. Once the starter cultures were ready (turbid media) 200µl of the starter cultures were transferred to a 250ml flask containing 100ml LB plus 100ug/ml of appropriate antibiotic, the flasks were placed in a shaker at 220rpm in a 37 ºC incubator.

2.5.5 Endofree maxi plasmid preparations

All plasmid preparations were carried out using Qiagen Endofree Maxi Prep kits (Qiagen), following the manufacturer's instructions. In brief: RNase was added to Buffer P1. Bacterial cells were pelleted by centrifugation at 6000x*g*, for 15 minutes at 4℃ in a 250ml centrifuge bottle and then resuspended in 10ml Buffer P1 and transferred to a 50ml tube. 10ml of Buffer P2 was added and mixed thoroughly by inverting the tube 6 times, then left at room temperature for 5 minutes. 10ml of pre-chilled Buffer P3 was added and mixed immediately and thoroughly by inverting the tube 6 times. The samples were then applied to the Qiafilter cartridge and incubated at room temperature for 10 minutes, the plunger was then inserted into the cartridge,

filtering the lysate into a 50ml tube. To the lysate 2.5ml buffer ER was added and mixed via inverting the tube 10 times. This was then incubated on ice for 30 minutes. The filtered lysate was then applied to a Qiagen-tip, after it had entered the resin it was washed 2 times with 30ml buffer QBT. The flow-through was then discarded and the tip was placed into a clean 50ml tube. 15ml Buffer QN was used to elute the DNA. The DNA was then precipitated by adding 10.5ml isopropanol and spinning at 5000xg for 1 hour. The supernate was decanted off and the pellet washed in 5ml of 70% ethanol and spun as above. The supernate was again decanted off and the pellet was left to air-dry and then subsequently re-suspended in 100µl sigma water. The optical density (O.D) was measured on the NanoDrop (ND-1000) to check both quantity and purity of plasmid preparations. Vector maps of plasmids used in this study are located in appendix A.

2.5.6 Restriction enzyme digestion

Plasmid preps were digested with *EcoR I* (Roche), a restriction endonuclease which cuts double stranded DNA at 5'-G^AATTC-3' producing cohesive 5' ends. 1µg of plasmid DNA was digested with 1µl *EcoR* I in the presence of 2.5µl 10X SuRE/Cut Buffer H along with water to give a final volume of 25µl. The mixture was then incubated at 37°C for 1 hour. The uncut and cut plasmid DNA was then visualised using gel electrophoresis to check the size of the plasmid and to indicate the presence of contaminating genomic DNA.

2.5.7 Transient transfection assay

Cells were trypsinised and then counted using a haemocytometer. Following this the cells were diluted to give a cell density of $1.5x10^5$cells/ml and 1ml of the cell dilution was seeded into each well of Nunc 6-well plates. Cells were then incubated

overnight at 37°C under 5% CO_2 atmosphere in complete growth media. The following day cells in each well were transfected with 4µl of appropriate plasmid (1µg/µl) in 625µl Opti-MEM added to 8µl Lipofectamine 2000 in 242µl OptiMEM the mixture was then incubated at room temperature for 20 minutes before 500µl was added to each well. During each transfection experiment one of the wells was transfected with pEGFP-NI so that the transfection efficiency could be monitored via visulation of GFP in transfected cells. The cells were incubated for 6 hours at 37ºC under a 5% CO_2 atmosphere. After 6 hours the medium was taken out of each well and cells were washed with 1ml Opti-MEM before 3ml Opti-MEM with 10% bovine serum was added to the well and the plate was placed back into incubator. At 24 hours post-transfection medium was changed to 3ml complete medium. The cells were then harvested at different time points using the methods described in sections 2.4.2 and 2.4.3.

2.6 Diagnostic PCR to check virus stocks

Diagnostic PCR reactions were carried out in 50µl volumes. Each reaction contained 0.5U of Platinum *Taq* DNA Polymerase (Invitrogen), 200nM of each oligonucleotide primer, 1x PCR buffer (20 mM Tris HCl, 50 mM KCl), 1.5mM $MgCl_2$ and 200µM Nucleotides (dATP, dCTP, dGTP and dTTP). All the primers were supplied by Sigma-Genosys or MWG-Eurofin and stored as stock solutions at 100µM at -20°C. A master PCR mix was prepared with above concentrations and 44µl of the master mix was aliquoted into 0.2ml microfuge tubes to which one µl of virus stock (or water in case of negative controls) was added along with one µl of 10mg/ml proteinase K (10µg). This was then heated at 65°C for 10 minutes before the enzyme

was inactivated by heating at 95℃ for 5 minutes. Taq polymerase was then diluted 1 in 5 in 1x PCR buffer and 5 µl of the diluted Taq was added to the PCR master mix. The PCR was run using the standard PCR amplification program, which consisted of an initial denaturation step at 95℃ for 5 min, followed by 35 cycles of denaturation at 94℃ for 1 min, annealing at a suitable annealing temperature, which in this case is 60℃ for 1 min, and primer extension at 72℃ for 1 min. Plus a final extension step of 5 min at 72℃. The Opticon 2 thermal cycler (BioRad) PCR machine was used for amplifications.

Table 2.2 Oligonucleotide primers used for diagnostic PCR and Southern blot probe.

Primer name	Primer sequence	Amplicon size (bp)	Annealing temperature (°C)
ORF37StopFA	GACATCGACGGAGGAAGCAG	340*	60
ORF37StopRB	GTCTTTGATGTTGCC AGGAG		
ORF37F652	CTGGACACTGCT TTCAATGTG	461	60
ORF37R55,221	GTAGTTGTGTGCAGGATTCAC		
5'b-actin	ACCCTAAGGCCAACCGTGAA	897	53.2-59.4
3'b-actin	AAACAAAGCCATGCCAATGT		

* If fragment contains 17bp insertion would expect a fragment size of 357bp

2.6.1 Validation of viral diagnostic PCR through restriction enzyme digestion

Following diagnostic PCR protocol, PCR products from MHV68, ORF37Stop and ORF37StopRev were digested with *Hpa*I (Roche), a restriction endonuclease which cuts double stranded DNA at 5'-GTT^AAC-3' producing blunt ends. 15 µl of PCR

product was digested with 1µl *Hpa*I in the presence of 2.5 µl 10X SuRE/Cut Buffer A and 6.5µl of water the mixture was then incubated at 37°C for 2 hours.

2.7 Preparation of cDNA for reverse transcription (RT)-PCR amplification

RNA extraction was performed using the RNeasy mini kit (Qiagen) along with the Qiagen RNase-free DNase kit following the manufacturer's instructions, in brief: RNA samples isolated from cells were defrosted and 1 volume of 70% ethanol was added and mixed well by pipetting. 700µl of the sample was added to an RNeasy spin column placed in a 2ml collection tube. Tubes were centrifuged for 15 seconds at 8000 x g (10,000 rpm) and the flow-through was discarded. Buffer RW1 (350 µl) was added to the RNeasy spin column and was centrifuged for 15 seconds. Following each centrifugation step the flow-through was discarded and unless otherwise stated all centrifugation steps were at 8000 x g (10,000 rpm). Then 10µl DNase I stock solution was added to 70µl Buffer RDD, which was subsequently pipette directly onto the RNeasy spin column membrane, and place on the benchtop (20–30°C) for 15 minutes. The spin column was then washed by adding 350µl Buffer RW1 and centrifuging for 15 seconds. Then 500µl buffer RPE was added to the RNeasy spin column and centrifuged for 15 seconds to wash the spin column. The column was then washed a second time in the same way as above, but this time the sample was spun for 2 minutes, to ensure that no ethanol is left in RNA sample. The RNeasy spin column was then placed in a 1.5ml microfuge tube and 50µl Sigma water was added directly to the spin column membrane, and centrifuged for 1 minute to elute the RNA. RNA concentration was measured using the Nanodrop (ND-1000) spectrophotometer.

cDNA was then synthesised using the following protocol. Initially, a mixture was made that consisted of 2µg of RNA, 1µl random primers (250ng), 2µl dNTPs (5mM) made up to 13µl with Sigma water. The reaction mixture was heated at 65^{o}C for 5 minutes and snap-cooled on ice for 5 minutes before a brief spin. To the mixture, four µl of first strand synthesis buffer was added along with two µl 0.1M DTT. The contents were gently mixed and incubated at 42^{o}C for two minutes. To the mixture one µl of SuperScript II was added and mixed by repeated pipetting before it was incubated at room temperature (25^{o}C) for 10 minutes. The contents were then incubated at 42^{o}C for two hours before it was inactivated by heating at 70^{o}C for 15 minutes. The temperature was then decreased to 37^{o}C for 10 minutes. After the contents had been spun briefly one µl of RNAse H was added, and incubated at 37^{o}C for 20 minutes. For each RNA preparation, a control reaction lacking the reverse transcriptase was also prepared.

2.7.1 Quantitative PCR (qPCR)

Quantitative PCR reactions were carried out in 20µl volumes. Each reaction contained 1 U of Platinum *Taq* DNA Polymerase, 500 nM of each oligonucleotide primer, 1x PCR buffer (20 mM Tris HCl, 50 mM KCl), 2.5 mM $MgCl_2$ and 200 µM nucleotides (dATP, dCTP, dGTP and dTTP), and one µl of cDNA. In addition, one µl of 10x SYBR green, one µl 3% Triton X-100 (v/v) and 0.4µg of BSA were also added to each reaction. All the primers used are listed in table 2.2 and were supplied by Sigma-Genosys or MWG-Eurofin and stored in a stock solution of 100µM at -20°C.

The qPCR amplification program consisted of an initial denaturation step at 95°C for 10 seconds, annealing at a gene-specific annealing temperature for 20 seconds, and primer extension at 72°C for 15 seconds. A final step of one second at 75°C was introduced to melt off any possible primer dimer formations before fluorescence readings were taken. To ensure only the fluorescence signal from the intended product was detected for cycle threshold (ct) calculations, melting curve analysis was performed at the end of each PCR reaction by melting the PCR products from 65°C to 95°C, with 0.2°C increments, with each temperature held for one second. The Opticon 2 thermal cycler (Bio-Rad) PCR machine was used for amplifications.

Where possible, absolute quantification of PCR products were performed by constructing standard curves using templates listed in table 2.4. The standards were serially diluted to give copy numbers ranging from $1x10^{11}$ to $1x10^{5}$ and PCR amplified in the same way as described above. Where absolute quantification was not feasible, the Pfaffl equation was used (Pfaffl 2001), which gives a ratio that takes into account both the efficiency and Ct value of the reaction:

$$\text{Ratio} = \frac{(E_{target})\ \Delta Ct\ \text{target (control-treated)}}{(E_{ref})\ \Delta Ct\ \text{ref (control-treated)}}$$

2.7.2 Oligonucleotide primers and templates for qPCR

Oligonucleotide primers used for qPCR assays are shown in Table 2.3 and templates used for qPCR standard curves are listed in Table 2.4.

Table 2.3 Oligonucleotide primer forward and reverse sequences and the optimum range of annealing temperatures.

Gene	Primer name	Primer sequence	Annealing temperature (°C)
c-fos	c-fosRT5' c-fosRT3'	GTCCGGTTCCTTCTATGCAG GGTGACCACGGGAGTACACA	59.4-61.4
cyclophilin	cyclophilinRT5' cyclophilinRT3'	GGATTTGGCTATAAGGGTTC CTGCCGCCAGTGCCATTATG	55.3-61.4
eEf_Tu	5'RTeEf_Tu 3'RTeEf_Tu	GTCACACAGCCCACATAGCA CGCCAGACTTCAGGAACTTG	59.4
18s rRNA	5'RT18SrRNA 3'RT18SrRNA	CATTGGAGGGCAAGTCTGGT CCCAAGATCCAACTACGAGC	59.4
β-actin	5'b-actin 3'b-actin	ACCCTAAGGCCAACCGTGAA AAACAAAGCCATGCCAATGT	53.2-59.4

Table 2.4 Gene templates used for producing qPCR standard curves.

Gene	Template sequence
c-fos	GTCCGGTTCCTTCTATGCAGCAGACTGGGAGCCTCTGCA CAGCAATTCCTTGGGGATGGGGCCCATGGTCACAGAGCT GGAGCCCCTGTGTACTCCCGTGGTCACC
cyclophilin	GGATTTGGCTATAAGGGTTCCTCCTTTAGAATTATTCCAG GATTCATGTGCCAGGGTGGTGACTTTACACGCCATATTG GCACTGGCGGCAG
eEf_Tu	GTCACACAGCCCACATAGCATGCAAGTTTGCTGAGCTTA AAGAAAAGATCCATCGTCGTTCTGGTAAGAAGCTGGAA GATGGCCCCAAGTTCCTGAAGTCTGGCG
18s rRNA	CATTGGAGGGCAAGTCTGGTGCCAGCAGCCGCGGTAATT CCAGCTCCAATAGCGTATATTAAAGTTGCTGCAGTTAAA AAGCTCGTAGTTGGATCTTGGG

2.8 Diagnostic PCR for plamid preps

All reaction were carried out in 20µl volumes using the same reaction mixture as the one stated in section 2.6, but without the addition of SYBR green, triton X-100 or BSA. The primers used are listed in table 2.2 and reactions were amplified using the same parameters stated in section 2.6.

2.9 Agarose gel electrophoresis

PCR products were resolved on 2% (w/v) agarose gels in 1X TAE Buffer. A size marker (Generuler DNA Ladder mix) was used on every gel throughout the project. Five µl of 10mg/ml ethidium bromide was added to 100 ml of agarose prior to pouring the gel. Unless stated otherwise, 10 µl of sample were mixed with 2µl of 6x loading dye (Fermentas) and the mixture was loaded into the wells of the gel. Plasmid DNA was run on 1% (w/v) agarose gel in the same way as described above. The gels were viewed under UV transillumination at a wavelength of 302 nm and images recorded using GeneSnap software (Syngene).

2.10 Sequencing

Sequencing was provided by Cogenics. Samples were prepared according to specifications provided by Cogenics, labelled with the respective codes and sent together with respective forward and reverse primers to Cogenics. Sequencing output was aligned using the BioEdit programme to compare sequences and check for insertion sequences.

2.11 Southern Blot

2.11.1 Isolation of viral genomic DNA for Southern blot hybridization

An appropriate amount of virus stock to give approximately $5x10^7$ pfu was added to a 38.5ml Beckman Ultracentrifuge tube, which was filled with media and were then spun in the Beckman Ultracentrifuge, SW28 rotor at 20,000 x g (11,000rpm) for two hours at 4^oC to pellet the virions. Media was removed and 400 µl of lysis buffer was added to the pellet, which was then incubated at 53^oC overnight. DNA was extracted with an equal volume of phenol/chloroform. Mixed gently by inversion of tube and then incubated at room temperature for 10 minutes followed by centrifugation at 13,000rpm for 10 minutes, then the top (aqueous) layer was carefully pipetted off. The phenol/chloroform extraction was then repeated two further times. Then DNA was extracted from the aqueous phase with an equal volume of chloroform and mixed gently by inversion of the tube. The samples were then incubated at room temperature for 10 minutes and centrifuged for 10 minutes at 13,000rpm and subsequently the top layer was removed. To the remaining DNA pellet 1/3 volume of ammonium acetate (7.5M) was added followed by two volumes of 96% ethanol, which was then mixed gently and left at -20^oC overnight. The following day the solution was spun at 13,000rpm for 10 minutes. Then carefully decanted off the waste supernate leaving the DNA pellet, to which 100µl of 70% ethanol was added to wash the pellet. After a further centrifugation at 13,000rpm for 15 minutes the supernate was removed and the pellet was left to air-dry for 10 minutes. DNA was re-suspended in 50µl of pure sterile water.

Restriction enzyme digests were carried out on viral genomic DNA in a similar way described in section 2.6.1.1. Digests were carried out in 40µl reactions, which

contained approximately 1U of the restriction enzyme *Hpa*I (Roche), and 1µg of DNA. Reactions were incubated at 37^{o}C overnight.

2.11.2 Southern blotting

Samples were dry-loaded and run on a 0.8% (w/v) gel in 1 x Tris/acetate/EDTA (TAE) buffer and run at 80V for 10 minutes. The gel was then completely submerged with running buffer and run at 60V for 4 hours. The gel was then washed in denaturing solution with gentle agitation for 30 minutes. This was followed by 2 x 30 minute washes in neutralisation solution. The transfer apparatus consisted of an electrophoresis tank partially filled with 10X SSC, with a long strip of 3MM filter paper trimmed to fit the width of the gel. One sheet of nylon membrane was then briefly soaked in ddH_2O and then in 2X SSC solution. The gel was rinsed in ddH_20 and placed on the tank. The nylon membrane was then placed onto the gel. The 3MM papers (same size as membrane) were then soaked and drained each in 2X SSC and placed on the membrane. Then a stack of paper towels were placed onto the membrane/filter stack along with a weight to facilitate transfer and left overnight. The following day the membrane was placed between two 3MM filter papers and oven-baked for 30 minutes at 120^{o}Cbefore being left to air dry at room temperature for 30 minutes.

2.11.3 Radio-labelling of DNA probes

A PCR product corresponding to 340bp fragment of ORF37 was used to generate radiolabelled probes. The 340bp fragment was amplified from MHV-68 WT virus stock using primers ORF37StopFA and ORF37StopRB listed in table 2.2 using the

PCR protocol detailed in section 2.6.1. The PCR product was then resolved on a 1% TAE low-melting point gel (microsieve). The DNA band corresponding to 340bp was cut out and DNA extracted using the Qiaquick Gel extraction kit (Qiagen) following the manufacturer's instructions. The purified PCR product was eluted in sterile water and the concentration was determined using the Nanodrop (ND-1000) spectrophotometer. Approximately 49ng of purified amplified DNA was made up to a volume of 45µl in Tris/EDTA (TE) buffer, which was subsequently denatured by heating at 100^{o}C for 2 minutes then placed immediately on ice. The denatured DNA was then added to Ready-to-go DNA labeling beads (Amersham) along with 5µl α-^{32}P dCTP (Perkin-Elmer), which was mixed by gentle pipetting. This was then incubated for 20 minutes at 37^{o}C. Prior to use, the probe was denatured at 100^{o}C for 2 minutes and then placed on ice. The probe was used within one week of synthesis.

2.11.4 Hybridisation and detection of nucleic acids

The blot was placed in a Techne hybridization tube along with 10 ml of pre-warmed (68^{o}C) Ultrahyb solution and incubated for 30 minutes at 42^{o}C in the hybridization incubator. Approximately, 15µl of probe was then added to the hybridization tube and left to hybridise overnight at 42^{o}C. The hybridization mix was decanted and the blot was washed 2x5 minutes with wash buffer 1 at 42^{o}C. This was followed by 2x15 minute washes with wash buffer 2 at 42^{o}C. The blot was then removed from the hybridization tube, covered with cling film and placed in a cassette with a PhosphorImager screen, which was left overnight and then scanned the following day. The PhosphorImager system is a quantitative imaging device, which is 15-250-fold more sensitive than x-ray when used to detect ^{32}P (Johnston *et al.* 1990).

2.12 Protein Assay

Total protein quantification of each sample was determined through the Bradford assay. Either immunoglobulin G or bovine serum albumin were used as standards (1 mg/ml to 31.25 µg/ml), prepared in 20µl of water. Each sample was subjected to two serial 2-fold dilutions, in 20µl of water. Samples were vortexed and spun down in between dilutions. Each of the samples and standards were added to 1ml of Bradford reagent, briefly vortexed and incubated at room temperature for 5 minutes. Absorbance of samples was measured in triplicate at 595 nm; the average of each standard was determined and used to plot a calibration curve. Samples absorbance was averaged and total protein concentration calculated using the calibration curve. A new calibration curve was determined for each assay.

2.13 Western blotting

2.13.1 SDS-PAGE

Glass plates were cleaned with ethanol and Biorad western blotting apparatus was assembled following manufacturer guidelines. Resolving gel was made, which consisted of a 10% (w/v) acrylamide concentration, to resolve proteins between 20-80kDa. After each component was added the glass universal was inverted gently to mix. Gel mix was added to each plate set, leaving sufficient room for the stacking gel, the gel was then overlayed with 100% ethanol and left to set. A 5% stacking gel was then made, again after adding each component the glass universal was inverted to mix. Once the resolving gel had set the plates were inverted to remove ethanol and then the stacking gel was pipetted on-top of resolving gel. The combs were inserted and the gel was left to set.

Once the gel had set the combs were removed and the wells were rinsed out with RO water. The gel was then mounted in the electrophoresis cell (gel facing inwards). The wells were then filled up with 1xSDS-PAGE running buffer and then 20-40µg of protein for each sample was added per well. The SDS-PAGE (1x) running buffer was poured into the inner buffer compartment covering the wells and then the rest of the running buffer was poured into the outer compartment. The gel was then run at 40mA (200V) at a constant current for 30-40 minutes until the dye front migrated off the end of the gel. Apparatus was dismantled and the glass plates were gently prised apart using the plastic wedge. Then using the sharp end of the wedge the stacking gel was removed from the main gel.

2.13.2 Sample preparation

An equal volume of 2x sample buffer (Appendix C) was added to each protein sample to give a final 1x concentration of sample buffer. The sample was then heated at 95°C for 4 minutes and then spun for 30 seconds to pellet any debris or insoluble precipitate.

2.13.3 Protein transfer to membranes

The Hybond-P membrane was cut to the size and pre-wetted in RO water. The membrane was then equilibrated in transfer buffer for 15 minutes. Then the gel was soaked in the above mentioned transfer buffer for 15 minutes along with 4 pieces of thin filter paper to pre-wet. Two sheets of filter paper were placed on the anode of the Bio-Rad Transblot semi-dry transfer cell and the membrane was placed on the top. The gel was placed on top of the membrane and then sandwiched between two more pieces of filter paper. The cathode was then placed on top of the stack and the

latches engaged. Once the plastic safety cover was on the transfer cell was plugged into the power supply and transfer took place at 10V for one hour. Efficiency of transfer was assessed by staining the transferred gel in Coomassie blue.

2.13.4 Colourmetric detection of blotted proteins

Following transfer, the membrane was rinsed in 20ml of TBS (1 x Tris-Buffered Saline) for 2 minutes and then blocked in 10 ml of blocking buffer for one hour at room temperature or overnight at 4ºC. The membrane was then incubated in the first antibody, which was either rabbit anti-βactin (Abcam), rabbit anti-myc or mouse anti-penta His (Qiagen) in 10ml antibody dilution buffer at room temperature for one hour with gentle agitation. The membrane was then washed 3 x 5 minutes with wash buffer. The second biotinylated antibody, goat anti-rabbit (Vector labs) or rabbit anti-mouse (Sigma) was then added to the membrane and left at room temperature for one hour with gentle agitation. Approximately 15 minutes before the end of incubation with the second antibody, the ABC Vectastain solution (Vector labs) was prepared: to 10ml of 1 x PBS, 2 drops of solution A were added followed by 2 drops of solution B the solution was mixed by inverting the tube a few times. The membrane was then washed in 1x PBS (3 x 5 minutes). The ABC complex was added to the blot and agitated for 30 minutes before it was rinsed in PBS (3 x 5 minutes). The membrane was then incubated in 100mM Tris-HCL pH 9.5 for 10 minutes with agitation. The BCIP/NBT solution (Vector labs) was then made 5 minutes before use, the solution was mixed well following the addition of each reagent: to 5ml 100mM Tris-HCL pH 9.5, 2 drops of reagent 1, 2 drops of reagent 2, 2 drops of reagent 3 and 1 drop of levamisole were added. The NBT substrate mix was added to

the membrane with constant agitation and the colour development was monitored. The substrate solution was decanted and water added to the blot to stop the reaction.

2.13.5 Enhanced chemiluminescence (ECL) detection of blotted proteins

After transfer from gels, the ECL (nitrocellulose) membrane was rinsed in TBS (1 x Tris-Buffered Saline) for 2 minutes and then blocked in 10ml of blocking buffer for one hour at room temperature or overnight at 4ºC. The membrane was then incubated in the first antibody, which was either rabbit anti-βactin (Abcam) or mouse anti-penta His (Qiagen) in 10ml antibody dilution buffer at room temperature for one hour with gentle agitation. The membrane was then washed 3x 5 minutes with wash buffer. The second HRP-conjugated antibody, ECL anti-rabbit (GE Heathcare) or anti-mouse HRP-linked was then added to the membrane and left at room temperature for one hour with gentle agitation. The membrane was then washed as stated above and the Immobilon Western chemiluminescent HRP substrate (Millipore) was prepared just prior to use, by mixing equal volumes of the two reagents in a universal. Excess wash buffer was drained from the membrane and then 3ml of the ECL reagent was applied, covering the membrane, which was then left for 5 minutes. After draining excess ECL reagent from membrane, it was placed on a glass plate and wrapped in cling film. The blot was then placed in an X-ray film cassette and in the dark room Amersham hyperfilm-ECL (GE Healthcare) was placed onto blot and exposed for between 30 seconds and 10 minutes, then placed in developer. After approximately 30 seconds the film was rinsed in running water for one minute and then into fixer for 5 minutes and again rinsed in running water and finally hung to dry.

2.14 *In vivo* infection

2.14.1 Infection

Groups of αβRKO female mice were inoculated intranasally with 4 x 10^5 pfu MHV-68, ORF37Stop or ORF37StopRev virus. Approximately 40µl of virus was administered intranasally to lightly anaesthetized (halothane anaesthesia) mice. After three days and six days post-infection mice were euthanised following Schedule 1 procedures using CO_2. Lungs, spleens and mediastinal lymph nodes (MLN's) were harvested and kept at -80 ºC (Dutia *et al.* 1999).

2.14.2 Harvesting and homogenisation of organs for virus titration

Using a sterile disposable blade, one of the lobes of the lung was removed and placed into a cryovial for further work. The rest of the lung was left to thaw completely on ice. Once thawed the lung tissue was placed into a glass homogenizer. Tissues were homogenised with 10 strokes in the homogeniser and then allowed to cool down for 2 minutes on ice. This process was repeated until no large tissue fragments could be seen by the naked eye. The debris was allowed to settle in the homogenizer. Using a long neck glass Pasteur pipette, the clear supernate was removed placed in a cryovials and kept at -80ºC.

2.14.3 Titration of virus isolated from organs

Lung homogenates were freezed-thawed twice to disrupt any remaining intact cells and to facilitate the release of virus particles. This entailed samples being placed on dry ice for 10 minutes, before thawing in a 37^{o}C water bath for 2 minutes. This cycle was repeated once more and the tubes were then spun at 3000rpm for 5 minutes. The virus preparation was then serially diluted by adding 440µl of the supernate to 4 ml

of medium, giving a 1 in 10 dilution. 440µl was then taken and placed in a tube containing 4 ml of medium to give a 1 in 100 dilution. This process was repeated up to the 10^{-6} dilution. 440µl was removed fromthe last dilution and discarded. To each dilution, 200µl of cells (1×10^6) was added and tubes were placed on a shaker (300rpm) at 37°C for one hour. From each bijou tube, two ml was removed and added to a 60 mm Petri dishes. Each preparation resulted in two Petri dishes (duplicated plates). Each Petri dish was topped up with three ml of fresh medium to bring up the total volume in each dish to 5ml. A control was set up which consisted of two petri dishes with cells only. Dishes were left in the incubator for four days, fixed with formaline and then stained with 0.1% toluidine blue. Finally, plaques were counted and the pfu/ml calculated.

2.15 mRNA Poly (A) tail Assay

2.15.1 Labelling of poly (A) tails

Poly (A) tail labelling was carried out using a reaction master mix which consisted of 4µl 5X Poly (A) buffer, 0.33µl Poly (A) enzyme (<100 units), 1µl [α-32P]dATP (10µCi) made up to a total volume of 10µl with sigma water. The master mix was added to 10 µl of RNA (5µg), mixed by pipetting and then incubated at 37 °C for one hour. Following the incubation period 30µl of water was added to bring up the volume to 50µl. Then 50µl of phenol/chloroform was added, mixed by vortexing and spun for 5 minutes at room temperature. The upper aqueous phase was transferred into a new tube and 50µl of chloroform was added, mixed by vortexing and microfuge spun for 5 minutes at room temperature, the upper aqeuous phase was then removed. Ethanol precipitation was then carried out using 0.3 volume of NaAc (3M, pH 5) and 2.5x volume of 100% ethanol. The mixture was inverted several

times and incubated at -20°C overnight. The following day, samples were spun for 15 minutes at RT and the supernate was removed. The pellet was rinsed in 100µl of 70% ethanol and spun for 5 minutes at room temperature. After removing the alcohol, pellets were allowed to air dry for 15 minutes before being re-suspended in 20 µl of Sigma water.

To make sure equal amunts of labelled RNA were used in subseqauent steps, labelling efficiency was measured by a scintillation counter. For this, two µl of each sample of labelled RNA was added to two ml of scintillation liquid and counted. From the counts, the volume giving one million counts was determined for the next step. One million cpm counts of each RNA sample were then added to the RNA digestion master mix (two µl 10X RNaseA/T1 buffer, four µl of yeast tRNA (5 µg/µl), two µl of RNaseA/T1) in a total volume of 20µl. The reaction mix was placed on ice until further use.

The samples were incubated at 30°C for 30 minutes. The RNA digestion was stopped using a stop solution (appendix C), which was added to the RNA and incubated at 37°C for 30 minutes. Following this step the samples were ethanol precipitated and pellets dried as above. Dried pellets were re-suspended in five µl of water. Samples were kept at -20C until ready to run on acrylamide/urea gel.

2.15.2 Preparation of denaturing gels to resolve poly(A) tails

Labelled poly(A) RNA was separated on 10% polyacrylamide/urea gels using a Bio-Rad Sequi-Gen GT sequencing apparatus. Initially the glass plate were cleaned using water and ethanol, the bottom plate was then wiped with Sigmacoat silicon (Sigma)

and left for 5 minutes, following which the plate was cleaned with ethanol. The gel apparatus was then assembled and a shark-tooth comb was placed in between the the glass plates. The 10% gel mixture (appendix C) was prepared and then added to the glass plates using a syringe, ensuring that there were no bubbles in the gel. The gel was then left to set for a couple of hours wrapped in cling fim overnight.

2.15.3 Running of poly (A) tail gels and visualisation of bands

Once the gel had set the Bio-Rad Sequi-Gen GT sequencing apparatus was assembled with 0.5x TBE as the running buffer. The gel was pre-heated to approximately 40^{o}C. Then one µl gel loading buffer (Ambion) was then added to each labelled RNA sample before loading into the gel. Gels were then run at 2000v for one to two hours (depending on separation). Gels were removed from glass plates using 3MM filter paper and dried at 80^{o}C for one hour. Once the gel had dried it was placed against a PhosphorImager reactive screen and left overnight. The screens were then scanned using the PhosphorImager and data were analyzed with the ImageQuant.

Chapter Three

Characterising the growth of an ORF37Stop mutant MHV68

3.1 Introduction

Recent evidence has demonstrated a central role for the *ORF37* gene product in mediating loss of cellular transcripts in KSHV and MHV-68 infections and for the EBV homologue BGLF5 (Glaunsinger and Ganem 2004b; Rowe *et al.* 2007; Covarrubias *et al.* 2009). The first study to address the question of how host shutoff within the γ-herpesvirus family may be mediated was demonstrated in KSHV-infected cell lines by Glaunsinger and Ganem in 2004, using a GFP screening method. This entailed transfection of a GFP expressing cell line with each of the selected viral genes. Cells were sorted by flow cytometry to identify viral gene(s) whose expression caused reduced or loss of GFP expression. This screening approach demonstrated that a single viral gene product caused a significant loss of GFP. This gene product was encoded by KSHV *ORF37* (Glaunsinger and Ganem 2004b). This was followed by similar observations in MHV68 (Covarrubias *et al.* 2009) and EBV (Rowe *et al.* 2007).

Over the last few years, much work has been undertaken to characterise the *ORF37* gene product, however, progress has been impeded by the inability of producing viable *ORF37* mutant viruses, which proved difficult to grow and yield infectious virus progeny (Covarrubias *et al.* 2009; Feederle *et al.* 2009). The EBV mutant virus ΔBGLF5, was produced using homologous recombination to substitute part of the BGLF5 gene with a gene which encodes for kanamycin resistance. It was observed that this virus did not replicate efficiently and quantitative assays looking at the viral

genome levels showed a 17 to 21-fold decrease in viral genome copies present in cells infected with the mutant EBV virus (Feederle *et al.* 2009). In another study, a deletion mutant of MHV-68 *ORF37* was constructed using allelic exchange (Covarrubias *et al.* 2009). Similar to the EBV study, the MHV-68 *ORF37* mutant virus was also unable to yield infectious progeny (Covarrubias *et al.* 2009). More recently, Richner *et al.* have produced another MHV-68 ORF37 mutant virus R443I, which has a single amino acid substitution, within a domain which they believe to be linked to host shutoff (Richner *et al* 2011). They found that on a murine fibroblast cell line, R443I was able to replicate to similar levels as MHV-68 and their marker rescue virus. They suggest that the reason for the mutant being able to replicate is due to the DNase function of ORF37 still being intact and so allowing the normal viral DNA packaging to take place. However some cellular mRNA degradation was still seen with this mutant virus, which may be due to incomplete inactivation of the host shutoff function (Richner *et al.* 2011). The different approaches used to produce ORF37 mutant viruses (Covarrubias *et al.* 2009; Feederle *et al.* 2009; Richner *et al.* 2011) along with the possible problems associated with them indicates (Richner *et al.* 2011) the need for further study of ORF37 mutant viruses to further elucidate its importance during infection.

3.2 Experimental design

The experimental approach undertaken in this chapter was aimed at investigating the growth characteristics of an engineered MHV-68 ORF37 mutant (ORF37Stop) and its corresponding revertant, ORF37StopRev *in vitro* and *in vivo*. This strategy involved the infection of the mutant, revertant and WT viruses on cell lines aswell as infection in mice. Growth characteristics were investigated using plaque assays to

ascertain if the mutant virus would follow a similar infection path to the revertant and WT viruses. The viruses were engineered in collaboration with Dr Bernadette Dutia (Edinburgh University) using BAC technology (see Chapter 2.3.1 and Figure 2.1).

3.3 Results

3.3.1 Construction of MHV-68 ORF37 mutant and revertant viruses

To produce an ORF37Stop mutant virus a 17bp sequence, which contained three stop codons along with a restriction enzyme cut site for *Hpa*I was inserted at the beginning of ORF37 at nt 54157. The 17bp sequence was inserted into a PCR product spanning the Hpy991 site at nt 53949 and the SacI site at nt 54270 (Figure 3.1A). After the ORF37Stop and ORF37StopRev viruses had been produced (see chapter 2.3.1) a Southern blot was carried out to check for presence of the mutation in the viral genomic DNA using a probe encompassing nt 53949-54270 (Figure 3.1B). After RE digest the mutant virus was expected to cut the probed area into two fragments for the ORF37Stop virus, but would yield just one fragment from the ORF37StopRev virus. Figure 3.1B shows the Southern blot which confirmed that the mutation had been inserted into ORF37 and at the correct position.

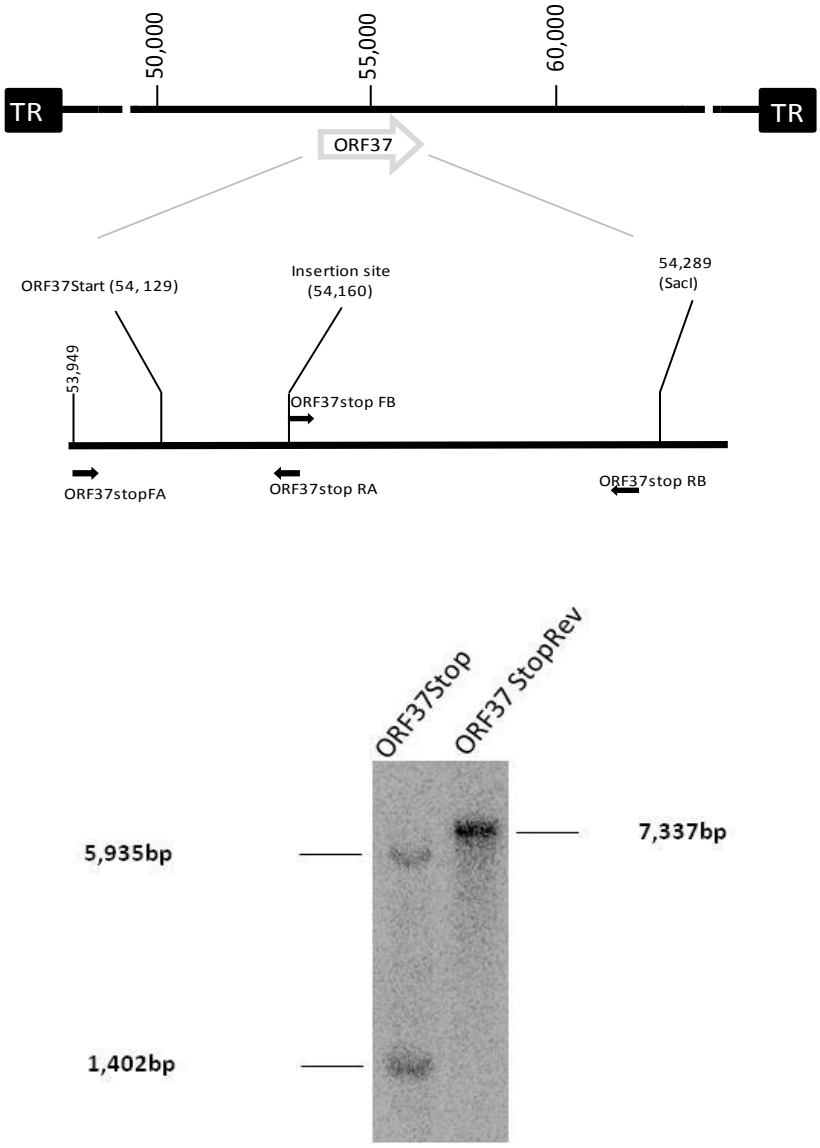

Figure 3.1 Construction of MHV-68 ORF37Stop mutant and revertant viruses. A) The ORF37 gene begins at nt 54129, the 17bp sequence was inserted at nt 54157 which corresponds to the end of ORF36. Arrows indicate position of primers used during construction of ORF37Stop and ORF37StopRev viruses. **B)** Virus stocks were pelleted at high speed, before undergoing phenol/chloroform extraction and ethanol precipitation. The viral DNA was then cut overnight with the RE *Hpa*I. 20µg of gDNA was then ran on a 1% (w/v) TAE gel along with a DNA ladder, the gel was imaged to later decipher fragment size before being transferred overnight onto nylon membrane. The membrane was then probed with a 340bp radiolabelled probe for the area of interest. Southern blot shows ORF37Stop (mutant) and ORF37StopRev (revertant), sizes of fragments are indicated on the left-hand side.

3.3.2 Diagnostic PCR to verify mutation within *ORF37* gene

A diagnostic PCR was carried out on ORF37Stop (mutant), ORF37StopRev (revertant) and WT MHV68. The primers used amplify a 340bp fragment for WT and revertant viruses and a 357bp fragment for mutant viruses (Figure 3.2A). After PCR was carried out each of the viral PCR products was cut using the restriction enzyme *Hpa*I. Because there is no *Hpa*I site in either WT virus or revertant virus, then the expected outcome would be a single product of 340bp. In contrast, the presence of the *Hpa*I site within the mutant virus should yield two products of 230 and 137 bp sizes (Figure 3.2A). Figure 3.2B clearly shows the digestion of PCR products from cells infected with WT and revertant viruses with *Hpa*I yielding a single PCR product of 340 bp, whereas digestion of PCR products from cells infected with ORF37Stop virus yielded two products. Taken together these data clearly show that (1) the insertion (to generate mutant virus) and removal (to obtain the revertant virus) within the ORF37 had been successful, and (2) the mutant virus did not show any signs of revertion to wild type genotype. Amplified PCR products were also sequenced to confirm that the 17bp fragment contained the three stop codons. Figure 3.2C shows the sequencing results from the forward primer for ORF37Stop and ORF37StopRev, which confirmed that the three stop codons were present in the 17 bp insertion sequence in the ORF37Stop virus, along with the *Hpa*I cut site. The diagnostic PCR and RE digest were carried out throughout experiments to ensure that the mutation was present and that reversion did not occur due to repeated infections.

A

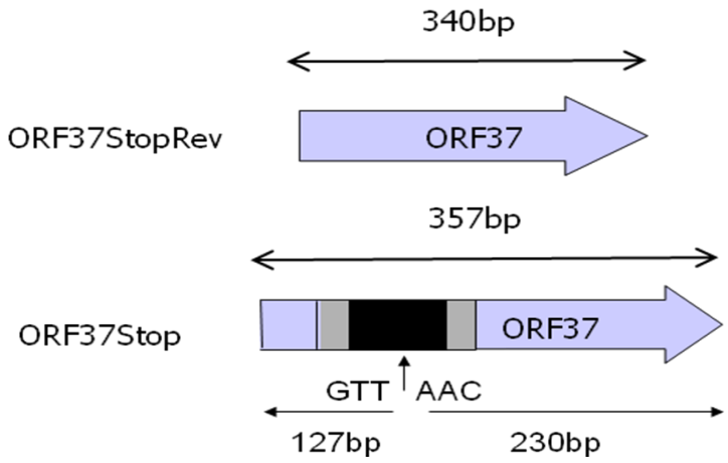

B

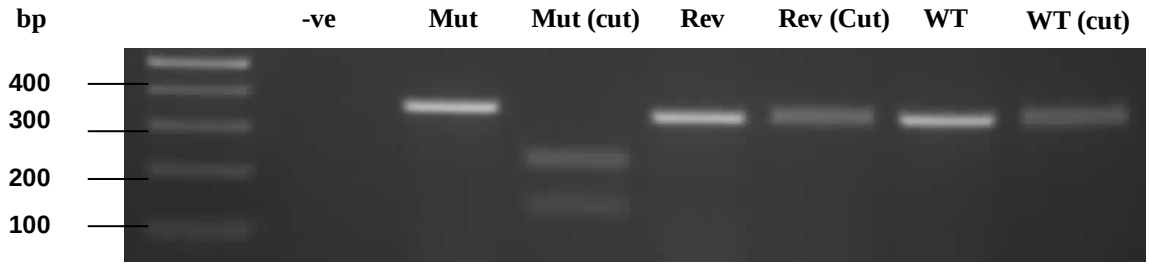

C

GGATTTTTTTGA~~~~~~~~~~~~~~~~~~~~~~AAAGGATGATTTGCTGGAAGT **ORF37StopRev**

GGATTTTTTTGAGCGTA*GTTAA*CGTGTAGAAAGGATGATTTGTTGGAAGT **ORF37Stop**

Figure 3.2 Diagnostic PCR to identify ORF37 mutant virus. A) Schematic of ORF37 gene depicting PCR fragment size and size of RE cut fragments. **B)** PCR amplification of ORF37 from virus stocks. Amplification was performed with primers to yield a 340bp fragment or 357bp fragment if mutation was present. After RE digest with *Hpa*I 15µl of PCR product was run on a 2% (w/v) TAE electrophoresis gel. Bands correspond to PCR products for ORF37Stop (Mut), ORF37StopRev (Rev) and MHV68 (WT), cut and uncut. **C)** Sequencing data from ORF37StopRev and ORF37Stop from forward primer amplification, ORF37Stop contains the 17 bp inserted sequence with three stop codons highlighted in red and the *Hpa*I RE site in italics.

3.3.3 Growth characteristics of ORF37Stop and revertant viruses *in vitro*

Previous work had found that growth of a mutant ORF37 virus was severely attenuated in NIH3T3 cells (Dutia and Ebrahimi, pers. Comm.). One possible obstacle to virus growth is inhibition by type I interferons. Therefore, an attempt was made to propagate the mutant viruses in cells which cannot respond to type I IFN, and as result, are unable to mount an effective anti-viral response (Dutia *et al.* 1999).

To characterise the growth of the ORF37 mutant virus compared to WT and revertant MHV-68 viruses in an immuno-compromised cell line, IFNαβRKO cells were infected with each virus. After infection, cells were harvested every five hours until 30 hours post-infection. The virus titre was determined using plaque assays, the pfu/ml was calculated and the growth curve for each virus was plotted (Figure 3.3). After initially replicating to $3x10^2$ pfu/ml at 5 hours post-infection (hpi) the ORF37Stop virus titre raised steadily to $1.4x10^5$ pfu/ml at 30 hpi. As can be seen from Figure 3.3 both MHV-68 and the revertant viruses followed similar infection paths to the mutant virus indicating that there was no attenuation of mutant virus growth. This can also be seen as there is no significant difference between the end titres at 30 hpi of mutant virus ($1.4x10^5$) compared to either revertant ($1.4x10^5$) or WT ($2.7x10^5$) (p values > 0.05). Figure 3.3 depicts the results from one experiment, however the one step growth curve was conducted twice, showing similar results to those seen in figure 3.3. These findings meant that further work could be carried out using ORF37Stop in IFNαβRKO cells as it could be compared to WT and revertant viruses without bias because of impeded growth.

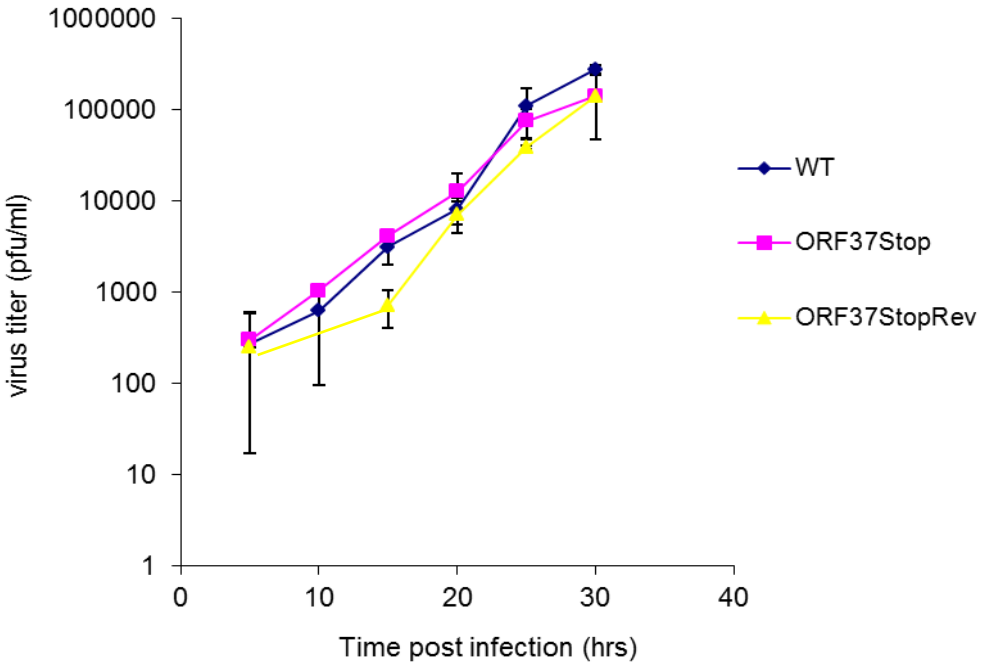

Figure 3.3 Growth characteristics of MHV68 ORF37 mutant and revertant viruses in IFNαβRKO cells. Six-well plates were seeded with $5x10^5$ IFNαβRKO cells, the following day the cells were infected with ORF37Stop, ORF37StopRev and WT MHV68 at an MOI of 5. At 5 hour intervals cells were harvested until 30 hours post-infection. Samples then underwent three freeze-thaw cycles before each sample was diluted in media to give five dilutions ranging from 10^{-1} to 10^{-5}, to each dilution $1x10^6$ cells were added and bijoux were incubated at 37ºC for one hour. Following incubation each sample was added to 4ml media in 60mm petri dishes and incubated at 37ºC. After four days cells were fixed with formalin and stained with toluidine blue, plaques were counted and the pfu/ml was calculated. Results are from one experiment, values are an average of three replicates +/- SD.

3.3.4 Growth characteristics of ORF37Stop and revertant viruses in IFNαβRKO mice

Once it had been established that the mutant virus did not show any attenuated growth *in vitro* (Figure 3.3), the next step was to characterise growth of the ORF37 mutant virus *in vivo*. This is an important step as characteristics identified in cells may differ *in vivo*, this is due to the increased complexity of the immune response to the virus (reviewed by Randall and Goodbourn 2008). Therefore, IFNαβRKO mice were infected with the ORF37Stop virus and the corresponding revertant virus via the intra-nasal (respiratory) route. Lungs were harvested on days three and six post-infection. Lungs from each mouse were divided into two equal parts: one half was homogenised and viral titres were determined using plaque assays; the other half was used to obtain RNA for use in the diagnostic PCR assay to assess the likelihood of reversion to wild type genotype with respect to ORF37.

After three days of infection plaques were identified from samples from lungs of IFNαβRKO mice infected with all three viruses. Interestingly the mutant ORF37Stop virus titre was higher than the WT virus titre although revertant virus titre was the highest of the three. Taken together these results pointed to the fact that ORF37Stop can cause lytic infection in IFNαβRKO mice, levels of which were similar to virus titres from mice infected with revertant and wild type viruses. However a significant difference was seen in virus titres from mice infected with ORF37Stop compared to mice infected with ORF37StopRev ($p=0.02$) and WT ($p=0.003$) at 6 dpi. This difference can best be visualised when comparing how much the virus titre has increased from three dpi to six dpi, with the ORF37Stop pfu/ml only increasing by 1.8-fold compared to a 56-fold increase in revertant virus-infected lungs. These

results suggest that once the infection has become established in the lungs the mutant virus growth is restricted by other immune response factors.

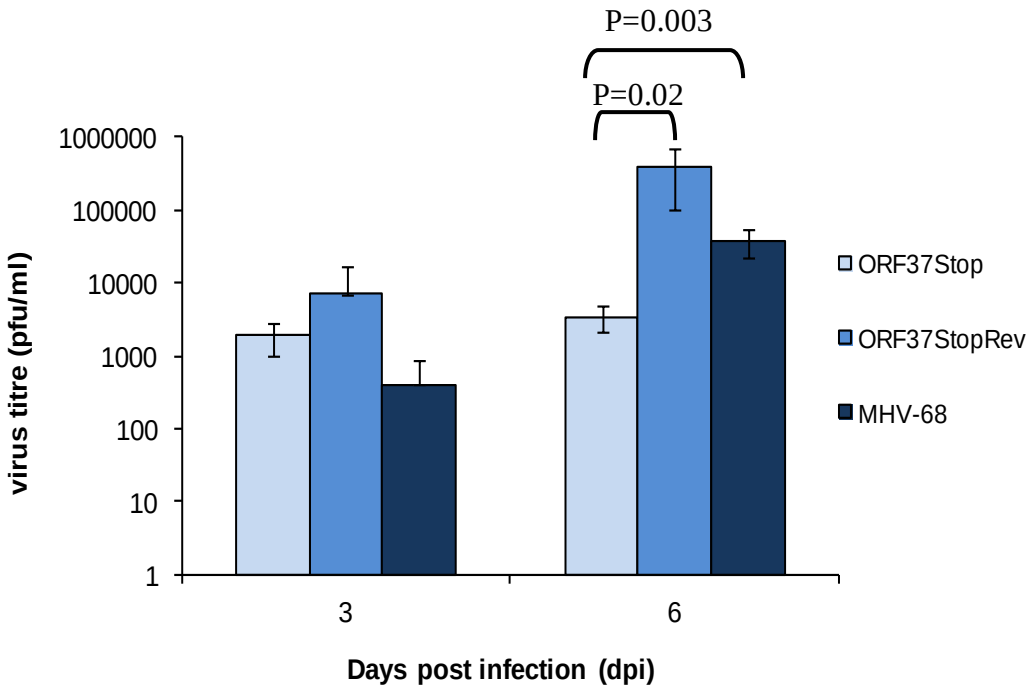

Figure 3.4 Growth characteristics of ORF37 mutant and revertant viruses in IFNαβRKO mice lungs IFNαβRKO mice were intranasally infected with 40µl of either MHV68, ORF37Stop or ORF37StopRev at $4x10^5$pfu/mouse. At three and six days post-infection, the mice were euthanised and their lungs were harvested. Half of each mouse lung was homogenised to release virus particles and viral titres were determined by plaque assay. ORF37Stop (3 & 6 dpi) n=4, ORF37StopRev (3 dpi) n=4, ORF37StopRev (6 dpi) n=3, MHV-68 (3 & 6 dpi) n=3. Each bar on the graph is the average titre of half mouse lungs +/- SD.

3.4 Discussion

Investigating the role of ORF37 and its homologues during viral infection has proved difficult. This has been due to the inability to produce mutant viruses that could replicate to the same levels as WT viruses in immunocompetent cell lines (Covarrubias *et al.* 2009; Feederle *et al.* 2009). The recent study by Richner *et al*., which used a host shutoff point mutation virus to study ORF37, found unexpected results. However the reliability of these results must be brought into question as they still saw increased mRNA degradation compared to mock infected cells, suggesting that they may have only partially inactivated host shutoff (Richner *et al.* 2011). This chapter has addressed the previously seen problems, through the use of a complete ORF37 mutant virus in an immuno-compromised cell line, the results of which insinuate a role for ORF37 in innate immune evasion, which was then also seen *in vivo.*

Retrieval of the ORF37Stop BAC virus from immunocompetent MEF cells had proved difficult. These data suggest that lack of function (s) afforded by the ORF37 product is vital in virus growth and subsequent egress from infected cells. This phenotype has also been identified in other studies where the partial or complete deletion of the ORF37 gene or its homologues has taken place (Covarrubias *et al*. 2009; Feederle *et al*. 2009). Studies carried out on an ORF37 deletion mutant had suggested that the reason for the lack of mutant virus replication was due to ORF37 playing an essential role in viral DNA replication (Covarrubias *et al.* 2009). Work carried out on the EBV BGLF5 null virus also found that deletion of the ORF37 homologue led to impaired nucleocapsid maturation, reduced egress and a reduction in viral DNA synthesis. Although they did find that despite these impairments

morphologically intact BGLF5-null viruses could be identified, suggesting that BGLF5 plays a modulatory role, rather than an essential role in viral replication (Feederle *et al.* 2009). How essential ORF37 is in MHV-68 infection has also been addressed using signature-tagged mutagenesis, with conflicting results, as it was found to be non-essential in BHK-21 cells (Song *et al.* 2005), but attenuated in Vero cells (Moorman *et al.* 2004), suggesting that the cell type in which the mutant virus is grown will have an impact on the ability of these viruses to complete a successful cycle of infection. However these results are difficult to explain as Vero cells are derived from African green monkey kidney cells and have been found to be defective for interferon production (Desmyter *et al.* 1968). The importance of the innate immune response to MHV-68 is well documented (Dutia *et al.* 1999; Nash *et al.* 2001). This along with the increased susceptibility of HSV-1 vhs mutant viruses to IFNα and IFNβ (Suzutani *et al.* 2000) leads to the possibility that the ORF37 gene product may provide a window of opportunity for the virus to grow in the presence of type I IFN-mediated antiviral mechanisms, hence a mutation in ORF37 will leave the virus susceptible. This led to the hypothesis that the ORF37Stop virus would be able to grow in IFNαβRKO cells, which have an impaired innate immune response.

The findings in Figure 3.3 confirmed our hypothesis and are in concordance with work carried out on HSV-2 vhs mutant viruses which also showed attenuated growth in immunocompetent MEF cells, growth of which was partially or completely restored in IFNαβRKO cells (Duerst and Morrison 2004). Taken together these data suggest that the *ORF37* product is playing a similar role to HSV-2 vhs. However how the host shutoff mechanism interacts with the host immune response is an intricate process as differences have been identified with the highly related vhs

proteins of HSV-1 and HSV-2, as HSV-2 vhs has been found to interfere with the PKR-activated pathway (Duerst and Morrison 2004), a phenotype which has not been identified in HSV1 (Pasieka *et al.* 2008).

The results from the *in vitro* growth curve also show that the ORF37Stop mutant virus is capable of going through all stages of virus entry, uncoating, gene expression, encapsidation, and egress similar to ORF37StopRev and WT viruses (Figure 3.3). Our observation that MHV-68 ORF37 mutant was capable of forming plaques in immunompetent cells is also similar to observations made with HSV-1 AE mutants, where it was shown that infection of HSV-1 AE mutants could grow in Vero cells (Weller *et al.* 1990). This and other studies also showed viral AE is not essential for viral DNA synthesis (Weller *et al.* 1990; Smiley 2004). This raises the issue of how nuclease mutant viruses process their genomic DNA for example in resolution of viral DNA intermediates. It was shown that plasmid DNA recombination can occur with very high efficiency in cells infected with an AE mutant of HSV-1, suggesting a role for cellular nucleases in resolution of Holliday junctions, which exist during herpesviral genomic DNA replication (Martinez *et al.* 1996). A number of cellular nucleases have since been shown to share a significant amino acid and structural similarities to viral nucleases, for example flap endo/exonucleases (Lieber 1997; Tomlinson *et al.* 2010). Of relevance here is the observation that HSV-1 vhs (but not HSV-1 AE) shares a significant amino acid sequence homology to a flap endo/exonucleases, FEN-1 (Smiley 2004). Therefore, in some circumstances, cell-derived nucleases can compensate for loss of viral nuclease activity, which may explain, at least in part, plaque formation in exonuclease mutant viruses.

The next step was to investigate the growth characteristics of the mutant virus *in vivo*. This is an important step as the interplay between a virus and the *in vivo* immune response is a complex one (reviewed by Randall and Goodbourn 2008), which may highlight differences between viral growth in cells compared to the animal model. An example of this has been seen with the HSV-1 vhs mutant virus, which upon infection in cells exhibited no attenuation of growth. In contrast upon *in vivo* infection the mutant vhs virus showed up to a 100-fold loss of replication at sites of both lytic and latent infection (Strelow and Leib 1995). The results from the *in vivo* experiment indicated that after initially reaching a similar level in mice lungs 3dpi the ORF37stop virus infection was restricted by 6dpi when compared to WT and revertant titres (Figure 3.4). These findings concord well to work carried out on HSV-2 vhs mutants, which also showed no attenuation of virus growth in IFNαβRKO cells (Duerst and Morrison 2004), but attenuated growth was observed in the genital mucosa (site of HSV2 lytic infection) in IFNαβRKO mice after reaching similar titres during the first two days post infection (Murphy *et al.* 2003). These findings along with the results from Figure 3.3 & 3.4 imply that *in vivo* the ORF37 (or vhs in HSV-2) mutant viruses may be more susceptible to other immune mediators.

The findings in this chapter and by Murphy *et al.* implicate the importance of host shutoff afforded by vhs (for HSV-2) and ORF37 (in γ-herpesviruses) for evading immune responses during lytic infection (Murphy *et al.* 2003). Paradoxically, the study by Richner *et al* found that growth of a host shutoff mutant of MHV-68 in C57BL/6 mice lungs was not attenuated, suggesting that host shutoff does not play an important role in lytic infection, whereas it was suggested that virus host shutoff

activity played a role in establishment of latency (Richner *et al.* 2011). One possible reason for the discrepancy between our study (and HSV-2 vhs) and Richner *et al.* is that host shutoff mutant virus, by Richner and colleagues, was generated via a point mutation, which still showed residual mRNA degradation compared to mock infected cells. It was suggested by Richner *et al.* that the host shut off activity still present in infection with their ORF37 mutant virus may be due to either incomplete inactivation of the host shutoff function or other viral genes contributing towards host shutoff (Richner *et al.* 2011).

Chapter Four

Investigating mRNA decay in IFNαβRKO cells infected with ORF37Stop

4.1. Introduction

The global downregulation of cellular genes during lytic MHV68 infection was first identified using microarray technology (Ebrahimi *et al.* 2003). This global downregulation of cellular genes or host shutoff was then also identifed in both KSHV (Glaunsinger and Ganem 2004b) and EBV (Rowe *et al.* 2007) and was found to be linked to enhanced mRNA turnover (Glaunsinger and Ganem 2004b; Rowe *et al.* 2007; Covarrubias *et al.* 2009). Understanding how ORF37 (and its homologues) cause host shutoff has been hampered by an inability to generate ORF37 mutants of these viruses (Covarrubias *et al.* 2009; Feederle *et al.* 2009). Therefore, much of our understanding of host shutoff in infections with these viruses has come from ORF37 or BGLF5 gene constructs in transient transfection experiments often using GFP as a marker for loss of mRNA. And a number of different methodologies have then been employed to monitor the loss of GFP mRNA and protein in the presence or absence of ORF37 (Glaunsinger and Ganem 2004b; Rowe *et al.* 2007a; Covarrubias *et al.* 2009).

Microarray technology was originally used to investigate the effect of MHV68 and KSHV on cellular genes (Ebrahimi *et al.* 2003; Glaunsinger and Ganem 2004a). In more recent years qPCR and RNAseq have been employed to further study the effect of ORF37 on cellular genes (Clyde and Glaunsinger 2011). The study by Clyde and Glaunsinger used qPCR to validate their RNAseq results, they selected a number of

different genes and compared their results from the two methodologies. Their findings showed a good overall conformity between the two methods, although some differences could be seen and they suggest that this may be due to both methods being less reliable for rare transcripts than more abundant ones (Clyde and Glaunsinger 2011).

4.2 Experimental design

The primary objective of this chapter was to study the effect of ORF37Stop mutant virus compared to ORF37StopRev virus and WT MHV68 in IFNαβRKO cells on mRNA degradation and loss of protein. A selection of cellular genes, previously shown to be degraded because of MHV-68 infection (Ebrahimi *et al*. 2003), were used as markers of host shutoff using qPCR. The cytoskeletal protein β-actin was chosen for Western blotting, as it is a highly conserved, abundant cellular protein.

4.3. Results

4.3.1 Role of MHV-68 ORF37 in mediating loss of mRNA in IFNαβRKO cells.

To study the role of ORF37 in cellular mRNA degradation during infection the immuno-compromised cell line, IFNαβRKO cells were infected at an MOI of 5 with either MHV-68, ORF37Stop or ORF37StopRev. At different times post-infection RNA was harvested from cells and was subsequently synthesised into cDNA and DNase I treated before qPCR was carried out. A selection of genes was chosen to be investigated, which had previously shown a loss of mRNA upon MHV-68 infection (Ebrahimi *et al.* 2003). The cellular gene 18s rRNA was chosen for normalisation, as it is highly abundant and has been used in other studies for normalisation (Taddeo *et al.* 2003). As MHV-68 infection is known to cause loss of cellular mRNA, firstly the

18s rRNA gene which had been chosen for normalisation needed to be tested to ensure that its mRNA was not being degraded. The qPCR results for 18s mRNA for ORF37Stop and ORF37StopRev looked similar with almost identical average copy numbers (data not shown). These results were in accordance with a HSV study which investigated the effectiveness of housekeeping genes for RT-qPCR for their study, the results of which indicated that 18s rRNA was the best for normalisation (Nystrom *et al.* 2004).

Original experiments looked at comparing mRNA transcript levels in ORF37Stop and ORF37StopRev infected cells. The expected result would be to see loss of cellular transcripts in ORF37StopRev cells compared to ORF37Stop. However this was not seen for eEf_Tu at either 12 or 24 hpi (Figure 4.1) or other cellular genes investigated (data not shown), as a clear difference could not be seen, with p-values > 0.05. This led onto a different approach, so that instead of comparing the revertant and mutant infections together they would be compared to mock infected cells, which produced interesting results. A significant loss of ORF37Stop infected mRNA transcripts was seen when compared to levels of mock infected transcripts for the three cellular genes investigated. Loss of mRNA was also seen for cells infected with MHV-68 and ORF37StopRev (Figure 4.2 – Figure 4.4). Comparing the results seen for ORF37Stop and ORF37StopRev indicated that there was no significant difference between the transcript levels of the two infections ($p > 0.05$), suggesting that a similar level of mRNA degradation is taking place in ORF37Stop infected cells when compared to ORF37StopRev. Taken together these results suggest that loss of certain cellular transcripts is seen in the presence or absence of ORF37 in IFNαβRKO cells when compared to mock infected cells

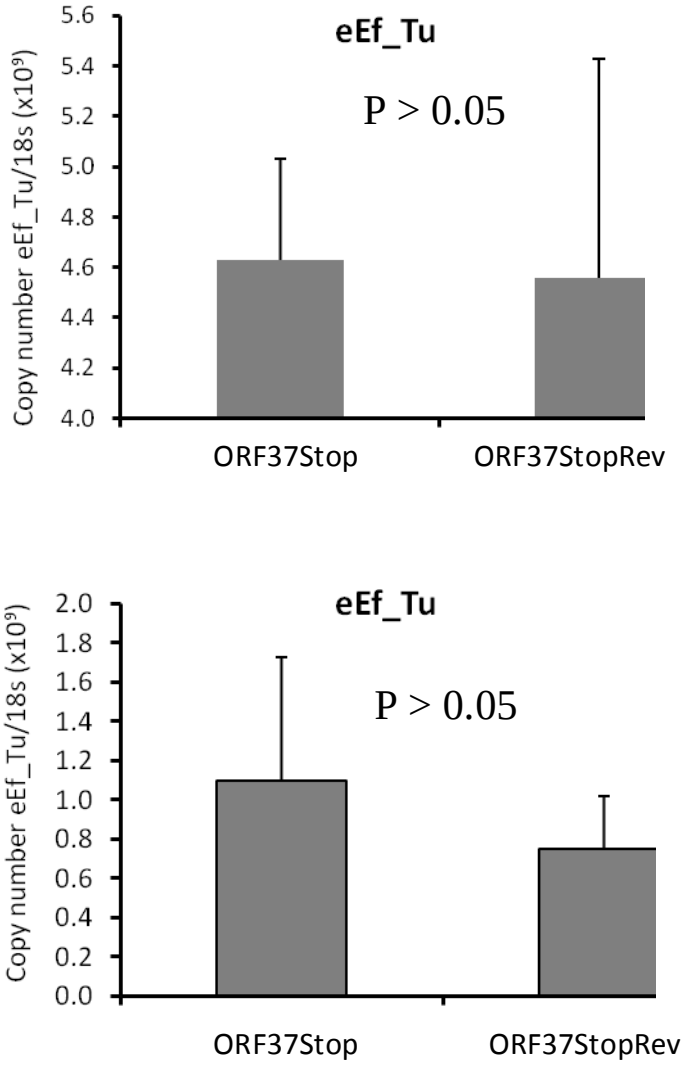

Figure 4.1 Comparison of ORF37Stop and ORF37StopRev eEf_Tu mRNA copy numbers. IFNαβRKO cells were infected with either ORF37Stop or ORF37StopRev at an MOI 5. After 12 and 24 hpi cells were harvested and RNA was extracted using the Qiagen RNeasy kit, after which cDNA synthesis took place. qPCR was then carried out using primers (Table 2.3) for 18s and eEf_Tu. **a)** Represented is copy number of eEf_Tu normalised against 18s, 12 hpi, each bar represents 3 biological replicates, of which there were 2 experimental replicates +/- SD. **b)** Graph depicts the average copy number of eEf_Tu normalised against 18s, 24 hpi, each bar represents 3 biological replicates, of which there were 2 experimental replicates +/-SD.

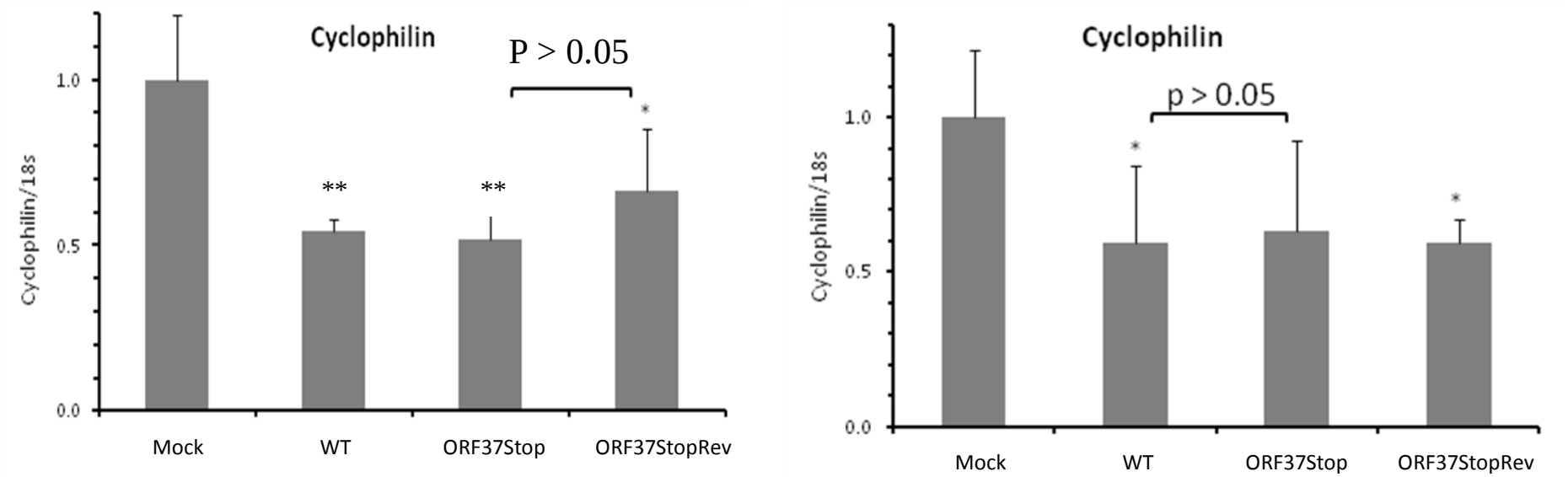

Figure 4.2 Fold change of cyclophilin mRNA in infected cells compared to mock infected mRNA levels. IFNαβRKO cells were infected with either ORF37Stop, ORF37StopRev or WT at an MOI 5 or mock infected. After 12 and 24 hpi cells were harvested and RNA was extracted using Qiagens RNeasy kit, after which cDNA synthesis took place. qPCR was then carried out using primers (Table 2.3) for 18s and cyclophilin. **A)** Represented is fold loss of abundance of cyclophilin transcript normalised against 18s, 12 hpi, each bar represents 3 biological replicates, of which there were 2 experimental replicates +/- SD. **B)** Graphs depict the fold loss of abundance of cyclophilin transcript normalised against 18s, 24 hpi, each bar represents 3 biological replicates, of which there were 2 experimental replicate +/- SD (* = $p < 0.05$ ** = $p < 0.01$).

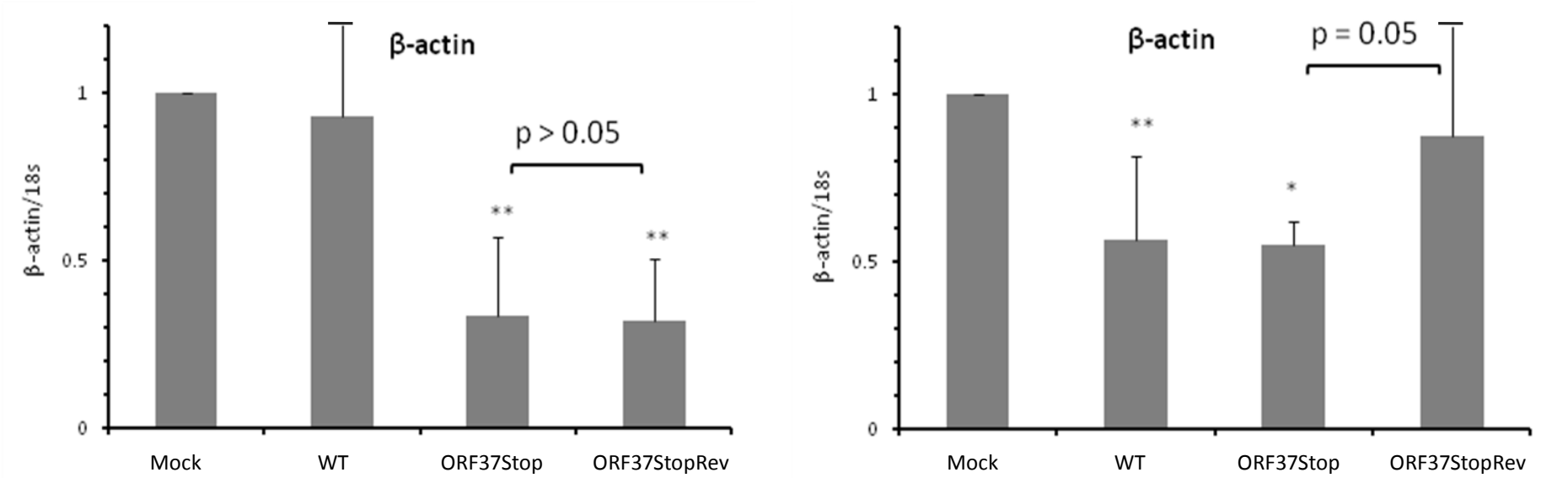

Figure 4.3 Fold change of β-actin mRNA in infected cells compared to mock infected mRNA levels. IFNαβRKO cells were infected with either ORF37Stop, ORF37StopRev or WT at an MOI 5 or mock infected. After 12 and 24 hpi cells were harvested and RNA was extracted using Qiagens RNeasy kit, after which cDNA synthesis took place. qPCR was then carried out using primers (Table 2.3) for 18s and β-actin. **A)** Represented is fold loss of abundance of β-actin transcript normalised against 18s, 12 hpi, each bar represents 3 biological replicates, of which there were 2 experimental replicates +/- SD, calculated from ct values using pfaffl equation. **B)** Graphs depict the fold loss of abundance of β-actin transcript normalised against 18s, 24 hpi, each bar represents 3 biological replicates, of which there were 2 experimental replicate +/- SD, calculated from ct values using pfaffl equation (* = $p < 0.05$ ** = $p < 0.01$).

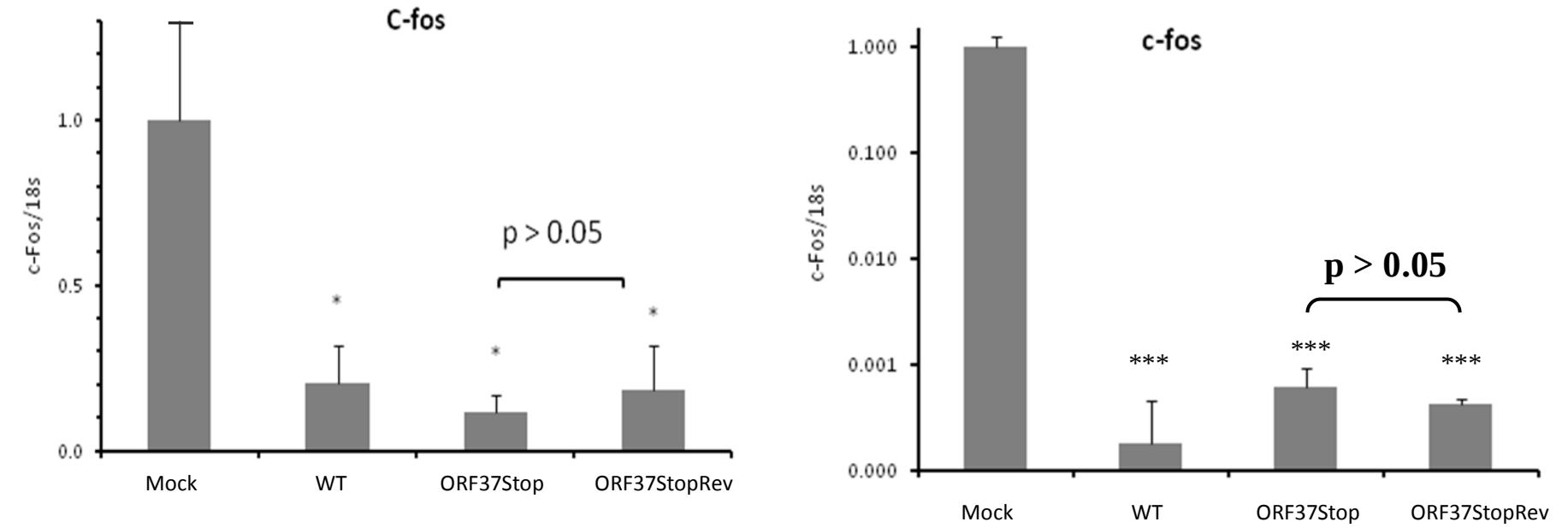

Figure 4.4 Fold change of c-fos mRNA in infected cells compared to mock infected mRNA levels. IFNαβRKO cells were infected with either ORF37Stop, ORF37StopRev or WT at an MOI 5 or mock infected. After 12 and 24 hpi cells were harvested and RNA was extracted using Qiagens RNeasy kit, after which cDNA synthesis took place. qPCR was then carried out using primers (Table 2.3) for 18s and cyclophilin. **A)** Represented is fold loss of abundance of c-fos transcript normalised against 18s, 12 hpi, each bar represents 3 biological replicates, of which there were 2 experimental replicates +/- SD. **B)** Graphs depict the fold loss of abundance of c-fos transcript normalised against 18s, 24 hpi, each bar represents 3 biological replicates, of which there were 2 experimental replicate +/- SD (* = $p < 0.05$ ** = $p < 0.01$ *** = $p < 0.001$).

4.3.2 Role of MHV-68 ORF37 in mediating loss of cellular proteins in IFNαβRKO cells.

To confirm that the loss of mRNA seen in Figures 4.2 – 4.4 was then also seen at the protein level an SDS PAGE gel was run with lysates from IFNαβRKO cells, 24 and 48 hpi (Figure 4.5A). Infections were carried out using the same method as described in section 4.3.1 and at the indicated time point cells were harvested for protein and a protein assay was carried out to elucidate protein concentrations. The banding pattern on the gel appears to be slightly lighter for MHV68, ORF37Stop and ORF37StopRev lysates 24 and 48 hpi compared to mock infected lysates (Figure 4.5A), although this is a subjective method. So to further clarify the result in Figure 4.5 A, Western blotting was carried out on cell lysates, again 24 and 48 hpi, this time looking specifically for the house-keeping gene β-actin (Figure 4.5B & C). After 24 hpi there is no clear difference between mock infected and virally infected levels of β-actin (Figure 4.5B). However after 48 hpi a loss of β-actin protein can be seen in virally infected lysates compared to mock infected, as the bands from virally infected lysates are lighter than that of the mock infected lysate (Figure 4.5C). The results suggest loss of cellular protein is seen in the presence or absence of ORF37 when compared to levels of mock infected proteins.

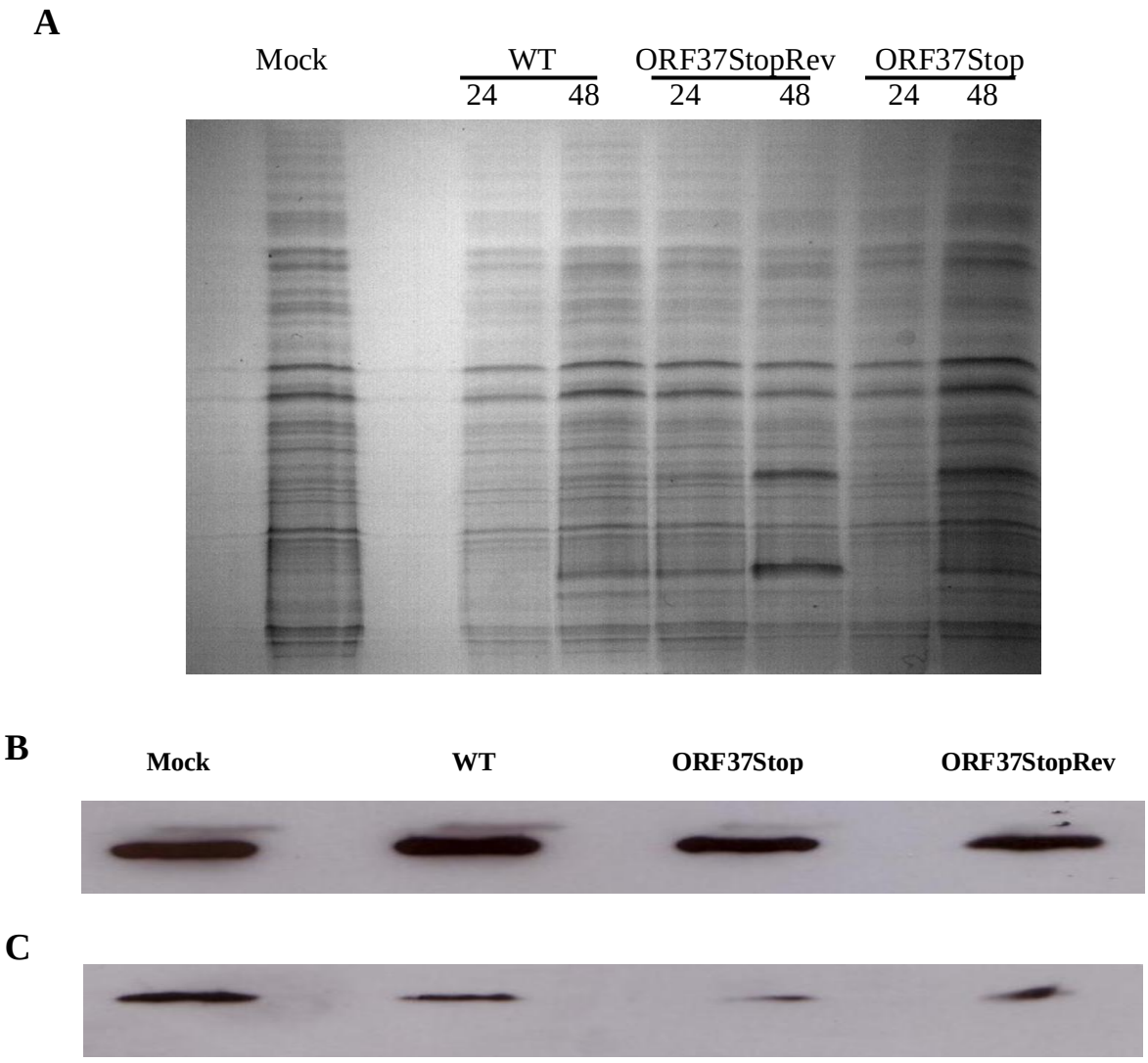

Figure 4.5 Protein levels from infected cells compared to mock infected cells. IFNαβRKO cells were infected with WT, ORF37Stop or ORF37StopRev and cells were harvested at 24 and 48 hours using cell lysis buffer. **A)** 20µg of cell lysates were resolved on 10% polyacrylamide gel. The gel was run at 40mA for 45 mins and then stained with coomassie blue for 30 mins before destaining **B)** Western blot for β-actin from protein lysates 24 hours post-infection. **C)** Western blot for β-actin from protein lysates 48 hours post-infection.

4.4 Discussion

Global downregulation of gene expression or host shutoff during MHV-68 infection was first identified using microarray technology (Ebrahimi *et al.* 2003). The gene identified as causing host shutoff was found to be the alkaline exonulease, ORF37 (Glaunsinger and Ganem 2004b), however the inability to produce ORF37 mutant viruses (Covarrubias *et al.* 2009; Feederle *et al.* 2009) has led to difficulties in studying the role of ORF37 during infection. Recently a partial deletion mutant virus has been produced via a point mutation, although some host shutoff was still seen during infection with this virus (Richner *et al.* 2011). As reported in Chapter 3 the ORF37Stop mutant virus was found to cause a productive infection in both IFNαβRKO cells and IFNαβRKO mice. So to study the effect of ORF37 during infection mRNA and protein levels were investigated from infected IFNαβRKO cells.

The results in this chapter led to the conclusion that loss of cellular mRNA and protein levels can take place independently of the ORF37 gene product in infected IFNαβRKO cells. Loss of cellular transcripts was observed in cells infected with ORF37Stop virus when compared to mock-infected cells (Figure 4.2 - 4.4). Moreover, loss of mRNA was also reflected at the protein level (Figure 4.5). These findings indicate that in an immuno-compromised cell line host shutoff is taking place regardless of the presence or absence of ORF37, suggesting that another host shutoff factor may be causing loss of mRNA. However CPE was seen during infections and so it is possible that some of the loss of mRNA and protein identified in infected cells when compared to mock infected cells may be due to lytic infection.

A dual method of host shutoff has been identified in HSV-1 infection, the first is through ICP27, which causes a re-distribution of snRNPs, disrupting the splicing machinery (Phelan *et al.* 1993; Hardwicke and Sandri-Goldin 1994) and the second is through the RNase activity of vhs protein (Zelus *et al*. 1996; Everly *et al.* 2002). These two proteins have been found to collaborate to cause loss of cellular mRNA (Smiley 2004) and more recently have been found to interact with each other when bound to certain proteins (Taddeo *et al.* 2010). However the complexities of these two proteins are still being investigated, as new studies discover more interactions and more functions associated with them (Esclatine *et al.* 2004b; Strand and Leib 2004; Taddeo *et al.* 2009; Taddeo *et al.* 2010).

A similar activity has also been identified in EBV linked to the ICP27 homologue, SM protein, which has been found to enhance intron-less gene expression and inhibit intron-containing gene expression (Ruvolo *et al.* 1998). ICP27 is conserved between all members of the herpesvirus family, although they differ in size and the overall sequence homolgy is low, as even the closest members of the family only share roughly 30% homology in their amino acid residues (reviewed by Majerciak and Zheng 2009). However EBV SM protein has been found to be able to compensate for ICP27 defects during viral infection, suggesting that they are linked to common pathways or have distinct activities which share a common phenotype (Boyer *et al.* 2002). The KSHV homologue of ICP27 is ORF57, a viral gene regulator, which has not been found to inhibit splicing of intron-containing genes. This difference in function is probably due to KSHV containing more than 30 intron-containing genes that require active splicing compared to just four in HSV-1 and in EBV just the latent genes contain introns

suggesting a role for SM in the lytic-latent switch (Ruvolo *et al.* 1998; Smiley 2004; Majerciak and Zheng 2009). Whether the MHV-68 ICP27 homologue, ORF57 is acting towards host shutoff has not been determined.

The fact that host shutoff has not, as yet, been linked to any other proteins in γ-herpesvirus infections may be due to the inability to produce mutant ORF37 viruses. The original study that lead to the discovery of ORF37 used a transfection method to screen each KSHV gene individually for its ability to cause host shutoff and their results indicated that ORF37 was the only gene linked to a significant decrease in GFP expression (Glaunsinger and Ganem 2004b), however other genes may cause host shutoff to a lesser degree and it may be that this can best be seen in an immuno-compromised cell line.

Taken together the results from this chapter suggest that more than one viral protein may cause host shutoff, as seen in HSV-1 (Smiley 2004). When infection studies have been carried out on MHV-68 with a deleted ORF37 gene there have been indications that an additional host shutoff factor may be at work. This was first suggested by Corruvbias *et al.* when they compared two different transfection experiments, as they saw a much decreased half-life of GFP in mRNA decay assays when cells were transfected with a deleted ORF37 BAC virus compared to a plasmid transfection in the absence of ORF37. They suggest that this difference may be due to GFP sequence differences and the fact that the transcripts were under the control of different promoters. However they also suggest that it may indicate additional viral host shutoff factors contributing to the instability of the BAC GFP (Covarrubias *et al.* 2009). This has also eluded to in the

recent paper by Richner *et al.* who produced an ORF37 point mutation virus and found that they still saw some mRNA degradation, which they suggest may be due to incomplete deactivation of ORF37 gene or other viral genes contributing to host shutoff (Richner *et al*. 2011).

The results from this chapter are in accordance with other MHV-68 ORF37 deletion studies and would back-up the suggestions that additional host shutoff factor (viral and/or cellular) may be involved. Identification of this other viral factor will however require much further work to be done to pinpoint where in the mRNA biogenesis process it is acting and how, as these are questions which are still being addressed for the already discovered ORF37.

Chapter Five

Investigating cellular mRNA decay in transfected cells with MHV-68 ORF37

5.1 Introduction

Global mRNA loss because of infection with MHV-68 and KSHV has been well-documented (Ebrahimi *et al.* 2003; Glaunsinger and Ganem 2004b). Moreover, it is now widely accepted that ORF37 homologues in the γ-herpesviruses play a key role in mediating host shutoff (Glaunsinger and Ganem 2004b; Rowe *et al.* 2007a; Covarrubias *et al.* 2009). Global loss of cellular mRNA upon infection of cells with MHV-68 was first identified using microarray technology (Ebrahimi *et al.* 2003). Gene expression microarrays have also been used to investigate further loss of cellular mRNA upon KSHV infection (Glaunsinger and Ganem 2004a). However the microarray studies that have been carried out have investigated host shutoff in the context of virus infection, which will have additional viral factors present that may influence mRNA levels. In order to investigate mRNA levels independent of lytic viral infection transfection, assays needed to be executed to examine the role ORF37 and its homologues.

Previous studies have employed a number of methodologies to investigate mRNA loss, the majority of which have used GFP as a marker for mRNA decay (Glaunsinger and Ganem 2004b; Rowe *et al.* 2007; Covarrubias *et al.* 2009). The first study that investigated possible host shutoff genes in KSHV used a GFP expressing cell line, which was individually transfected with each viral gene. Following this flow, cytometry

was used to identify genes that decreased GFP levels, the results of which implicated ORF37 in host shutoff (Glaunsinger and Ganem 2004b). The GFP protein was then used to investigate host shutoff in EBV infection. In the latter case, BGLF5 was co-transfected with a GFP expression vector and GFP levels were visualised using Northern blotting (Rowe *et al.* 2007). Covarrubias *et al.* employed similar methodologies to investigate host shutoff linked to MHV-68 ORF37, using Northern blotting of transfected cells to determine the GFP half-life in cells co-transfected with ORF37 (Covarrubias *et al.* 2009). However GFP is not a natural cellular protein, so it would appear that the next step would be to investigate loss of cellular mRNA in the presence or absence of ORF37.

The effect of MHV-68 ORF37 on cellular genes during transfection has been examined using Northern blotting to determine levels of the cellular genes (Covarrubias *et al.* 2009). However this is an area which requires further investigation as the effect of ORF37 on cellular genes may indicate possible host shutoff mechanisms, as the structures of both BGLF5 and SOX have been elucidated, both of which suggest that the nuclease may be interacting with other cellular proteins to cause mRNA degradation (Buisson *et al.* 2009; Dahlroth *et al.* 2009; Bagneris *et al.* 2011). Examining the direct effect of ORF37 on cellular genes may indicate elements that can protect mRNA degradation, such as AREs (Chandriani and Ganem 2007), which may point to possible decay mechanisms.

5.2 Experimental design

To assess whether MHV-68 ORF37 can directly (i.e. not in the context of a virus infection cycle) mediate mRNA degradation, murine NIH3T3 cells were transiently transfected with either the empty vector, pcDNA3.1 or pcDNA3.1 containing the ORF37 gene (FLORF37pcDNA3.1). Following transfection, cells were harvested at set time points and quantitative real-time PCR (qPCR) and Western blotting assays were carried out to analyse cellular mRNA and protein levels. The pcDNA3.1 construct is a 5.4 kb vector under the control of the immediate-early CMV promoter, containing myc and His-tagged epitopes. Cells were also transfected with pEGFP-N1, a GFP containing vector also under the control of the CMV promoter, GFP was used to check for transfection efficiency.

5.3 Results

5.3.1 Cellular mRNA decay in ORF37 transfected cells using qPCR

A selection of cellular genes which showed the greatest loss of mRNA upon MHV68 infection (Ebrahimi *et al.* 2003) was chosen to investigate loss of mRNA in cells transfected with ORF37. NIH3T3 cells were transfected with either an empty vector (pcDNA3.1) or a plasmid containing the ORF37 gene (FLORF37pcDNA3.1). Total RNA was harvested from cells, synthesized into cDNA and then used in qPCR assays. Figure 5.1 shows the results for eukaryotic elongation factor Tu (eEf_Tu) at 12, 24 and 36 hours post-transfection. The transcript copy number for eEf_Tu was comparable between cells transfected with empty vector and cells transfected with ORF37-containing plasmid. At 24 and 36 hours post-transfection, however, a greater loss of eEf_Tu mRNA was observed in the presence of ORF37, but, this was not statistically

significant ($p < 0.05$). Similar results were also seen for the cellular genes cfos and cyclophilin with no significant differences seen between cells transfected with either empty vector or cells transfected with FLORF37pcDNA3.1 (Figure 5.2).

A possible explanation for lack of mRNA loss in cells transfected with FLORF37pcDNA3.1 (compared to control cells transfected with pcDNA3.1) is lack of ORF37 protein expression from FLORF37pcDNA3.1 plasmid. To ascertain that indeed ORF37 was being expressed from FLORF37pcDNA3.1 plasmid, total RNA was isolated from transfected cells, DNase I-treated and synthesised into cDNA. A diagnostic PCR was then performed with primers to amplify a 416bp fragment within the ORF37 transcript. The same process was used to amplify the cellular β-actin transcript, which was used as an internal control. As can be seen in Figure 5.3A, the control transcript, β-actin, was detected in all samples indicating that comparable levels and quality of RNA were isolated from control and ORF37-transfected cells. In contrast, ORF37 transcript was only detected in cells transfected with FLORF37pcDNA3.1 and not in cells transfected with empty vector (Figure 5.2B). These results show that the ORF37 gene was transcribed from the expression vector in these cells. It is, however plausible to suggest that ORF37 transcript was not translated into protein.

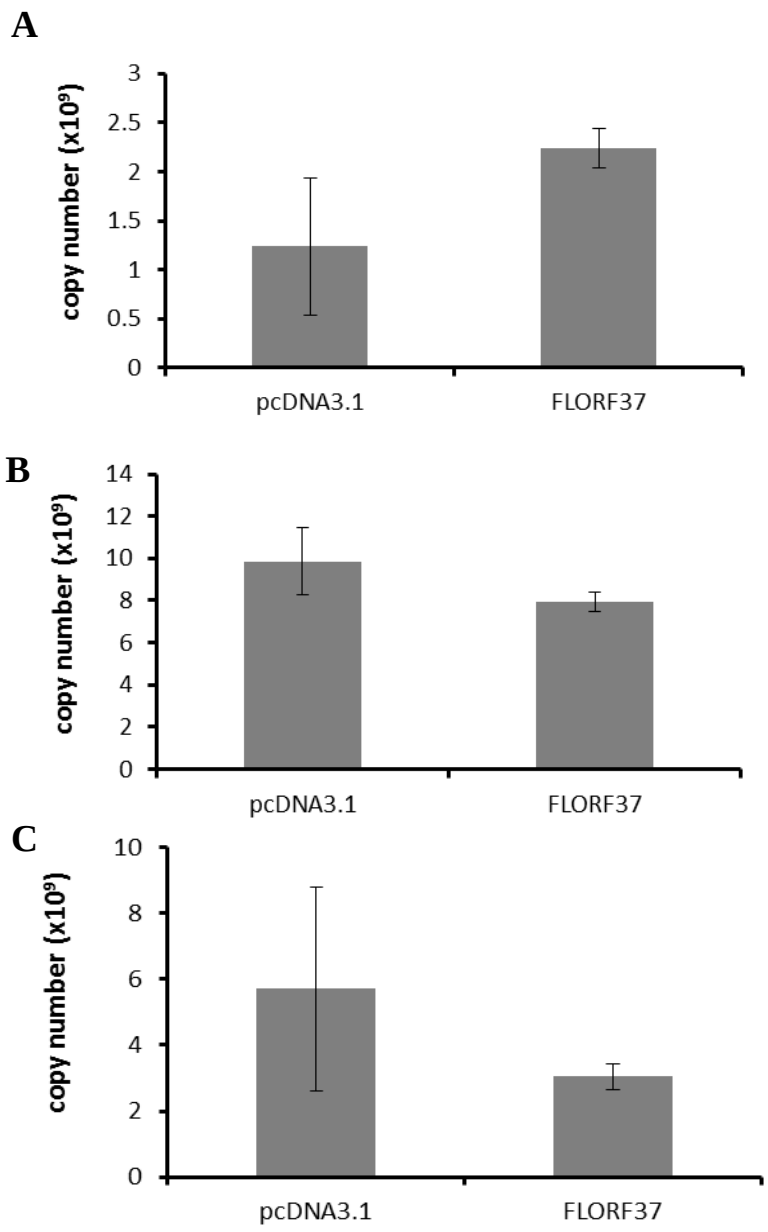

Figure 5.1 qPCR for cellular gene, eEf_Tu, in transiently transfected cells. NIH3T3 cells were transfected with either pCDNA3.1 or FLORF37pCDNA3.1 and cells were harvested for RNA, which was subsequently synthesised into cDNA. qPCR was then carried out using primers (table 2.3) for 18s and eEf_Tu. Graphs depict the average copy number of eEf_Tu normalised against 18s, each bar represents 3 biological replicates, of which there were 2 experimental replicates +/- SD **A)** 12 hours post-transfection **B)** 24 hours post-transfection **C)** 36 hours post-transfection.

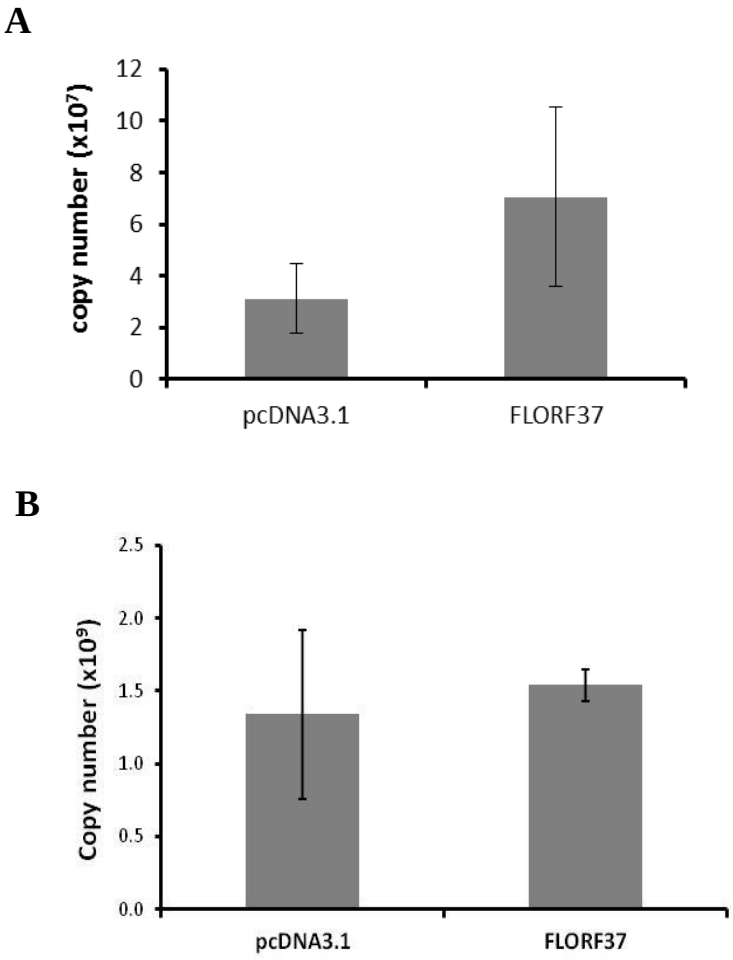

Figure 5.2 qPCR for cellular genes, c-fos and cyclophilin, 24 hours post-transfection. NIH3T3 cells were transfected with either pCDNA3.1 or FLORF37pCDNA3.1 and cells were harvested for RNA, which was subsequently synthesised into cDNA. qPCR was then carried out using primers (Table 2.3) for 18s and either c-fos or cyclophilin. Graphs depict the average copy number normalised against 18s, each bar represents 3 biological replicates, of which there were 2 experimental replicates +/- SD **A)** c-fos transript **B)** cyclophilin transcript.

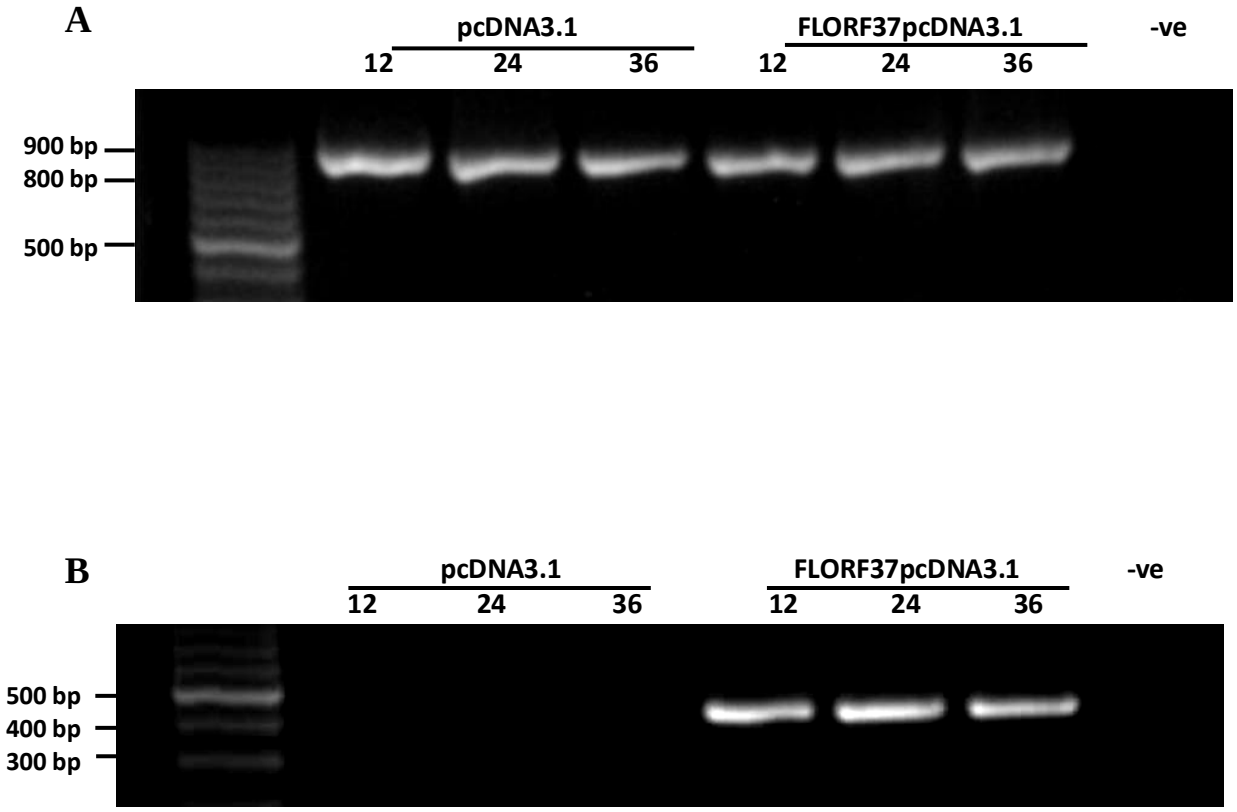

Figure 5.3 Diagnostic PCR for presence of ORF37 in transiently transfected cells. NIH3T3 cells were transfected with either pCDNA3.1 or FLORF37pCDNA3.1, 12, 24 and 36 hours post-transfection cells were harvested for RNA, which was subsequently synthesised into cDNA. A diagnostic PCR was then carried out using primers in table 2.2, PCR products were then run on a 2% (w/v) TAE electrophoresis gel. **A)** 897bp PCR products corresponding to β-actin. **B)** 461bp PCR products corresponding to ORF37.

5.3.2 Detection of epitope-tagged FLORF37 and β-actin using Western blotting

The presence of ORF37 transcript in transfected cells confirmed that the transfection experiment had been successful. As stated above, it is, plausible to suggest that ORF37 transcript was either expressed at very low levels or not translated. The pcDNA3.1 vector used in these transfection experiments contains both myc and His-tagged epitopes. Therefore, the expressed protein of interest (ORF37) could also be detected at the protein level. Western blotting for the myc tag using the ABC-alkaline phosphatase detection method was unsuccessful, as although bands could be seen they were around 70kDa, rather than the expected 56kDa and were also seen in the empty vector samples which should not contain the myc-tagged protein (Figure 5.4B). Western blotting for β-actin (Figure 5.4A) had been successful with clear bands seen at the expected size (43kDa), which indicated that the Western blotting method was working well. This leads to the conclusion that unspecific binding may be taking place in the Western blotting experiments for the myc-tagged protein due to the increased development time that was used in order to identify a band relating to the myc-tagged ORF37 protein. A number of underlying causes may explain these findings, one of which was lack of a positive control. We were able to obtain a His-tagged protein (M4) (courtesy of Dr Bernadette Dutia, Edinburgh University) to use as a positive control (Figure 5.4C). Original experiments used the ABC detection method for the His-tag. The ABC method uses the binding of the glycoprotein avidin to the small molecular weight vitamin, biotin. This process is used because of the extraordinarily high affinity that these two molecules have for each other, which is over one million times higher than that of an antibody for most antigens (Diamandis and Christopoulos 1991). These macromolecular complexes formed between avidin and biotinylated antibodies can then be visualised using alkaline

phosphatase or horseradish peroxidase. However experiments carried out using the ABC method gave weak results with unclear bands for both ORF37 and the 52kDa His-tagged M4 protein (the positive control) (Figure 5.5A). So to try to improve detection of the bands a similar method to ABC was used which uses a Streptavidin-AP conjugate (Roche) instead of avidin. Figure 5.5B shows the results from a Western blot for the His-tag developed using the Streptavidin method, which did show bands at the correct size for ORF37, but on this blot the positive control (M4) did not have a strong band. Extra bands were also seen in the FLORF37pcDNA3.1 lanes, which again may be due to unspecific binding of the secondary antibody due to long development times. Attempts were made to improve the detection limits included loading high quantities of total protein (40µg of protein/lane). However, the high viscosity of samples at high protein concentration levels gave poor results (data not shown).

To improve detection of ORF37, another antibody detection method, ECL, was used. ECL is a light emitting method that detects horseradish peroxidise-linked antibodies and is thought to be at least 10 times more sensitive than colourimetric assays (Amersham). As can be seen in Figure 5.6 B, β-actin was readily detected in all samples. With respect to ORF37, faint bands corresponding to the expected ORF37 protein were detected by this method. Taken together it appears that it is not possible to improve the intensity of the ORF37 protein from the samples described in this chapter.

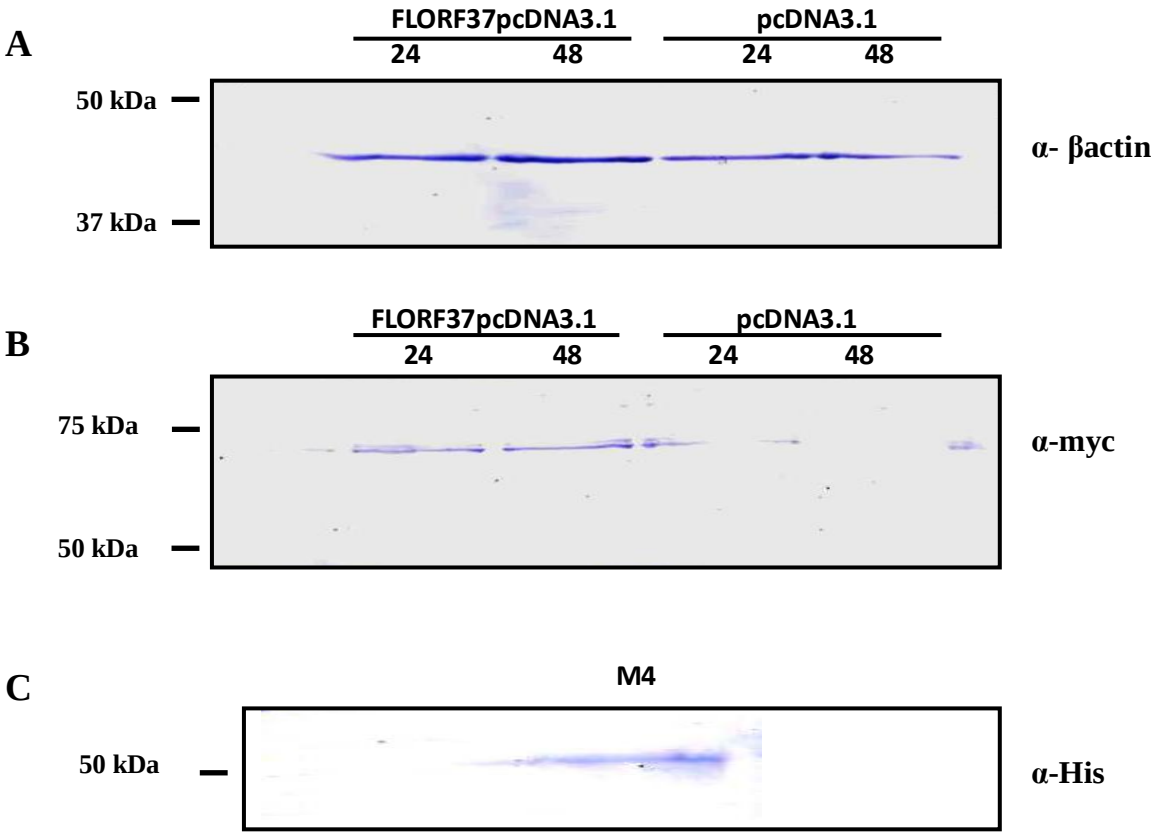

Figure 5.4 Detection of myc-tagged ORF37 protein and His-tagged M4 protein. NIH3T3 cells were transfected with either pCDNA3.1 or FLORF37pCDNA3.1, 24 & 48 hours post-transfection cells were harvested for protein. Protein concentration was calculated using Bio-Rad's protein assay and 20µg of protein was loaded into each well and samples were run using SDS-PAGE before blotting and staining of the membrane. Asterisks indicate bands of interest, M4 control is 52kDa, β-actin is 43kDa and myc-tagged ORF37 is 56kDa. **A)** Membrane stained with 1/2000 dilution of primary ab: rabbit α actin and a 1/2000 dilution of secondary ab: biotinylated goat α rabbit **B)** Membrane stained with 1/2000 dilution of primary ab: rabbit α myc and a 1/2000 dilution of secondary ab: biotinylated goat α rabbit **C)** Membrane stained with 1/500 dilution of primary ab: mouse penta His and a 1/2000 dilution of secondary ab: biotinylated rabbit α mouse. All bands visualised using ABC-alkaline phophatase staining**.**

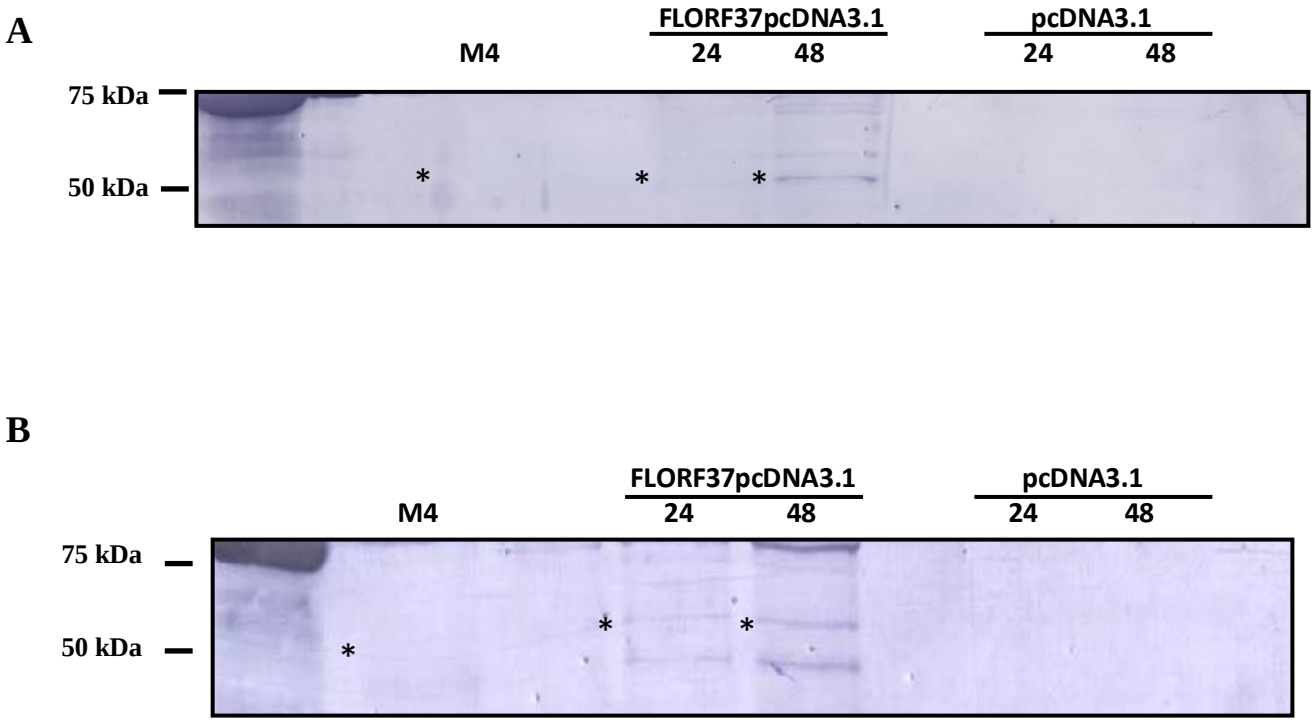

Figure 5.5 Detection of His-tagged ORF37 protein. NIH3T3 cells were transfected with either pCDNA3.1 or FLORF37pCDNA3.1, 24 and 48 hours post-transfection total cellular protein was harvested for protein assays. Protein concentration was measured using Bio-Rad's Bradford protein assay and 20µg of total cellular protein was loaded into each well and samples were run using SDS-PAGE before blotting and staining of the membrane. Asterisks indicate bands of interest, +ve control is 52kDa and His-tagged ORF37 is 56kDa. **A)** Membrane stained with 1/500 dilution of primary ab: mouse penta His and a 1/4000 dilution of secondary ab: biotinylated rabbit α mouse, bands visualised using ABC-alkaline phophatase followed by BCIP/NBT **B)** Membrane stained with 1/500 dilution of primary ab: mouse penta His and a 1/2000 dilution of secondary ab: biotinylated rabbit α mouse, bands visualised using streptavidin followed by BCIP/NBT.

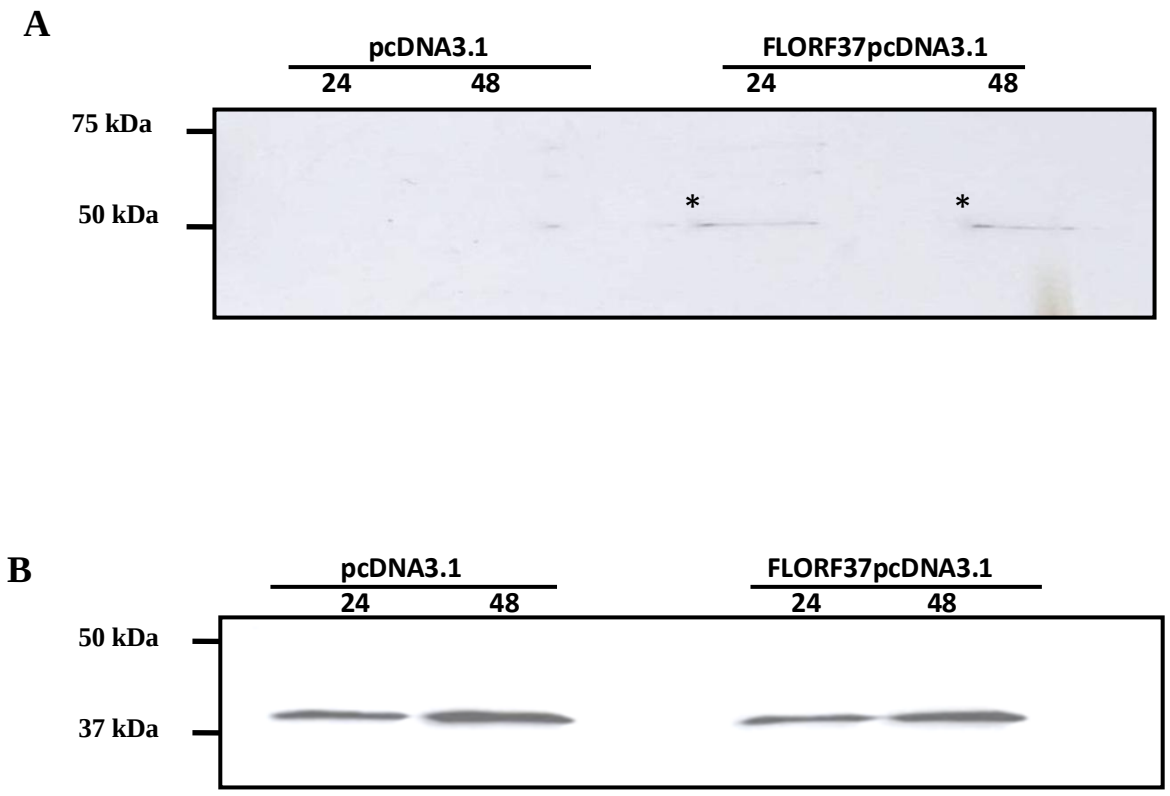

Figure 5.6 Detection of His-tagged ORF37 protein using ECL detection method. NIH3T3 cells were transfected with either pCDNA3.1 or FLORF37pCDNA3.1, 24 and 48 hours post-transfection cells were harvested for protein. Protein concentration was calculated using Bio-rad protein assay and 20µg of protein was loaded into each well and samples were run using SDS-PAGE before membrane transfer and visualization of bands using ECL chemiluminescence. **A)** Membrane stained with 1/500 dilution of primary ab: mouse α penta His and 1/10,000 dilution of secondary ab: α mouse-HRP-linked. Astrix points to bands of interest; His-tagged ORF37 is 56kDa. **B)** Membrane stained with 1/2000 dilution of primary ab: rabbit α actin and 1/20,000 dilution of secondary ab: α-rabbit-HRP-linked. Bands correspond to 43 kDa β-actin.

5.4 Discussion

Previous studies have focussed on the use of GFP levels as a marker for mRNA loss during co-transfection experiments with ORF37/ BGLF5 plasmids (Glaunsinger and Ganem 2004b; Rowe *et al.* 2007; Covarrubias *et al.* 2009). Glaunsinger *et al* investigated mRNA loss in the presence of ORF37 from KSHV using a plasmid containing a destabilised GFP gene with a reduced half life of 3 hours, the results of which indicated a clear loss of GFP mRNA when ORF37 was co-expressed (Glaunsinger and Ganem 2004b). This loss of GFP has also been seen in co-transfection experiments with MHV-68 ORF37 and EBV BGLF5 when mRNA decay assays have been conducted post-actinomycin D treatment (Rowe *et al.* 2007; Covarrubias *et al.* 2009). However these studies only examined loss of cellular mRNA in the context of viral infection. As a number of viral genes are expressed during lytic infection, to determine the effect of ORF37 on cellular mRNA, transfection experiments which focussed on cellular mRNA levels were required.

The qPCR method is a relatively simple method for the quantification of mRNA. The indications from previous viral infection studies (Ebrahimi *et al.* 2003; Glaunsinger and Ganem 2004b; Rowe *et al*. 2007) and GFP transfection experiments (Glaunsinger and Ganem 2004b; Rowe *et al.* 2007a; Covarrubias *et al.* 2009) led to the hypothesis that loss of cellular mRNA ought be seen in the presence of ORF37 alone. However as Figure 5.1 shows this was not seen for the cellular genes examined in this study, some loss was identified 24 and 36 hours post-transfection, but this was not statistically significant (Figure 5.1B & C). Similarly other cellular genes tested also did not exhibit a significant loss of mRNA and in the case of c-fos the mRNA level is actually higher in ORF37 transfected cells (Figure 5.2). This led

to the possibility that the ORF37 gene was not adequately expressed from the vector used in transient transfection studies. The FLORF37pcDNA3.1 plasmid was sequenced, which confirmed that the presence of ORF37 DNA sequence in the vector (data not shown). A diagnostic PCR was then conducted on cDNA synthesised from RNA to confirm that the ORF37 gene was being transcribed, the results of which clearly shows the presence of ORF37 mRNA (Figure 5.3).

The next logical step was to confirm that ORF37 transcript was translated into protein. This was facilitated by the presence of myc and His tags in the expression vectors used in this study. Initially, antibodies against the the myc tag were to detect ORF37 protein, but this gave very poor results (Figure 5.4B). The His-tag was then tested for the presence of ORF37 protein. Bands were visible at the expected size, but expressed at the level of detection with this approach (Figure 5.5 & 5.6). A number of different methods were used to improve the detection of ORF37 protein, and with varying antibody concentrations. These attempts, however, did not improve the quality of ORF37 protein detection. Taken together, these results show that the ORF37 gene was transcribed and translated at very low levels compared to the housekeeping gene β-actin. This observation correlates well with expression profiling of all MHV-68 genes by DNA microarrays, which showed low abundance of ORF37 compared to structural genes of MHV-68 (Ebrahimi *et al.* 2003; Martinez-Guzman *et al.* 2003). For example, 24 hours post MHV-68 infection there is approximately an 18-fold decrease in ORF37 expression compared to gp150 (Martinez-Guzman *et al.* 2003). This is expected, since ORF37 is an enzyme, and unlike structural genes, relatively minute quantities of this protein are required during the virus infection.

Furthermore, it is also plausible that not all cells were transfected leaving a number of harvested cells untransfected. Therefore, host shutoff effect of ORF37 on cellular mRNA would be masked with greater quantities of intact mRNA from untransfected cells. One way to circumnavigate this problem is to identify transfected cells using a marker. This method was used by Clyde and Glaunsinger. Therefore, only cells which harboured ORF37 (as green cells) were isolated by means of flow cytometry. This study focussed on the use of RNAseq for deep sequencing and used qPCR to validate the results. They compared mRNA levels for the housekeeping gene GAPDH for sorted and unsorted cells transfected with ORF37 compared to control cells and found that as expected a greater loss of mRNA was seen in the sorted cells, although some loss was still seen in unsorted cells (Clyde and Glaunsinger 2011). These results concord well with our findings as the cells in this study were in effect unsorted and did exhibit some loss of cellular mRNA, but not to a significant level (Figure 5.1). The findings from Clyde and Glaunsinger were in agreement with previous studies as they found a reduction in the levels of most cellular mRNAs in cells expressing ORF37. They did not detect any obvious similarities between cellular mRNAs that escape host shutoff, but they did notice that in the majority of cases the more abundant mRNAs experience a higher level of downregulation compared to rare mRNAs (Clyde and Glaunsinger 2011).

Chapter Six

Examining the mechanism of mRNA degradation in MHV68 infected cells

6.1 Introduction

The discovery of host shutoff within the γ-herpesvirus family has led to the question of how the multi-functional DNA exonuclease could be causing mRNA degradation. The first and most obvious answer would be that ORF37 (and homologues of ORF37) has direct RNase similar to HSV vhs (Everly *et al.* 2002). However, *in vitro* studies have not found this to be the case (Glaunsinger and Ganem 2004b; Rowe *et al.* 2007), leading to the possibility that the DNA exonuclease interacts with the host mRNA degradation pathways indirectly. The crystal structures of KSHV ORF37 and EBV BGLF5 have recently been elucidated and *in vitro* asays with these recombinant proteins suggest that ORF37 and BGLF5 possess a degree of RNase activity under *in vitro* conditions (Buisson *et al.* 2009; Bagneris *et al.* 2011). However SOX exhibited a low affinity for binding RNA. This, along with site-directed mutagenesis studies looking at residues required for SOX mediated host shutoff, suggest that SOX may interact with cellular mRNA decay pathways to degrade RNA (Bagneris *et al.* 2011).

Studies investigating the mRNA degradation activity of ORF37 have so far identified two phenotypes, both of which are linked to the 3' end of mRNA. The first phenotype is hyperadenylation, which was seen as an increase in poly(A) tail length, using RNase H and Northern blotting methods (Covarrubias *et al.* 2009; Lee and Glaunsinger 2009; Kumar and Glaunsinger 2010). The second phenotype was a

relocalisation of the cytoplasmic poly(A) binding protein (PABPC) to the nucleus, which was visualised using immunofluorescence assays (Covarrubias *et al.* 2009; Lee and Glaunsinger 2009; Kumar and Glaunsinger 2010). PABPC is a nuclear-cytoplasmic shuttling protein (Afonina *et al.* 1998) that plays a role in mRNA stability and translation (Tarun and Sachs 1995), hence its relocation may prevent export of nuclear mRNA and destabilise mRNA in the cytoplasm. However, no direct binding of ORF37 with PABPC was identified in these studies (Covarrubias *et al.* 2009; Lee and Glaunsinger 2009), suggesting that ORF37 is interacting with other cellular factors to cause these phenotypes. As can be seen from these studies host shutoff by ORF37 is a complex process which still needs further investigation.

6.2 Experimental design

Due to previous studies in KSHV and MHV-68 suggesting a link between mRNA decay and an increase in poly(A) tail length (Covarrubias *et al.* 2009; Lee and Glaunsinger 2009; Kumar and Glaunsinger 2010), the 3' end of cellular mRNA was investigated. Previous studies had used transfected cells and probes for GFP as the reporter mRNA. In this chapter the effect of ORF37 in the context of a lytic infection with MHV-68 on cellular poly(A) tail length mRNA was investigated. Total RNA was isolated from mock-infected, MHV-68-infected and ORF37Stop virus-infected cells. The poly(A) tail was radiolabelled followed by enzymatic digestions to remove mRNA. The labelled poly(A) tails were then resolved by PAGE and visualised using a PhosphorImager (Temme *et al.* 2004). Infections were carried out in immunocompetent NIH3T3 and IFNαβRKO cells.

6.3 Results

6.3.1 Poly(A) tail length in MHV-68 infected cells

To investigate the effect of MHV-68 infection on the 3' cellular mRNA poly(A) tail lengths, total cellular RNA was examined that was harvested from either mock-infected cells or cells infected with MHV-68 viruses of interest. NIH3T3 cells were either mock-infected or virus-infected and 24 hours post-infection total RNA was harvested from cells and DNase I treated. Poly(A) tails were labelled with [α-^{32}P] dATP, digested to remove mRNA and resolved on 10% polyacrylamide/urea gels. Figure 6.1 shows a representation of the banding pattern seen with the poly(A) tail assay of RNA from mock-infected and MHV-68-infected cells. Initial visual inspection of lanes corresponding to mock-infected and virus-infected samples did not show any apparent difference in the overall size distribution of poly(A) tail lengths, although MHV-68 infected profiles did appear to be slightly lighter near to the top of the lane in the region of higher molecular weight RNA. To quantify any possible difference in bulk poly(A) tail distribution between mock and virus-infected samples, images were analysed using the ImageQuant software that measures the intensity of bands. The relative intensity profiles of poly(A) tail lengths in samples from mock and virus-infected cells were found to be similar (Figure 6.2).

Previous studies had suggested that ORF37 causes hyperadenylation (Covarrubias *et al.* 2009; Lee and Glaunsinger 2009; Kumar and Glaunsinger 2010). Therefore, the gel region where higher molecular weight poly(A) tail fragments are expected to resolve were investigated using the poly(A) tail assay. Based on empirical observations, samples which were resolved over a two hour run period were chosen to investigate the impact of MHV-68 on lengthening on poly(A) tails. As Figure 6.1

shows, no apparent difference was observed in the population of mRNA with longer poly(A) tails between mock-infected and virus-infected samples . ImageQuant was then used to assess the band intensities of poly(A) tail fragments between the two samples. Again no obvious difference could be identified between the two profiles (Figure 6.3).

However, when the two poly(A) tail profiles from mock and WT MHV-68-infected mRNA for both shorter poly(A) tails (75-200 nt) and longer poly(A) tails (200-775 nt) were compared there were areas on both graphs that showed some difference (Figure 6.4). Statistical analysis of the data indicated that although some regions exhibited no difference in intensities other regions were significantly different ($p < 0.001$). For shorter poly(A) tails, there appeared to be a greater intensity of poly(A) tails in the regions of 80-100 nt and 130-155 nt in length in MHV-68 infected cells when compared to mock-infected cells with an average 10% increase in relative intensity in the regions highlighted (Figure 6.4A). In terms of the longer poly(A) tails, there was a decrease in poly(A) tail intensity at approximately 225-450 nt in MHV-68 infected cells compared to mock infected with an average 12% decrease in intensity (Figure 6.4B). Taken together, these results suggest a shortening of some poly(A) tails in MHV-68 infected cells.

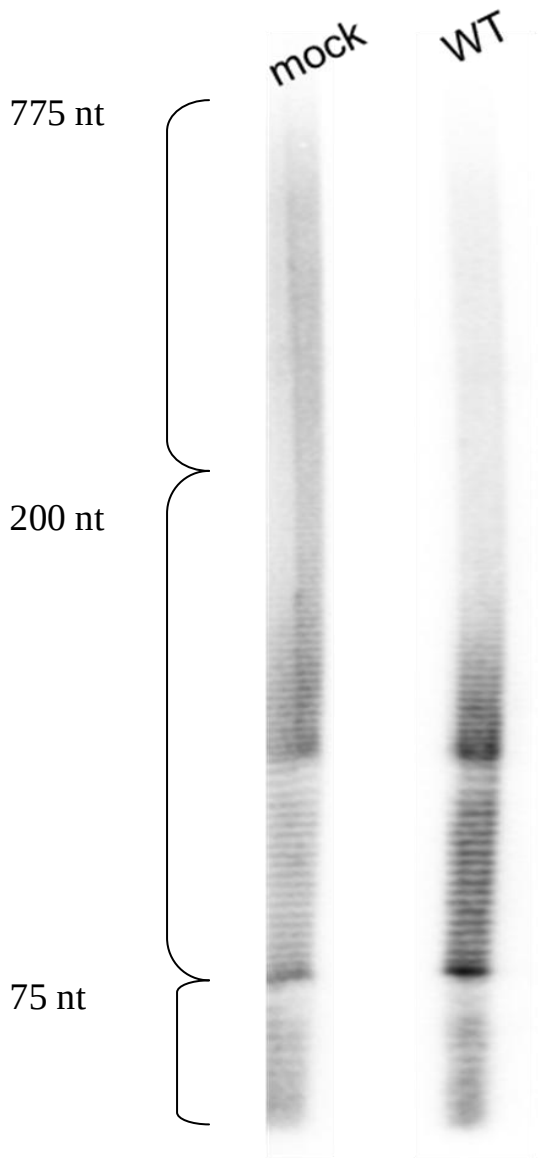

Figure 6.1 Poly(A) tail profile from mock and WT infected NIH3T3 cells. Five μg of total RNA was labelled with [α-^{32}P]dATP, the RNA was then purified by phenol/chloroform extraction and ethanol precipitation and re-suspend in 20 μl of Sigma water. Labelled RNA (10^6 counts) was digested with RNase A/T1, after 30 minutes the reaction was stopped and the remaining RNA was ethanol precipitated and separated on a 10% polyacrylamide/urea gel. Gels were analyzed on a PhosphorImager and data were analysed using the ImageQuant program. Representative banding pattern of poly(A) tail profiles of mock and WT MHV-68 infected NIH3T3 cells seen on 4 gels, with on average 3 RNA samples per infection ran in duplicate (approximate sizes are indicated).

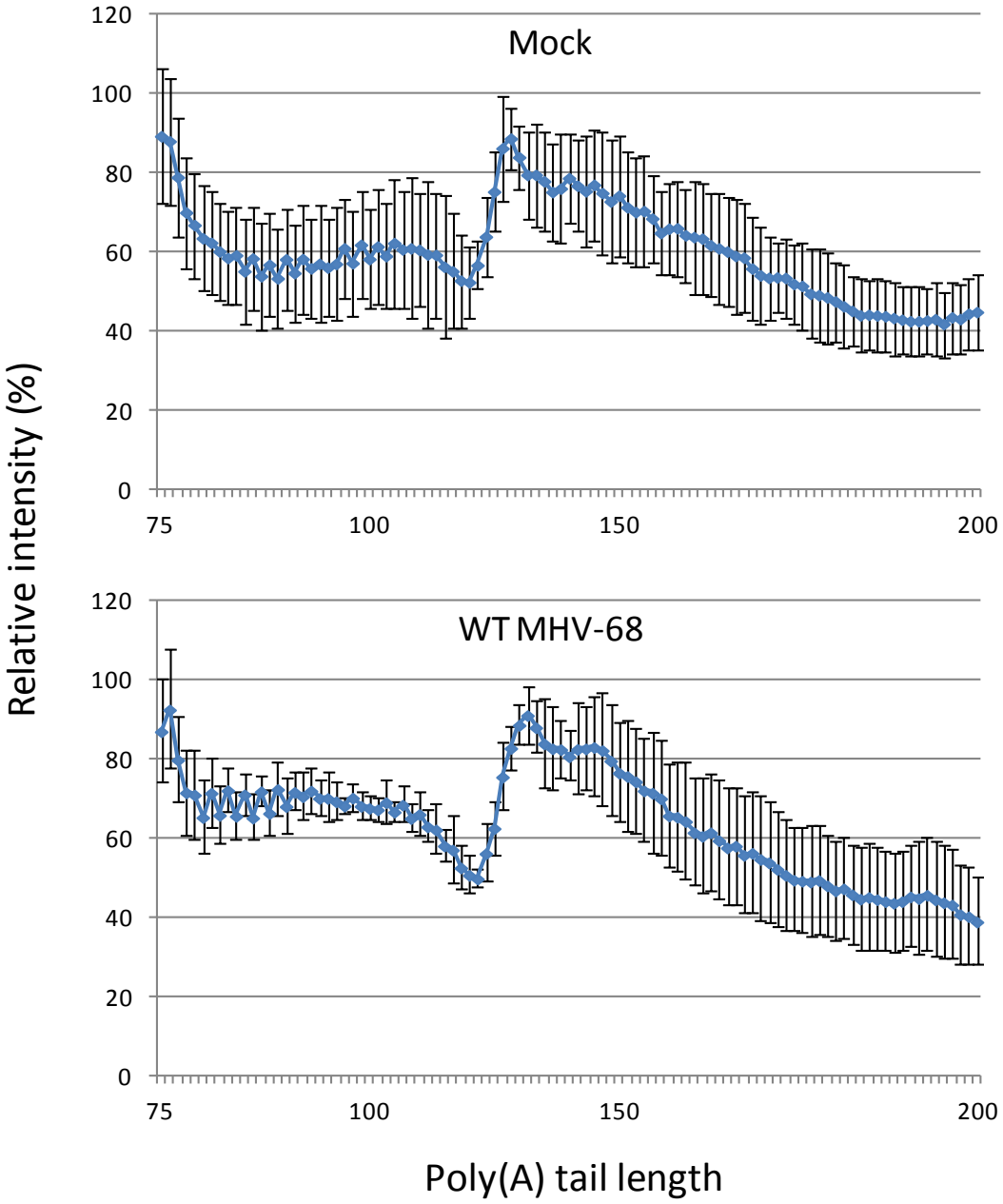

Figure 6.2 Comparison of poly(A) tail profile from mock- and WT-infected NIH3T3 cells. Total RNA was harvested and poly(A) tails labelled and resolved as described in figure legend 6.1. Gels were analyzed on a PhosphorImager and data were analysed using the ImageQuant program. Relative intensity of bands from mock and WT MHV-68 RNA covering 75-200 nt in length, information pooled from two gels +/-SD.

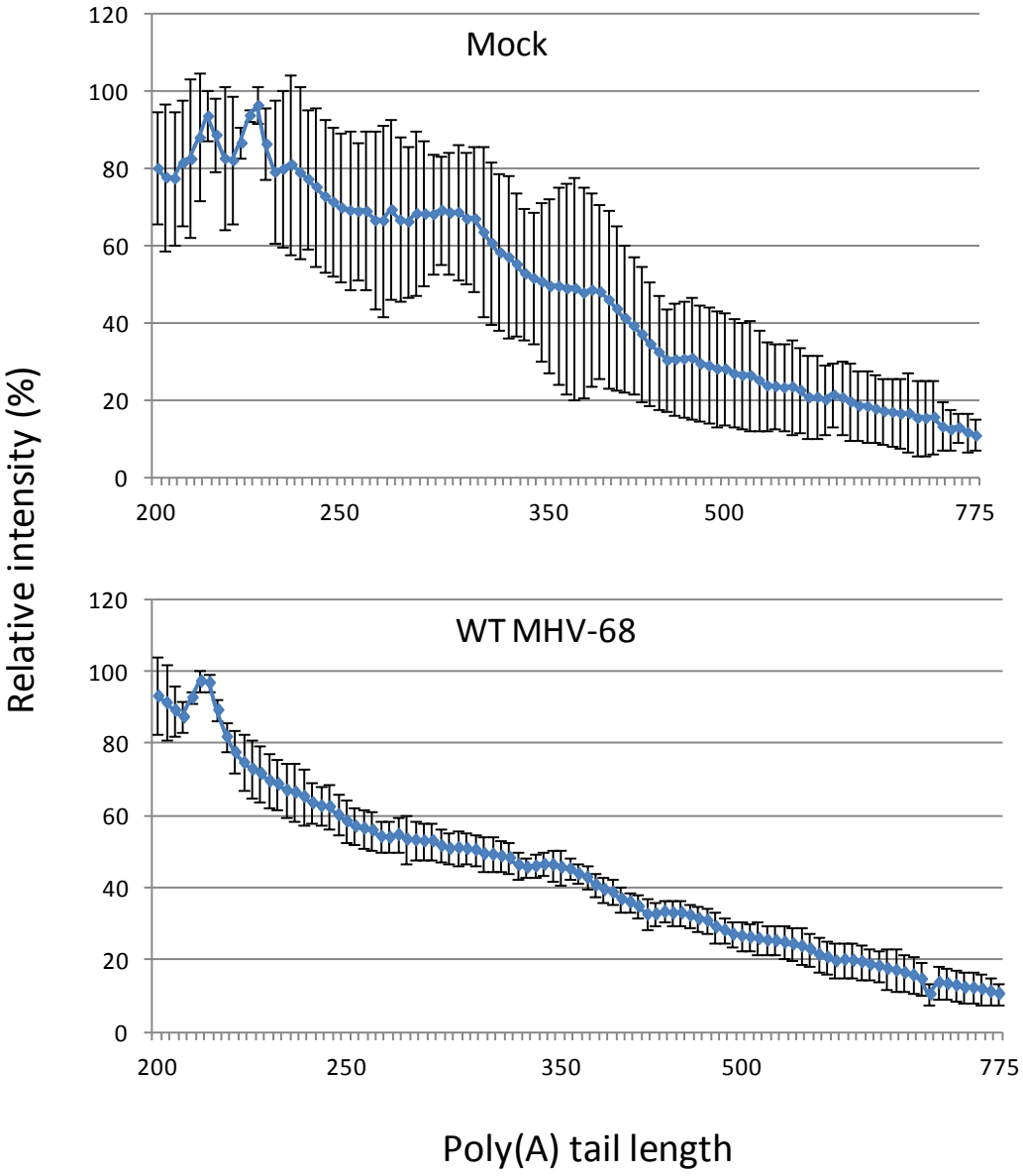

Figure 6.3 Analysis of longer poly(A) tail profile from mock and WT infected NIH3T3 cells. Total RNA was harvested and poly(A) tails labelled and resolved as described in figure legend 6.1. Gels were analyzed on a PhosphorImager and data were analysed using the ImageQuant program. Relative intensity of bands from mock and WT RNA covering 200-775 nt in length, information pooled from two gel +/-SD.

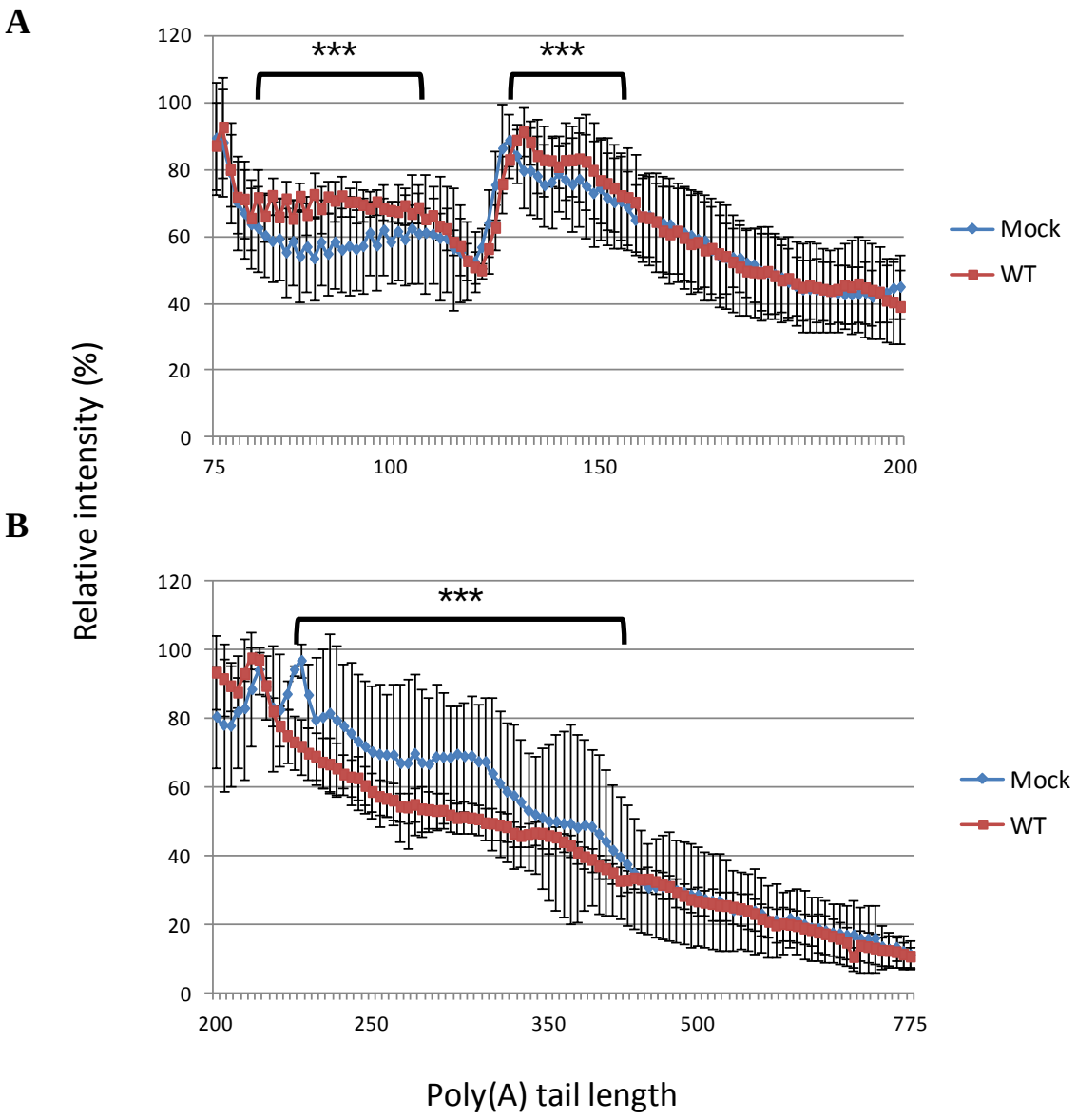

Figure 6.4 Analysis of longer poly(A) tail profile from mock and WT infected NIH3T3 cells. Total RNA was harvested and poly(A) tails labelled and resolved as described in figure legend 6.1. Gels were analyzed on a PhosphorImager and data were analysed using the ImageQuant program. **A)** Graph comparing relative intensity of Poly(A) tails in the region of 75-200 nt from mock and WT (MHV-68) infected cells +/- SD **B)** Graph comparing relative intensity of Poly(A) tails in the region of 200-775 nt from mock and WT (MHV-68) infected cells +/- SD. *** = p>0.001

6.3.2 Characterisation of poly(A) tail lengths in αβRKO cells infected with MHV-68, ORF37Stop and ORF37StopRev

As described in previous chapters, the ORF37Stop virus was found to cause mRNA degradation in IFNαβRKO cells in stark contrast to infection in immunocompetent cells thus suggesting host shutoff can still procced in an immune-compromised cellular enviroment and absence of ORF37. This led to the question of whether poly(A) tail distribution was similar or different in IFNαβRKO cells infected with MHV-68 or ORF37Stop mutant virus. To address this question, poly(A) tail distribution was assayed from mock-infected IFNαβRKO cells and IFNαβRKO cells infected with wild type MHV-68 and ORF37Stop mutant virus as described previously for NIH3T3 infections (Section 6.3.1).

The results from the gels showed comparable bulk poly(A) tail distributions (Figure 6.5). This was corroborated when images were analysed using the ImageQuant where the profiles for 75-200 nt in length were very similar between the groups (Figure 6.6). Similarly, when the bands from the top of the gel were analysed they also exhibited very similar poly(A) profiles for mock, MHV-68, and ORF37Stop infected cells (Figure 6.7). However, when the three profiles from Mock, MHV-68 and ORF37Stop infected cells were plotted on the same graph for both shorter poly(A) tails (Figure 6.8A) and longer poly(A) tails (Figure 6.8B) some areas appeared to show some differences. Figure 6.8A had two regions where a significant difference was identified ($P>0.001$); the first is at approximately 75-85 nt and in this region both MHV-68 and ORF37Stop infected cells exhibited a lower intensity of poly(A) tails compared to mock-infected samples. The second region is at approximately 140-170 nt and in this region the ORF37Stop infected cells show a

higher intensity of poly(A) tails when compared to MHV-68 and mock infected. Figure 6.8B had one area of significant difference in the region of 225-300 nt within this area the MHV-68 and ORF37Stop infected cells exhibited a lower intensity of poly(A) tails when compared to mock infected, similar to the result seen in NIH3T3 cells for wildtype virus (Figure 6.4B). Overall there was no obvious shift in poly(A) tail length distribution.

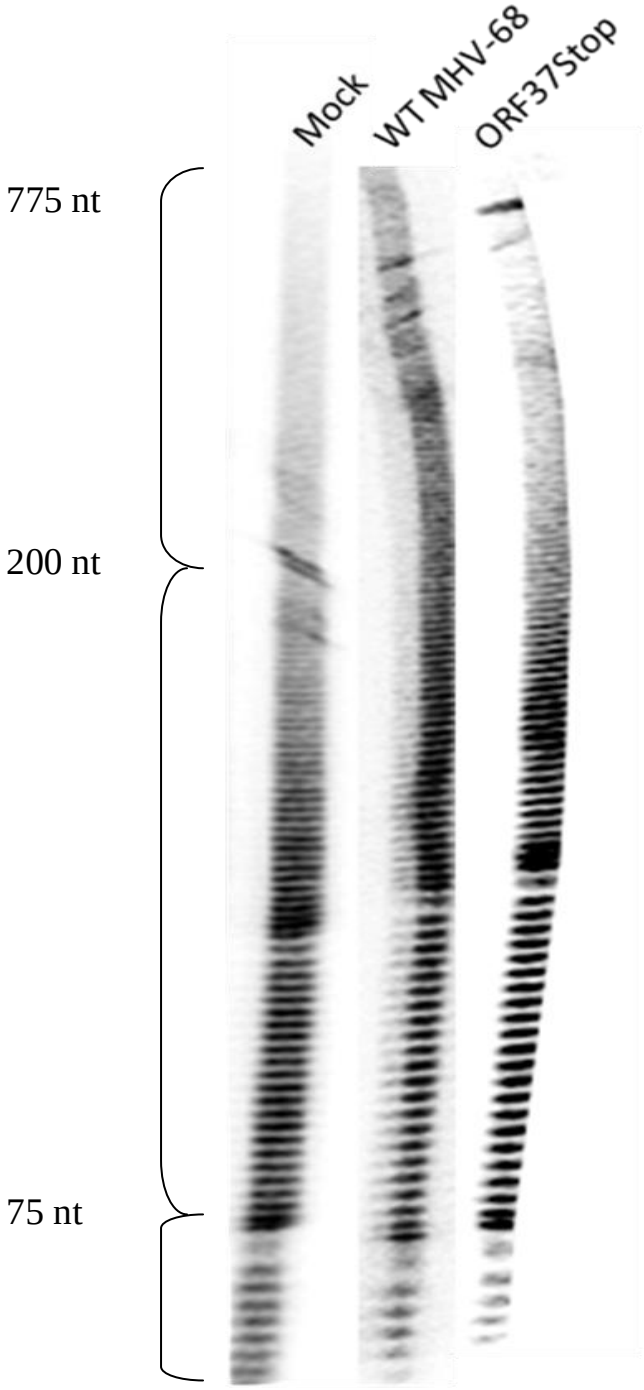

Figure 6.5 Poly(A) tail profiles in IFNαβRKO cells infected with wild type MHV-68 and ORF37Stop mutant virus. Total RNA was harvested and poly(A) tails labelled and resolved as described in figure legend 6.1. Representative banding patterns of poly(A) tail profiles from gels showing mock, WT MHV-68 and ORF37Stop infected αβRKO cells seen on 4 gels, with on average 3 RNA samples per infection ran in duplicate (approximate sizes are indicated).

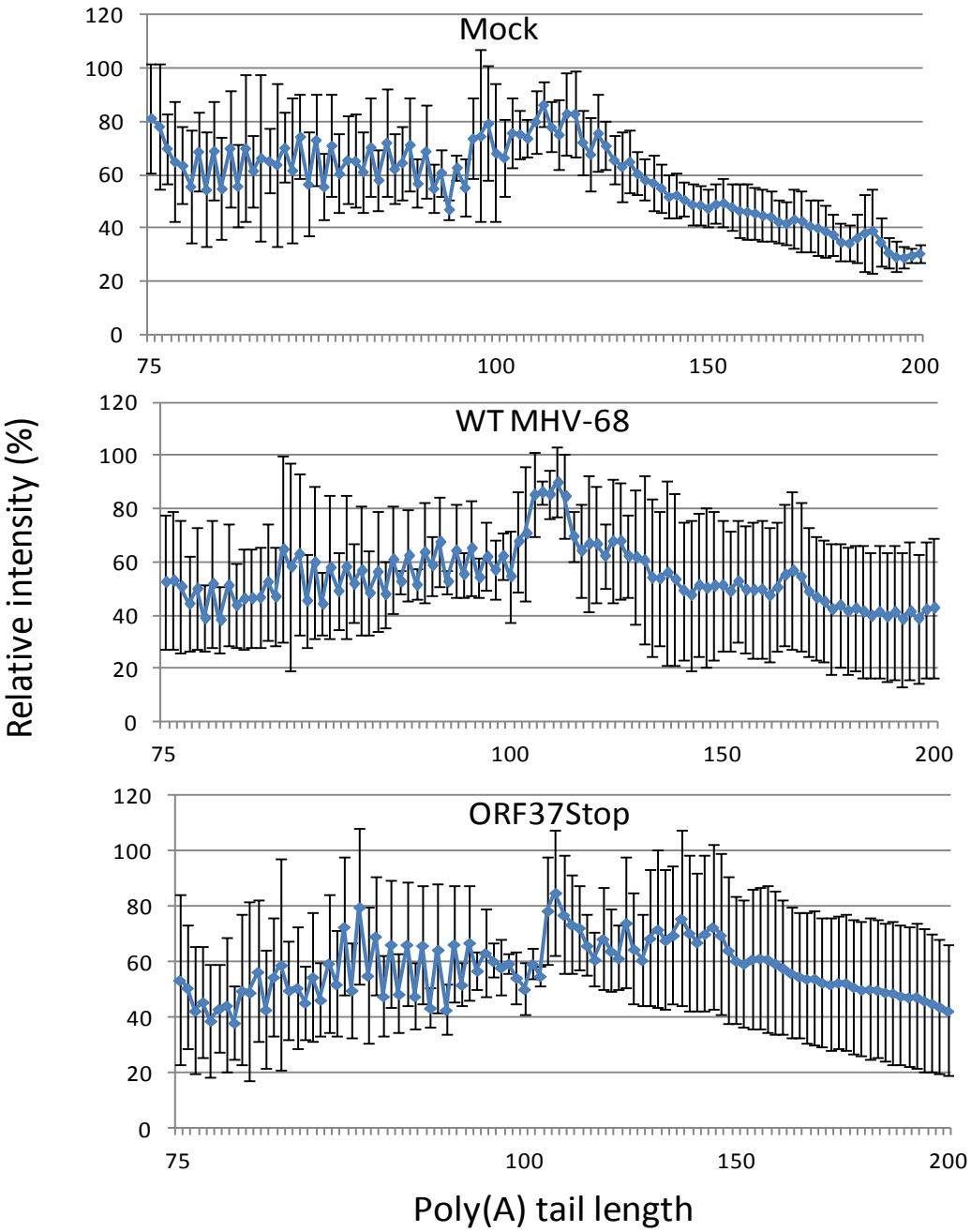

Figure 6.6 Comparison of poly(A) tail profiles from MHV-68 and ORF37Stop mRNA from IFNαβRKO cells. Total RNA was harvested and poly(A) tails labelled and resolved as described in figure legend 6.1. Gels were analyzed on a PhosphorImager and data were analysed using the ImageQuant program. Relative intensity of poly(A) tail bands from cells either mock-infected, infected with wild type virus or with ORF37Stop mutant virus covering 75-200 nt in length. Band intensities were obtained from two separate gels +/-SD.

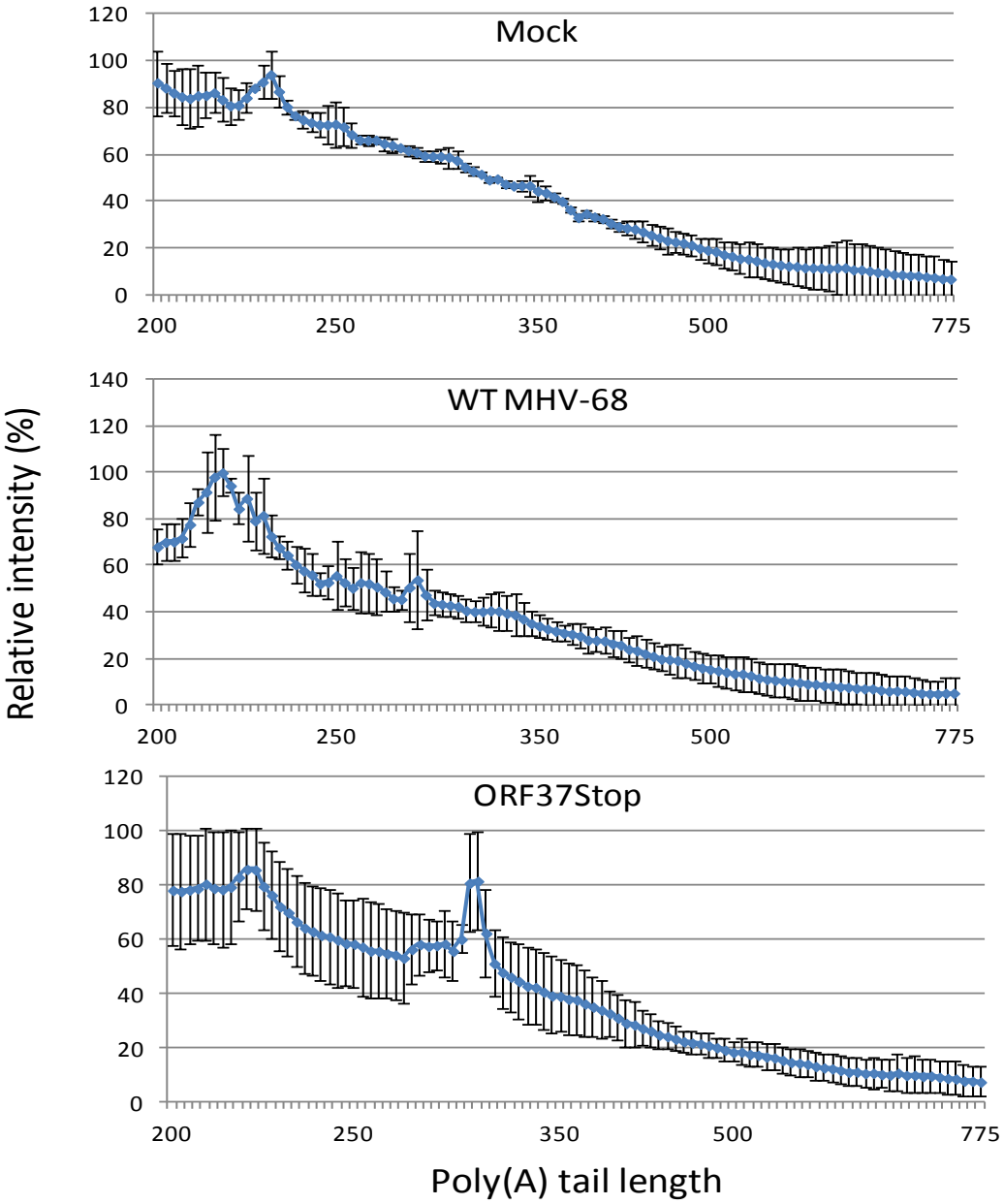

Figure 6.7 Comparison of poly(A) tail profiles from MHV-68 and ORF37Stop mRNA from IFNαβRKO cells. Total RNA was harvested and poly(A) tails labelled and resolved as described in figure legend 6.1. Gels were analyzed on a PhosphorImager and data were analysed using the ImageQuant program. Relative intensity of poly(A) tail bands from cells either mock-infected, infected with wild type virus or with ORF37Stop mutant virus covering 200-775 nt in length. Band intensities were obtained from two separate gels +/-SD.

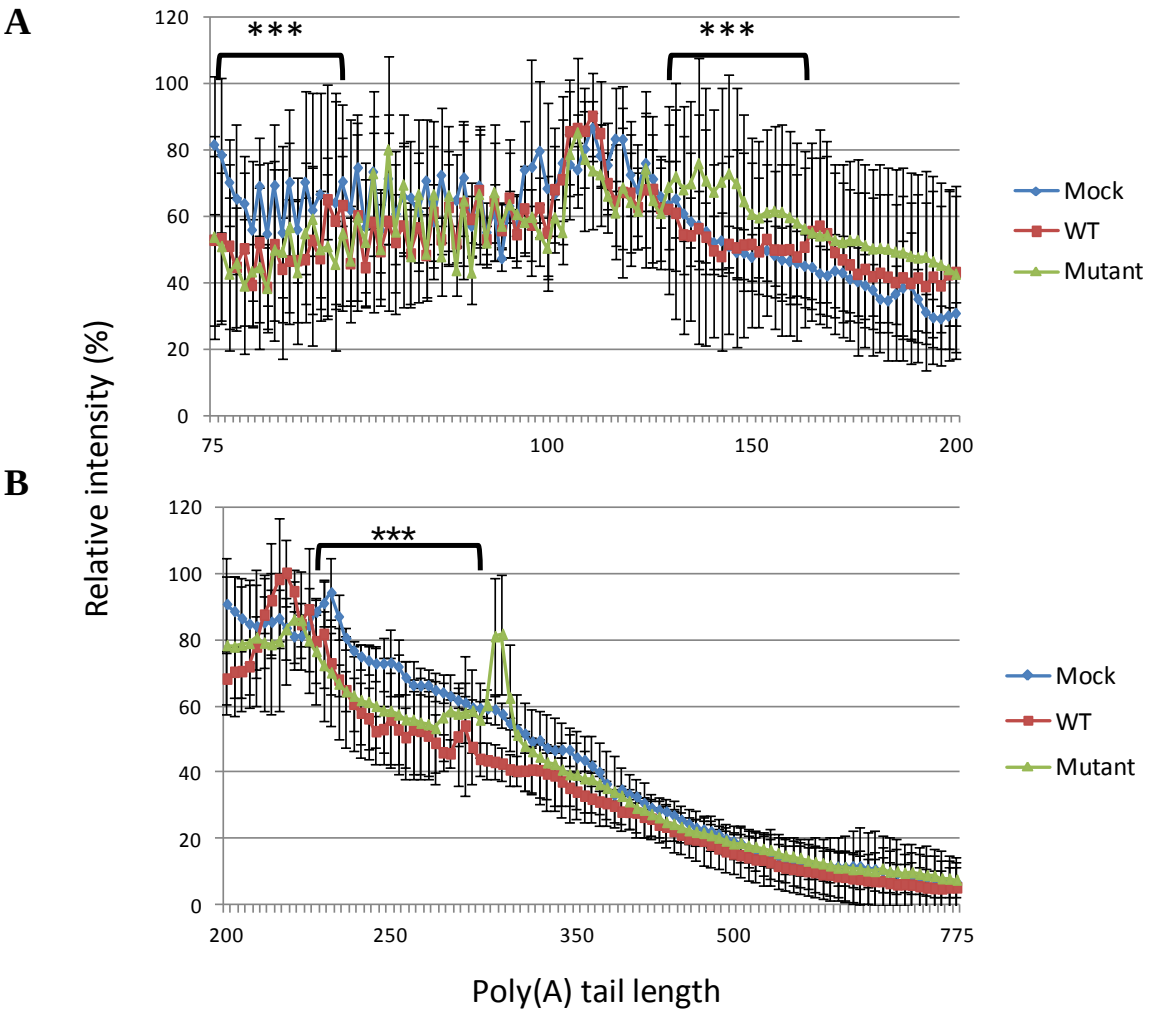

Figure 6.8 Comparison of poly(A) tail profiles from MHV-68 and ORF37Stop mRNA from IFNαβRKO cells. Total RNA was harvested and poly(A) tails labelled and resolved as described in figure legend 6.1. Gels were analyzed on a PhosphorImager and data were analysed using the ImageQuant program. Relative intensity of poly(A) tail bands from cells either **A)** Graph comparing relative intensity of Poly(A) tails in the region of 75-200 nt from mock, WT (MHV-68) or ORF37Stop infected cells +/- SD **B)** Graph comparing relative intensity of Poly(A) tails in the region of 200-775 nt from mock, WT (MHV-68) and ORF37Stop infected cells +/- SD. *** = p>0.001

6.4 Discussion

The method of radio labelling 3' RNA, digestion with RNases and visualisation using gel sequencing methods was first described by Ahlquist and Kaesburg in 1979, who used the method to examine the length distribution of viral RNAs (Ahlquist and Kaesberg 1979). Since then the method has been refined and updated and used in a number of studies to analyse poly(A) tail length in both fungi (Morozov *et al.* 2010) and flies (Temme *et al*. 2004). This method was employed in this chapter as a tool to investigate the bulk cellular poly(A) tail length distribution in both mock and MHV-68 infected cell, as previous studies have focused on GFP mRNA in transfected cell lines (Covarrubias *et al.* 2009; Lee and Glaunsinger 2009; Kumar and Glaunsinger 2010).

The results from Figures 6.1 and 6.2 suggest that there is little difference between bulk poly(A) tail lengths of mock and MHV-68 infected transcripts as the poly(A) profiles follow a similar trend for poly(A) tails ranging from 75-200 nt in length. The results from the NIH3T3 infections suggested that infection with MHV-68 was not affecting the poly(A) tail length (Figure 6.1 & 6.2). However previous studies using RNase H assays to look at the poly(A) tail length of GFP mRNA have suggested that ORF37 causes hyperadenylation (Covarrubias *et al.* 2009; Lee and Glaunsinger 2009; Kumar and Glaunsinger 2010). Therefore, the gel regions corresponding to higher molecular weight poly(A) tails were investigated further. The poly(A) tail distributions from these regions suggested that the mock infected poly(A) tails were slightly longer when compared to a similar region for poly(A) tail population in cells infected with WT-MHV-68, suggesting a decrease in poly(A) tails rather than hyperadenylation (Figure 6.1). Image analysis of the bands revealed that the relative

intensities were very similar (Figure 6.3). Further analysis of the data through plotting the data on the same graphs to highlight areas of difference along with looking for areas exhibiting significant differences did indicate that some changes may occur to poly(A) tail length in MHV-68 infected cells, as the poly(A) tails were shorter in virus-infected cells when compared to mock-infected controls (Figure 6.4).

As mRNA degradation had also been indentified in ORF37Stop infected immuno-compromised cells (Chapter 4), the next objective was to see if any variation could be identified in IFNαβRKO cells infected with ORF37Stop mutant when compared to cells infected with the wild type virus. This may indicate a difference in the mechanism of host shutoff employed in an ORF37 mutant virus in cells lacking a response to type I IFN (in IFNαβRKO cells) when compared to infection in immunocompetent cells. Therefore, IFNαβRKO cells were infected with these viruses and total RNA harvested for use in poly(A) tail assays. The results showed comparable band intensities and size distribution between the samples (Figure 6.5); very similar poly(A) tail profiles in the region of 75-200 nt (Figure 6.6) and in 200-775 nt regions (Figure 6.7). The findings from the comparison of intensity profiles did highlight some areas where a significant difference could be identified (Figure 6.8). However, the differences did not point to either a lengthening or shortening of poly(A) tails in infected cells and so would need to be investigated further. Also the poly(A) tails from ORF37Stop infected cells were very similar to MHV-68 infected cells with only one region showing a significant difference suggesting that the mutant virus is acting in a similar way to the WT virus.

The results described in this chapter were not as expected, as hyperadenylation was not seen in MHV-68 infected NIH3T3 or IFNαβRKO cells as was reported previously (Covarrubias *et al.* 2009; Lee and Glaunsinger 2009; Kumar and Glaunsinger 2010). One possible explanation is that their experiments focused on the use of transfection experiments using GFP as a marker, whereas our study used virus infections and their impact on global cellular mRNA. Another key observation identified in previous studies is the relocalisation of PABPC from the cytoplasm to the nucleus (Covarrubias *et al.* 2009; Lee and Glaunsinger 2009; Kumar and Glaunsinger 2010), which has also been seen upon infection with MHV-68 (Richner *et al.* 2011). The relocalisation of PABP is a feature seen in a number of viral infections (reviewed by Smith and Gray 2010) and so far in the γ-herpesviruses it has been linked to mRNA turnover, but not hyperadenylation (Lee and Glaunsinger 2009). A way forward will be the use of other assays such as the ligation-mediated poly(A) test (LM-PAT), which uses cDNA synthesis from an oligo(dT) primer followed by PCR amplification. Following PCR amplification samples are visualized on polyacrylamide gels with short tails producing a compact band and long tails appearing as a smear. Alternatively, the more direct method of RNase H assays can be conducted, which involves the removal of the poly(A) tail followed by the direct comparion of deadenylated mRNA with polyadenylated mRNA using Northen blotting (reviewed by Murray and Schoenberg 2008).

Chapter Seven

Final discussion

The γ-herpesviruses are double-stranded DNA viruses that are of medical and veterinary importance due to their ability to cause lymphoproliferative diseases, as well as lymphomas and non-lymphoid cancers in their respective hosts. The species specificity of γ-herpesviruses has limited the study of human γ-herpesviruses in animal models. Over the years, murine gammaherpesvirus 68 (MHV-68) has been developed as an amenable model to study γ-herpesviruses within their natural hosts (reviewed by Barton *et al.* 2011). Differences can be identified between MHV-68 and EBV and KSHV for example, MHV-68 is distantly related to the human γ-herpesviruses (McGeoch *et al.* 2005) and genome analysis has revealed that the γ-herpesviruses, including MHV-68 contain virus-specific genes (Virgin *et al.* 1997). However the MHV-68 genome also contains large blocks of conserved γ-herpesvirus genes (Virgin *et al.* 1997) and in terms of pathogenesis all γ-herpesviruses have conserved the ability to cause lymphoproliferative diseases. Therefore some aspects of γ-herpesvirus pathogenesis may be different, but the core pathogenic strategies appear to be conserved (reviewed by Barton *et al.* 2011). These observations and the relative ease of constructing gene deletion mutant MHV-68 viruses (Adler *et al.* 2000; Adler *et al.* 2003) have made MHV-68 a powerful model for the study of γ-herpesvirus pathogenesis.

A feature of infection with a number of lytic viruses is loss of cellular proteins, a phenomenon termed host shutoff (Tables 1.4 & 1.5). More recently host shutoff was identified in γ-herpesviruses linked to viral DNA exonuclease, encoded by ORF37

(in KSHV and MHV-68) and BGLF5 (in EBV) (Glaunsinger and Ganem 2004b; Rowe *et al.* 2007; Covarrubias *et al.* 2009). Furthermore, in γ-herpesviruses, ORF37 (and BGLF5)-mediated host shutoff is now believed to be post-transcriptional and at the level of mRNA (Glaunsinger and Ganem 2004b; Rowe *et al.* 2007). The significant loss of cellular mRNA is a key component of disease pathogenesis as a result of infection with these viruses and therefore an important area of herpesvirology research worldwide.

At the onset of this study, the role of ORF37 (and BGLF5) in mediating host shutoff was not entirely clear. This was because ORF37 and BGLF5 are primarily alkaline DNA exonucleases believed to play a role in viral genomic DNA encapsidation (Martinez *et al.* 1996; Goldstein and Weller 1998). This function had made deletion of these viral genes in their respective genomes difficult (Covarrubias *et al.* 2009; Feederle *et al.* 2009). Therefore, the primary purpose of this study was to generate a mutant of MHV-68 ORF37 to investigate the role of viral DNA exonuclease in host shutoff *in vitro* and *in vivo*. Initially, an ORF37 mutant virus (ORF37Stop) was constructed using the BAC technology in collaboration with Dr Bernadette Dutia (University of Edinburgh), which generates premature stop codons in all possible reading frames at the beginning of the ORF37 gene. Previously conducted experiments had indicated that retrieval of the ORF37Stop BAC virus from immunocompetent MEF cells was difficult. This suggested that lack of function (s) afforded by the ORF37 product is vital in virus growth and subsequent egress from infected cells. This phenotype has also been identified in other studies where the partial or complete deletion of the ORF37 gene or its homologues had taken place (Covarrubias *et al.* 2009; Feederle *et al.* 2009). Studies carried out on an ORF37

deletion mutant had suggested that ORF37 plays an essential role in viral DNA replication (Covarrubias *et al.* 2009). Furthermore, work carried out on the EBV BGLF5 null virus had found that maturation, egress and viral DNA synthesis were impaired in this mutant virus but BGLF5-null virus was morphologically intact, suggesting that BGLF5 plays a modulatory role, rather than an essential role in EBV replication (Feederle *et al.* 2009).

The observation that MHV-68 ORF37 mutant was severely restricted in forming plaques in immunocompetent cells is also similar to observations made with HSV-1 AE mutants, where it was shown that infection of HSV-1 AE mutants could grow, albeit in a significantly restricted manner in Vero cells (Weller *et al.* 1990). This and other studies also showed viral AE is not essential for viral DNA synthesis (Weller *et al.* 1990; Smiley 2004). This raises the issue of how nuclease mutant viruses process their genomic DNA for example in resolution of viral DNA intermediates. It was shown that plasmid DNA recombination can occur with very high efficiency in cells infected with an AE mutant of HSV-1, suggesting a role for cellular nucleases in resolution of Holliday junctions, which exist during herpesviral genomic DNA replication (Martinez *et al.* 1996). A number of cellular nucleases have since been shown to share amino acid and structural similarities to viral nucleases, for example flap endo/exonucleases (Lieber 1997; Tomlinson *et al.* 2010). Of relevance here is the observation that HSV-1 vhs (but not HSV-1 AE) shares amino acid sequence homology to a flap endo/exonucleases, FEN-1 (Smiley 2004). Therefore, in some circumstances, cell-derived nucleases can compensate for loss of viral nuclease activity, which may explain, at least in part, plaque formation in exonuclease mutant viruses. Studies carried out using signature-tagged mutagenesis to identify essential

and attenuated genes in MHV-68 infection, had found ORF37 to be non-essential in BHK-21 cells (Song *et al.* 2005), but attenuated in Vero cells (Moorman *et al.* 2004), suggesting that the cell type in which the mutant virus is grown will have an impact on the ability of these viruses to complete a successful cycle of infection. These observations prompted attempts to grow MHV68 ORF37Stop virus in other cell types.

Type I interferons are the most potent anti-viral cytokines known to-date. The importance of the innate immune response to MHV-68 is well documented (Dutia *et al.* 1999; Nash *et al.* 2001). This along with the increased susceptibility of HSV1 vhs mutant viruses to IFNα and IFNβ highlights the importance of the Type I interferons (Suzutani *et al.* 2000). Therefore, attempts were made to propagate the MHV-68 ORF37Stop virus in cells defective in type I IFN receptor knockout cells.

As shown in chapter three, the ORF37Stop virus was able to grow in IFNαβRKO cells, which was in concordance with work carried out on HSV-2 vhs mutant viruses which also showed attenuated growth in immunocompetent MEF cells, growth of which was partially or completely restored in IFNαβRKO cells (Duerst and Morrison 2004). Replication of the ORF37Stop virus was then investigated in lungs (site of lytic infection) of IFNαβRKO mice. When compared to WT and ORF37StopRev the viral titres were similar three days post infection, but were attenuated six days post infection (Figure 3.4). These results accord well with work carried out on HSV-2 vhs mutants, which also showed no attenuation of virus growth in IFNαβRKO cells (Duerst and Morrison 2004), but attenuated growth was observed in the genital mucosa (site of HSV-2 lytic infection) in IFNαβRKO mice after reaching similar

titres for first two days post infection (Murphy *et al.* 2003). These findings along with the results from this study imply that *in vivo* the ORF37 (or vhs in HSV-2) mutant viruses may be more susceptible to other immune mediators.

The findings in chapter three and data from Murphy *et al.* implicate the importance of host shutoff afforded by vhs (for HSV-2) and ORF37 (in γ-herpesviruses) for evading immune responses during lytic infection (Murphy *et al.* 2003). Paradoxically, the study by Richner *et al* found that growth of a host shutoff mutant of MHV-68 in C57BL/6 mice lungs was not attenuated, suggesting that host shutoff does not play an important role in lytic infection, whereas it was suggested that virus host shutoff activity played a role in establishment of latency (Richner *et al.* 2011). One possible reason for the discrepancy between our study (and HSV-2 vhs) and Richner *et al.* is that the host shutoff mutant virus constructed by Richner and colleagues, was generated via a point mutation, which still showed residual mRNA degradation compared to mock infected cells. It was suggested by Richner *et al.* that the host shutoff activity still present in infection with their ORF37 mutant virus may be due to either incomplete inactivation of the host shutoff function or other viral genes contributing towards host shutoff (Richner *et al.* 2011).

To study further the effect of ORF37 during infection mRNA and protein levels were investigated from IFNαβRKO infected cells. Loss of cellular transcripts was observed in cells infected with ORF37Stop virus when compared to mock-infected IFNαβRKO cells (Figures 4.2-4.4). Moreover, loss of mRNA was also reflected at the protein level (Figure 4.5). These findings led to the conclusion that in immune-compromised cells host shutoff is taking place regardless of the presence or absence

of ORF37, suggesting that another host shutoff factor (cellular/viral) may be causing loss of mRNA. Host shutoff has not, as yet, been linked to any other proteins in γ-herpesvirus infections. The original study that led to the discovery of ORF37 used a transfection method to screen each KSHV gene individually for its ability to cause host shutoff and their results indicated that ORF37 was the only gene linked to a significant decrease in GFP expression (Glaunsinger and Ganem 2004b). However, other genes may cause host shutoff to a lesser degree and it may be that this can best be seen in an immune-compromised cell line.

A dual method of host shutoff has been well characterised in HSV-1 infection, the first is through ICP27, which causes a re-distribution of snRNPs, disrupting the splicing machinery (Phelan *et al.* 1993; Hardwicke and Sandri-Goldin 1994) and the second is through the RNase activity of vhs protein (Zelus *et al.* 1996; Everly *et al.* 2002). These two proteins have been found to cause loss of cellular mRNA (reviewed by Smiley 2004) and more recently have been found to interact with each other when bound to other proteins (Taddeo *et al.* 2010). ICP27 is conserved between all members of the herpesvirus family, although they differ in size and the overall sequence homology is low, as even the closest members of the family only share 30% homology in their amino acid residues (reviewed by Majerciak and Zheng 2009). The EBV ICP27 homologue, SM protein, displays similar properties to ICP27 as it has been found to enhance intron-less gene expression and inhibit intron-containing gene expression (Ruvolo *et al.* 1998). The KSHV homologue of ICP27 is ORF57, a viral gene regulator, which has not been found to inhibit splicing of intron-containing genes. This difference in function is probably due to KSHV containing more than 30 intron-containing genes that require active splicing compared to just

four in HSV-1; in EBV only latent genes contain introns suggesting a role for SM in the lytic-latent switch (Ruvolo *et al.* 1998; Smiley 2004a; Majerciak and Zheng 2009). Whether the MHV-68 ICP27 homolog, ORF57, is acting towards host shutoff has not been determined.

Although no obvious link has been made between γ-herpesviruses and a dual host shutoff system infection studies have been carried out on MHV-68 with a deleted ORF37 gene that have indicated that an additional host shutoff factor may be at work. This was first suggested by Covarrubias *et al.* when they compared two different transfection experiments, as they saw a much decreased half-life of GFP in mRNA decay assays when cells were transfected with a deleted ORF37 BAC virus compared to a plasmid transfection in the absence of ORF37. They suggest that this difference may be due to GFP sequence differences and the fact that the transcripts were under the control of different promoters. However they also suggested that it may indicate additional viral host shutoff factors contributing to the instability of the BAC GFP (Covarrubias *et al.* 2009). As discussed previously, a recent paper by Richner *et al.* produced an ORF37 point mutation virus and found that they still observed some mRNA degradation, which they suggest may be due to incomplete deactivation of ORF37 gene or other viral genes contributing to host shutoff (Richner *et al.* 2011).

To gain further insight into the direct effect of MHV-68 ORF37 on mRNA degradation, transient transfections of immunocompetant cells were carried out with an empty vector and a plasmid containing the ORF37 gene and mRNA and protein levels were analysed. Previous studies had used co-transfection of ORF37/BGLF5

plasmids along with GFP as a marker for mRNA loss in mRNA decay assays (Glaunsinger and Ganem 2004b; Rowe *et al.* 2007; Covarrubias *et al.* 2009). However these studies only examined the effect of ORF37/BGLF5 on GFP and not on cellular mRNA. Therefore, the effect of ORF37 on cellular mRNA was investigated in cells transfected with an ORF37 expression vector (FLORF37pcDNA3.1) in transient transfection experiments.

The indications from previous viral infection studies (Ebrahimi *et al.* 2003; Glaunsinger and Ganem 2004b; Rowe *et al.* 2007) and GFP transfection experiments (Glaunsinger and Ganem 2004b; Rowe *et al.* 2007; Covarrubias *et al.* 2009) led to the hypothesis that loss of cellular mRNA ought to be seen in the presence of ORF37 alone. However the qPCR results seen in chapter five were equivocal. Expression of ORF37 at both mRNA and protein levels were confirmed in these experiments (Figures 5.3 & 5.6). One possible explanation is that since transfection efficiency is usually in the order of 20%, the host shutoff activity of ORF37 would have been masked by the majority of the cell population which is untransfected. A recent study by Clyde and Glaunsinger used a marker method to overcome this problem, therefore, only cells which harboured ORF37 (as green cells) were isolated by means of flow cytometry. They found a reduction of most cellular mRNAs in sorted cells, although some loss was still seen in unsorted cells (Clyde and Glaunsinger 2011). These results are in accordance with our findings as the cells were in effect unsorted and did exhibit a degree of loss of cellular mRNA, but not at a significant level. In searching for patterns in mRNA degradation, Clyde and Glaunsinger did notice that in the majority of cases the more abundant mRNAs experience a higher level of downregulation compared to rare mRNAs (Clyde and Glaunsinger 2011). However

this correlation is imperfect as increasing the abundance of some cellular genes did not make them susceptible to SOX, suggesting that some cellular genes can escape host shutoff (Glaunsinger and Ganem 2004a; Clyde and Glaunsinger 2011). In contrast to a previous study which had suggested that the presence of AREs in their 3' UTR of mRNAs may lead to stabilisation of mRNA (Chandriani and Ganem 2007) no correlation was identified between the presence of AREs and their loss when compared to transcripts lacking ARE motifs (Clyde and Glaunsinger 2011). These findings have led to the conclusion that other viral factors such as KSHV kaposin B may stabilise ARE containing mRNAs (McCormick and Ganem 2005). Taken together the results from Clyde and Glaunsinger suggest that multiple mechanisms may influence SOX-mediated decay (Clyde and Glaunsinger 2011).

Another important question to be addressed is how MHV-68 ORF37 is causing mRNA degradation. The original studies which identified DNA exonucleases SOX/BGLF5 as the causative agent of mRNA degradation failed to find a direct RNase activity linked to these proteins (Glaunsinger and Ganem 2004b; Rowe *et al.* 2007). Subsequently, protein structure studies demonstrated that SOX and BGLF5 were able to mediate RNA degradation *in vitro*, but only in the presence of high levels of metal ions (Mg^{2+} and Mn^{2+}) (Buisson *et al.* 2009; Bagneris *et al.* 2011). Nucleases utilise metal ions as cofactors for cleavage, although the types and concentrations of metals required vary magnesium and manganese are the most commonly required metals for catalysis (reviewed by Nishino and Morikawa 2002). Whether metal ions at such high concentrations would be found within cells is questionable. In addition SOX exhibits a lower affinity for binding RNA than DNA. Furthermore RNase activity was still seen following mutation of residues which had

previously been found to play an essential role in host shutoff (Bagneris *et al.* 2011). These findings led to the conclusion that other factors such as cellular mRNA decay machinery may be required for host shutoff.

Previous studies using RNase H assays to look at the poly(A) tail length of GFP mRNA have suggested that ORF37 causes hyperadenylation (Covarrubias *et al.* 2009; Lee and Glaunsinger 2009; Kumar and Glaunsinger 2010). In our current study, a method of radio-labelling all poly(A) tails was used to analyse poly(A) tail length distribution in infected cells (Ahlquist and Kaesberg 1979; Temme *et al.* 2004; Morozov *et al.* 2010). The results from chapter six did indicate that some changes may occur in poly(A) tail lengths in MHV-68-infected cells in NIH3T3 cells, as poly(A) tails appeared to be shorter in virus-infected cells when compared to mock-infected cells (Figure 6.4). As mRNA degradation had also been identified in ORF37Stop infected immune-compromised cells (Chapter 4), the next objective was to see if any variation could be observed in poly(A) tail lengths in IFNαβRKO cells infected with ORF37Stop mutant when compared to cells infected with the wild type virus. Comparison of poly(A) tail intensity profiles highlights an apparent difference in these samples (Figure 6.8). However, the apparent differences in band intensities did not point to either lengthening or shortening of poly(A) tails in infected cells. Also the poly(A) tails from ORF37Stop infected cells were very similar to MHV-68 infected cells with only one region showing a significant difference suggesting that the mutant virus is acting in a similar way to the wild type virus. Further detailed analysis of poly(A) tail length distribution are warranted.

In contrast to a previous report, no obvious hyperadenylation was seen in either MHV-68-infected NIH3T3 or IFNαβRKO cells (Covarrubias *et al.* 2009; Lee and Glaunsinger 2009; Kumar and Glaunsinger 2010). One possible explanation for this discrepancy may be that previous experiments used transfected GFP mRNA as a marker. This is in contrast to the approach in this study, where impact of MHV-68 infection was investigated on cellular transcripts and on a global scale. Furthermore, Lee and Glaunsinger found that hyperadenylation was linked to newly transcribed nuclear transcripts rather than the bulk of transcripts located in the cytoplasm. Taking this into consideration, this may explain the discrepancy between the two studies; bulk poly(A) tail more than likely does not represent newly transcribed cellular mRNA. Even so, this does not explain how poly(A) tail lengthening could explain loss of mRNA in virus-infected cells, since almost 50% of cellular mRNA are lost as a result of MHV-68 infection. Therefore, one would expect to detect a significant population of transcripts with lengthened poly(A) tail. The latter was not the case in this study. Interestingly, hyperadenylation was found to be necessary, but not sufficient for host shutoff as inhibition of hyperadenylation resulted in only a partial reduction in mRNA turnover (Lee and Glaunsinger 2009). Another key observation identified in previous studies is the relocalisation of poly A binding protein (cytoplasmic), PABPC, from cytoplasm to nucleus (Covarrubias *et al.* 2009; Lee and Glaunsinger 2009; Kumar and Glaunsinger 2010), which has also been seen upon infection with MHV-68 (Richner *et al.* 2011). The relocalisation of PABPC is a feature seen in a number of other viral infections (reviewed by Smith and Gray 2010). In KSHV, knockdown of PABPN (nuclear) and PABPC (cytoplasmic) leads to a strong inhibition of SOX-induced mRNA degradation highlighting their importance in host shutoff (Lee and Glaunsinger 2009). In contrast to the study by

Lee and Glaunsinger, which found that the poly(A) tail participates in targeting of mRNAs for turnover by SOX in KSHV and MHV-68, a more recent study has suggested a different mRNA degradation process is occurring which is not linked to poly(A) tail (Lee and Glaunsinger 2009; Covarrubias *et al.* 2011). The process that they describe is a two-step mechanism that involves initial removal of the 5' sequences of mRNA via endonucleolytic cleavage followed by exonucleolytic degradation of the fragments by the cellular Xrn1 enzyme. They found that this process occurred during early stages of translation and bypassed the regulatory decapping and deadenylation pathways (Covarrubias *et al.* 2011). Although these studies suggest different mechanisms of SOX-induced mRNA degradation and are in contrast to our findings they also suggest that multiple mechanisms govern SOX-induced host shutoff in the γ-herpesviruses (Figure 7.1). Additionally, the discovery of the relocalisation of PABPC may be in agreement with our findings as it may lead to a destabilization of mRNA leading to deadenylation. Conversely, our results may also indicate that a viral factor other than SOX is causing the differences in poly(A) tail length as no obvious difference was identified between wild type MHV-68 and mutant ORF37Stop infected IFNαβRKO cells, although this will require further investigation.

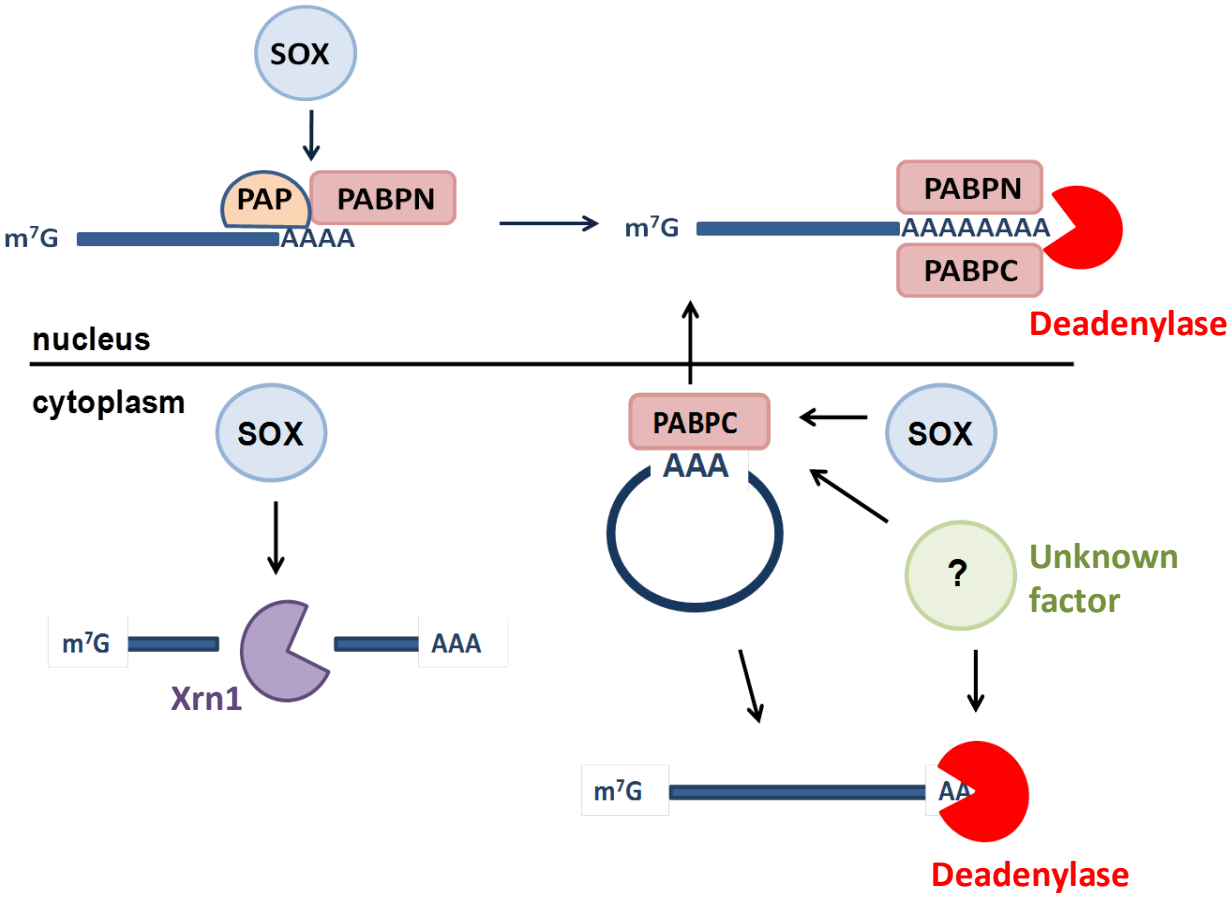

Figure 7.1 Possible mRNA degradation mechanisms employed by ORF37/SOX. ORF37 may induce different mechanisms to induce host shutoff. One such mechanism is via direct endonuclease activity, which in turns leads to the recruitment of the cellular exonuclease Xrn1. Another mechanism is hyperadenylation of newly transcribed transcripts via PABPN and PAP activity, which are then retained in the nucleus and degraded by deadenylases. The other possible process that could be occurring is the relocalisation of PABPC from the cytoplasm to the nucleus, which may destabilize the mRNA leading to degradation via host factors. Additionally another viral or cellular factor may initiate shortening of poly(A) tails, as MHV-68 and ORF37 mutant viruses appear to cause similar effects in IFNαβRKO cells (Information from Lee and Glaunsinger 2009; Covarrubias *et al.* 2011).

In conclusion, the results from this study have shown that an ORF37 mutant can grow in IFNαβRKO cells to a similar level seen in wild-type MHV-68, suggesting the importance of host shutoff in the evasion of the type I IFN response during lytic MHV-68 infection. Furthermore, an ORF37 mutant virus can also be propagated *in vivo*, however, ORF37 does afford a degree of robustness *in vivo*. Interestingly, host shutoff can proceed in IFNαβRKO cells even in the absence of ORF37, suggesting that additional viral/cellular factors may lead to host shutoff in immunocompromised cells. Future investigation into the effect of ORF37 in transfection experiments would require the use of a reporter system, to remove the effect of untransfected cells. The mechanism behind ORF37-induced mRNA degradation appears to be more complex and may involve shortening of cellular poly(A) tails.

7.1 Future work

There are two main areas which require further investigation: (1) the link between the ORF37Stop virus and the Type I IFN system; and (2) mRNA degradation pathways linked to ORF37. One approach would be to conduct *in vivo* experiments to examine the effect of ORF37 mutation during the latent phase of infection. The study by Richner *et al.* found that an ORF37 point mutation virus caused little defect during lytic infection, but decreased latency establishment in immunocompetant mice (Richner *et al.* 2011). It would be interesting to examine latent infection in immunocompromised mice to see if any parallels can be drawn between the ORF37 deletion and point mutation viruses. In addition, it would be interesting to conduct RNA profiling experiments using microarrays or RNAseq on ORF37Stop infected IFNαβRKO cells compared to MHV-68-infected and also compared to MHV-68 infection in an immunocompetant cell line to gauge if differences can be seen in

mRNAs that are down regulated. In addition, mutational analysis of the MHV-68 genome, similar to those carried out by Glaunsinger and Ganem in KSHV (Glaunsinger and Ganem 2004b) could also be executed to try to decipher if another viral factor is causing additional host shutoff in IFNαβRKO cells.

The mRNA degradation mechanism employed by MHV-68 requires further investigation. Although the findings in chapter six are in contrast to previous studies (Lee and Glaunsinger 2009; Covarrubias *et al*. 2011) they do warrant further examination as they may suggest a shortening of some transcripts. A way forward will be the use of other assays such as the LM-PAT assay and the more direct method of RNase H (Murray and Schoenberg 2008).

Other possible mRNA degradation pathways require further investigation such as those described by Covarrubias *et al.* 2011, to see if a link can be made between ORF37 and the cellular degradation machinery. For example co-immunoprecipitation could be used to try to identify protein-protein interactions between ORF37 and cellular mRNA degradation proteins or alternatively biomolecular fluorescence complementation (BiFC) could also be used to identify protein-protein interactions.
Overall the findings from this study have highlighted the importance of MHV-68 ORF37 in innate immune avoidance and in addition have also suggested that another factor may cause host shutoff in the absence of ORF37 in an immunocompromised environment. Furthermore, this study has used a global cellular poly(A) tail assay to investigate mRNA degradation, which suggests that ORF37 may cause poly(A) tail shortening, which along with previously published work points to the highly complex nature of mRNA degradation by ORF37.

References

Ackermann, M. (2006). "Pathogenesis of gammaherpesvirus infections." Vet Microbiol **113**(3-4): 211-222.

Adler, B., E. Schaadt, B. Kempkes, U. Zimber-Strobl, B. Baier and G. W. Bornkamm (2002). "Control of Epstein-Barr virus reactivation by activated CD40 and viral latent membrane protein 1." Proc Natl Acad Sci U S A **99**(1): 437-442.

Adler, H., M. Messerle and U. H. Koszinowski (2003). "Cloning of herpesviral genomes as bacterial artificial chromosomes." Rev Med Virol **13**(2): 111-121.

Adler, H., M. Messerle, M. Wagner and U. H. Koszinowski (2000). "Cloning and mutagenesis of the murine gammaherpesvirus 68 genome as an infectious bacterial artificial chromosome." J Virol **74**(15): 6964-6974.

Afonina, E., R. Stauber and G. N. Pavlakis (1998). "The human poly(A)-binding protein 1 shuttles between the nucleus and the cytoplasm." J Biol Chem **273**(21): 13015-13021.

Ahlquist, P. and P. Kaesberg (1979). "Determination of the length distribution of poly(A) at the 3' terminus of the virion RNAs of EMC virus, poliovirus, rhinovirus, RAV-61 and CPMV and of mouse globin mRNA." Nucleic Acids Res **7**(5): 1195-1204.

Ahmed, M. and D. S. Lyles (1998). "Effect of vesicular stomatitis virus matrix protein on transcription directed by host RNA polymerases I, II, and III." J Virol **72**(10): 8413-8419.

Akula, S. M., P. P. Naranatt, N. S. Walia, F. Z. Wang, B. Fegley and B. Chandran (2003). "Kaposi's sarcoma-associated herpesvirus (human herpesvirus 8) infection of human fibroblast cells occurs through endocytosis." J Virol **77**(14): 7978-7990.

Alvarez, E., A. Castello, L. Menendez-Arias and L. Carrasco (2006). "HIV protease cleaves poly(A)-binding protein." Biochem J **396**(2): 219-226.

Aranda, M. and A. Maule (1998). "Virus-induced host gene shutoff in animals and plants." Virology **243**(2): 261-267.

Areste, C. and D. J. Blackbourn (2009). "Modulation of the immune system by Kaposi's sarcoma-associated herpesvirus." Trends Microbiol **17**(3): 119-129.

Arts, G. J., S. Kuersten, P. Romby, B. Ehresmann and I. W. Mattaj (1998). "The role of exportin-t in selective nuclear export of mature tRNAs." EMBO J **17**(24): 7430-7441.

Bagneris, C., L. C. Briggs, R. Savva, B. Ebrahimi and T. E. Barrett (2011). "Crystal structure of a KSHV-SOX-DNA complex: insights into the molecular mechanisms underlying DNase activity and host shutoff." Nucleic Acids Res.

Barton, E., P. Mandal and S. H. Speck (2011). "Pathogenesis and host control of gammaherpesviruses: lessons from the mouse." Annu Rev Immunol **29**: 351-397.

Bellare, P. and D. Ganem (2009). "Regulation of KSHV lytic switch protein expression by a virus-encoded microRNA: an evolutionary adaptation that fine-tunes lytic reactivation." Cell Host Microbe **6**(6): 570-575.

Bieniasz, P. D. (2006). "Late budding domains and host proteins in enveloped virus release." Virology **344**(1): 55-63.

Blackman, M. A. and E. Flano (2002). "Persistant Gamma-herpesvirus Infections: What Can We Learn from an Experimental Mouse Model?" J. Exp. Med **195**(7): F29-F32.

Blasdell, K., C. McCracken, A. Morris, A. A. Nash, M. Begon, M. Bennett and J. P. Stewart (2003). "The wood mouse is a natural host for Murid herpesvirus 4." J Gen Virol **84**(Pt 1): 111-113.

Blaskovic, D., M. Stancekova, J. Svobodova and J. Mistrikova (1980). "Isolation of five strains of herpesviruses from two species of free living small rodents." Acta Virol **24**(6): 468.

Boo, K. H. and J. S. Yang (2010). "Intrinsic cellular defenses against virus infection by antiviral type I interferon." Yonsei Med J **51**(1): 9-17.

Boyer, J. L., S. Swaminathan and S. J. Silverstein (2002). "The Epstein-Barr virus SM protein is functionally similar to ICP27 from herpes simplex virus in viral infections." J Virol **76**(18): 9420-9433.

Brierley, M. M. and E. N. Fish (2002). "Review: IFN-alpha/beta receptor interactions to biologic outcomes: understanding the circuitry." J Interferon Cytokine Res **22**(8): 835-845.

Brinkmann, M. M., M. Pietrek, O. Dittrich-Breiholz, M. Kracht and T. F. Schulz (2007). "Modulation of host gene expression by the K15 protein of Kaposi's sarcoma-associated herpesvirus." J Virol **81**(1): 42-58.

Bronstein, J. C. and P. C. Weber (1996). "Purification and characterization of herpes simplex virus type 1 alkaline exonuclease expressed in Escherichia coli." J Virol **70**(3): 2008-2013.

Buisson, M., T. Geoui, D. Flot, N. Tarbouriech, M. E. Ressing, E. J. Wiertz and W. P. Burmeister (2009). "A bridge crosses the active-site canyon of the Epstein-Barr virus nuclease with DNase and RNase activities." J Mol Biol **391**(4): 717-728.

Bujnicki, J. M. and L. Rychlewski (2001). "The herpesvirus alkaline exonuclease belongs to the restriction endonuclease PD-(D/E)XK superfamily: insight from molecular modeling and phylogenetic analysis." Virus Genes **22**(2): 219-230.

Bushell, M. and P. Sarnow (2002). "Hijacking the translation apparatus by RNA viruses." J Cell Biol **158**(3): 395-399.

Campadelli-Fiume, G. (2007). The egress of alphaherpesviruses from the cell. Human Herpesviruses. A. e. a. Arvin.

Carbone, A., A. Gloghini and G. Dotti (2008). "EBV-associated lymphoproliferative disorders: classification and treatment." Oncologist **13**(5): 577-585.

Cassady, K. A., M. Gross and B. Roizman (1998). "The herpes simplex virus US11 protein effectively compensates for the gamma1(34.5) gene if present before activation of protein kinase R by precluding its phosphorylation and that of the alpha subunit of eukaryotic translation initiation factor 2." J Virol **72**(11): 8620-8626.

Castello, A., D. Franco, P. Moral-Lopez, J. J. Berlanga, E. Alvarez, E. Wimmer and L. Carrasco (2009). "HIV- 1 protease inhibits Cap- and poly(A)-dependent translation upon eIF4GI and PABP cleavage." PLoS One **4**(11): e7997.

Chandriani, S. and D. Ganem (2007). "Host transcript accumulation during lytic KSHV infection reveals several classes of host responses." PLoS One **2**(8): e811.

Chandriani, S. and D. Ganem (2010). "Array-based transcript profiling and limiting-dilution reverse transcription-PCR analysis identify additional latent genes in Kaposi's sarcoma-associated herpesvirus." J Virol **84**(11): 5565-5573.

Chang, Y., E. Cesarman, M. S. Pessin, F. Lee, J. Culpepper, D. M. Knowles and P. S. Moore (1994). "Identification of herpesvirus-like DNA sequences in AIDS-associated Kaposi's sarcoma." Science **266**(5192): 1865-1869.

Chen, D. H., H. Jiang, M. Lee, F. Liu and Z. H. Zhou (1999). "Three-dimensional visualization of tegument/capsid interactions in the intact human cytomegalovirus." Virology **260**(1): 10-16.

Choi, J. K., B. S. Lee, S. N. Shim, M. Li and J. U. Jung (2000). "Identification of the novel K15 gene at the rightmost end of the Kaposi's sarcoma-associated herpesvirus genome." J Virol **74**(1): 436-446.

Clark, M. E., P. M. Lieberman, A. J. Berk and A. Dasgupta (1993). "Direct cleavage of human TATA-binding protein by poliovirus protease 3C in vivo and in vitro." Mol Cell Biol **13**(2): 1232-1237.

Clyde, K. and B. A. Glaunsinger (2011). "Deep sequencing reveals direct targets of gammaherpesvirus-induced mRNA decay and suggests that multiple mechanisms govern cellular transcript escape." PLoS One **6**(5): e19655.

Cole, C. N. and J. J. Scarcelli (2006). "Transport of messenger RNA from the nucleus to the cytoplasm." Curr Opin Cell Biol **18**(3): 299-306.

Coller, J., & Parker, R. (2004). "Eukaryotic mRNA Decapping." Annual Reviews in Biochemistry **73**: 861-890.

Connolly, S. A., J. O. Jackson, T. S. Jardetzky and R. Longnecker (2011). "Fusing structure and function: a structural view of the herpesvirus entry machinery." Nat Rev Microbiol **9**(5): 369-381.

Covarrubias, S., M. M. Gaglia, G. R. Kumar, W. Wong, A. O. Jackson and B. A. Glaunsinger (2011). "Coordinated destruction of cellular messages in translation complexes by the gammaherpesvirus host shutoff factor and the mammalian exonuclease Xrn1." PLoS Pathog **7**(10): e1002339.

Covarrubias, S., J. M. Richner, K. Clyde, Y. J. Lee and B. A. Glaunsinger (2009). "Host shutoff is a conserved phenotype of gammaherpesvirus infection and is orchestrated exclusively from the cytoplasm." J Virol **83**(18): 9554-9566.

Crump, C. M., C. Yates and T. Minson (2007). "Herpes simplex virus type 1 cytoplasmic envelopment requires functional Vps4." J Virol **81**(14): 7380-7387.

Cuesta, R., Q. Xi and R. J. Schneider (2000). "Adenovirus-specific translation by displacement of kinase Mnk1 from cap-initiation complex eIF4F." EMBO J **19**(13): 3465-3474.

Dahlroth, S. L., D. Gurmu, J. Haas, H. Erlandsen and P. Nordlund (2009). "Crystal structure of the shutoff and exonuclease protein from the oncogenic Kaposi's sarcoma-associated herpesvirus." FEBS J **276**(22): 6636-6645.

Dai-Ju, J. Q., L. Li, L. A. Johnson and R. M. Sandri-Goldin (2006). "ICP27 interacts with the C-terminal domain of RNA polymerase II and facilitates its recruitment to herpes simplex virus 1 transcription sites, where it undergoes proteasomal degradation during infection." J Virol **80**(7): 3567-3581.

Dai, W., Q. Jia, E. Bortz, S. Shah, J. Liu, I. Atanasov, X. Li, K. A. Taylor, R. Sun and Z. H. Zhou (2008). "Unique structures in a tumor herpesvirus revealed by cryo-electron tomography and microscopy." J Struct Biol **161**(3): 428-438.

Das, S., A. Vasanji and P. E. Pellett (2007). "Three-dimensional structure of the human cytomegalovirus cytoplasmic virion assembly complex includes a reoriented secretory apparatus." J Virol **81**(21): 11861-11869.

Davison, A. J., R. Eberle, B. Ehlers, G. S. Hayward, D. J. McGeoch, A. C. Minson, P. E. Pellett, B. Roizman, M. J. Studdert and E. Thiry (2009). "The order Herpesvirales." Arch Virol **154**(1): 171-177.

DeLuca, N. A. and P. A. Schaffer (1987). "Activities of herpes simplex virus type 1 (HSV-1) ICP4 genes specifying nonsense peptides." Nucleic Acids Res **15**(11): 4491-4511.

Deng, W., Roberts .S. G. E (2007). "TFIIB and the regulation of transcription by RNA polymerase II." Chromosoma **116**: 417-429.

Desmyter, J., J. L. Melnick and W. E. Rawls (1968). "Defectiveness of Interferon production and of Rubella virus interference in a line of African Green Monkey Kidney cells (Vero)." J Virol **2** (10): 955-961.

Diamandis, E. P. and T. K. Christopoulos (1991). "The biotin-(strept)avidin system: principles and applications in biotechnology." Clin Chem **37**(5): 625-636.

Doepker, R. C., W. L. Hsu, H. A. Saffran and J. R. Smiley (2004). "Herpes simplex virus virion host shutoff protein is stimulated by translation initiation factors eIF4B and eIF4H." J Virol **78**(9): 4684-4699.

Dohner, K., A. Wolfstein, U. Prank, C. Echeverri, D. Dujardin, R. Vallee and B. Sodeik (2002). "Function of dynein and dynactin in herpes simplex virus capsid transport." Mol Biol Cell **13**(8): 2795-2809.

Duerst, R. J. and L. A. Morrison (2004). "Herpes simplex virus 2 virion host shutoff protein interferes with type I interferon production and responsiveness." Virology **322**(1): 158-167.

Dutia, B. M., D. J. Allen, H. Dyson and A. A. Nash (1999). "Type I interferons and IRF-1 play a critical role in the control of a gammaherpesvirus infection." Virology **261**(2): 173-179.

Ebrahimi, B., B. M. Dutia, K. L. Roberts, J. J. Garcia-Ramirez, P. Dickinson, J. P. Stewart, P. Ghazal, D. J. Roy and A. A. Nash (2003). "Transcriptome profile of murine gammaherpesvirus-68 lytic infection." J Gen Virol **84**(Pt 1): 99-109.

Efstathiou, S., Y. M. Ho and A. C. Minson (1990). "Cloning and molecular characterization of the murine herpesvirus 68 genome." J Gen Virol **71 (Pt 6)**: 1355-1364.

Engelhardt, O. G. E., Foder (2006). "Functional association between viral and cellular transcription during influenza virus infection." Reviews in Medical Virology **16**: 329-345.

Erkmann, J. A. and U. Kutay (2004). "Nuclear export of mRNA: from the site of transcription to the cytoplasm." Exp Cell Res **296**(1): 12-20.

Esclatine, A., B. Taddeo, L. Evans and B. Roizman (2004a). "The herpes simplex virus 1 UL41 gene-dependent destabilization of cellular RNAs is selective and may be sequence-specific." Proc Natl Acad Sci U S A **101**(10): 3603-3608.

Esclatine, A., B. Taddeo and B. Roizman (2004b). "The UL41 protein of herpes simplex virus mediates selective stabilization or degradation of cellular mRNAs." Proc Natl Acad Sci U S A **101**(52): 18165-18170.

Etchison, D., S. C. Milburn, I. Edery, N. Sonenberg and J. W. Hershey (1982). "Inhibition of HeLa cell protein synthesis following poliovirus infection correlates with the proteolysis of a 220,000-dalton polypeptide associated with eucaryotic initiation factor 3 and a cap binding protein complex." J Biol Chem **257**(24): 14806-14810.

Eulalio, A., I. Behm-Ansmant and E. Izaurralde (2007). "P bodies: at the crossroads of post-transcriptional pathways." Nat Rev Mol Cell Biol **8**(1): 9-22.

Everly, D. N., Jr., P. Feng, I. S. Mian and G. S. Read (2002). "mRNA degradation by the virion host shutoff (Vhs) protein of herpes simplex virus: genetic and biochemical evidence that Vhs is a nuclease." J Virol **76**(17): 8560-8571.

Faria, P. A., P. Chakraborty, A. Levay, G. N. Barber, H. J. Ezelle, J. Enninga, C. Arana, J. van Deursen and B. M. Fontoura (2005). "VSV disrupts the Rae1/mrnp41 mRNA nuclear export pathway." Mol Cell **17**(1): 93-102.

Feederle, R., H. Bannert, H. Lips, N. Muller-Lantzsch and H. J. Delecluse (2009). "The Epstein-Barr virus alkaline exonuclease BGLF5 serves pleiotropic functions in virus replication." J Virol **83**(10): 4952-4962.

Feng, P., J. Everly, D. N. and G. S. Read (2005). "mRNA Decay during Herpes Simplex Virus (HSV) Infections: Protein-Protein Interactions Involving the HSV Virion Host Shutoff Protein and Translation Factors eIF4H and eIF4A." Journal of Virology **79**(15): 9651-9664.

Feng, X., Y. G. Thompson, J. B. Lewis and G. B. Caughman (1996). "Expression and function of the equine herpesvirus 1 virion-associated host shutoff homolog." J Virol **70**(12): 8710-8718.

Folkmann, A. W., K. N. Noble, C. N. Cole and S. R. Wente (2011). "Dbp5, Gle1-IP6 and Nup159: a working model for mRNP export." Nucleus **2**(6): 540-548.

Fuld, S., C. Cunningham, K. Klucher, A. J. Davison and D. J. Blackbourn (2006). "Inhibition of interferon signaling by the Kaposi's sarcoma-associated herpesvirus full-length viral interferon regulatory factor 2 protein." J Virol **80**(6): 3092-3097.

Ganem, D. (2006). "KSHV infection and the pathogenesis of Kaposi's sarcoma." Annu Rev Pathol **1**: 273-296.

Garmashova, N., R. Gorchakov, E. Frolova and I. Frolov (2006). "Sindbis virus nonstructural protein nsP2 is cytotoxic and inhibits cellular transcription." J Virol **80**(12): 5686-5696.

Gill, M. B., L. Gillet, S. Colaco, J. S. May, B. D. de Lima and P. G. Stevenson (2006). "Murine gammaherpesvirus-68 glycoprotein H-glycoprotein L complex is a major target for neutralizing monoclonal antibodies." J Gen Virol **87**(Pt 6): 1465-1475.

Gillet, L., S. Colaco and P. G. Stevenson (2008). "The murid herpesvirus-4 gH/gL binds to glycosaminoglycans." PLoS One **3**(2): e1669.

Gillet, L., M. B. Gill, S. Colaco, C. M. Smith and P. G. Stevenson (2006). "Murine gammaherpesvirus-68 glycoprotein B presents a difficult neutralization target to monoclonal antibodies derived from infected mice." J Gen Virol **87**(Pt 12): 3515-3527.

Gingras, A. C., Y. Svitkin, G. J. Belsham, A. Pause and N. Sonenberg (1996). "Activation of the translational suppressor 4E-BP1 following infection with encephalomyocarditis virus and poliovirus." Proc Natl Acad Sci U S A **93**(11): 5578-5583.

Glaunsinger, B., L. Chavez and D. Ganem (2005). "The Exonuclease and Host Shutoff Functions of the SOX protein of Kaposi's Sarcoma -Associated Herpesvirus Are Genetically Separable." Journal of Virology **79**(12): 7396-7401.

Glaunsinger, B. and D. Ganem (2004a). "Highly selective escape from KSHV-mediated host mRNA shutoff and its implications for viral pathogenesis." J Exp Med **200**(3): 391-398.

Glaunsinger, B. and D. Ganem (2004b). "Lytic KSHV Infection Inhibits Host Gene Expression by Accelerating Global mRNA Turnover." Molecular Cell **13**: 713-723.

Goldstein, J. N. and S. K. Weller (1998). "The exonuclease activity of HSV-1 UL12 is required for in vivo function." Virology **244**(2): 442-457.

Goldstrohm, A. C. and M. Wickens (2008). "Multifunctional deadenylase complexes diversify mRNA control." Nat Rev Mol Cell Biol **9**(4): 337-344.

Goodbourn, S., L. Didcock and R. E. Randall (2000). "Interferons: cell signalling, immune modulation, antiviral response and virus countermeasures." J Gen Virol **81**(Pt 10): 2341-2364.

Greene, W. and S. J. Gao (2009). "Actin dynamics regulate multiple endosomal steps during Kaposi's sarcoma-associated herpesvirus entry and trafficking in endothelial cells." PLoS Pathog **5**(7): e1000512.

Gu, M. and C. Lima, D. (2005). "Processing the message: structural insights into capping and decapping mRNA." Current Opinion in Structural Biology **15**: 99-106.

Guo, H., S. Shen, L. Wang and H. Deng (2010). "Role of tegument proteins in herpesvirus assembly and egress." Protein Cell **1**(11): 987-998.

Halbert, D. N., J. R. Cutt and T. Shenk (1985). "Adenovirus early region 4 encodes functions required for efficient DNA replication, late gene expression, and host cell shutoff." J Virol **56**(1): 250-257.

Hahn, A.S., Kaufmann, J.K., Wies, E., Naschberger, E., Panteleev-lvlev, J., Schmidt, K., Holzer, A., Schmidt, K., Chen, J., Konig, S., Ensser, A., Myoung, J., Brockmeyer, N. H., Sturzl, M., Fleckenstein, B and F. Neipel (2012). "The ehrin receptor tyrosine kinase A2 is a cellular receptor for Kaposi's sarcoma-associated herpesvirus." Nat Med **18**(6): 961-966

Harb, M., M. M. Becker, D. Vitour, C. H. Baron, P. Vende, S. C. Brown, S. Bolte, S. T. Arold and D. Poncet (2008). "Nuclear localization of cytoplasmic poly(A)-binding protein upon rotavirus infection involves the interaction of NSP3 with eIF4G and RoXaN." J Virol **82**(22): 11283-11293.

Hardwicke, M. A. and R. M. Sandri-Goldin (1994). "The herpes simplex virus regulatory protein ICP27 contributes to the decrease in cellular mRNA levels during infection." J Virol **68**(8): 4797-4810.

He, B., M. Gross and B. Roizman (1997). "The gamma(1)34.5 protein of herpes simplex virus 1 complexes with protein phosphatase 1alpha to dephosphorylate the alpha subunit of the eukaryotic translation initiation factor 2 and preclude the shutoff of protein synthesis by double-stranded RNA-activated protein kinase." Proc Natl Acad Sci U S A **94**(3): 843-848.

Her, L. S., E. Lund and J. E. Dahlberg (1997). "Inhibition of Ran guanosine triphosphatase-dependent nuclear transport by the matrix protein of vesicular stomatitis virus." Science **276**(5320): 1845-1848.

Herskowitz, J. H., M. A. Jacoby and S. H. Speck (2005). "The murine gammaherpesvirus 68 M2 gene is required for efficient reactivation from latently infected B cells." J Virol **79**(4): 2261-2273.

Hinkley, S., A. P. Ambagala, C. J. Jones and S. Srikumaran (2000). "A vhs-like activity of bovine herpesvirus-1." Arch Virol **145**(10): 2027-2046.

Hoffmann, P. J. and Y. C. Cheng (1978). "The deoxyribonuclease induced after infection of KB cells by herpes simplex virus type 1 or type 2. I. Purification and characterization of the enzyme." J Biol Chem **253**(10): 3557-3562.

Hoffmann, P. J. and Y. C. Cheng (1979). "DNase induced after infection of KB cells by herpes simplex virus type 1 or type 2. II. Characterization of an associated endonuclease activity." J Virol **32**(2): 449-457.

Huang, C., K. G. Lokugamage, J. M. Rozovics, K. Narayanan, B. L. Semler and S. Makino (2011). "SARS coronavirus nsp1 protein induces template-dependent endonucleolytic cleavage of mRNAs: viral mRNAs are resistant to nsp1-induced RNA cleavage." PLoS Pathog **7**(12): e1002433.

Hwang, S., K. S. Kim, E. Flano, T. T. Wu, L. M. Tong, A. N. Park, M. J. Song, D. J. Sanchez, R. M. O'Connell, G. Cheng and R. Sun (2009). "Conserved herpesviral kinase promotes viral persistence by inhibiting the IRF-3-mediated type I interferon response." Cell Host Microbe **5**(2): 166-178.

Jacoby, M. A., H. W. t. Virgin and S. H. Speck (2002). "Disruption of the M2 gene of murine gammaherpesvirus 68 alters splenic latency following intranasal, but not intraperitoneal, inoculation." J Virol **76**(4): 1790-1801.

Jainchill, J. L., S. A. Aaronson and G. J. Todaro (1969). "Murine sarcoma and leukemia viruses: assay using clonal lines of contact-inhibited mouse cells." J Virol **4**(5): 549-553.

Joachims, M., P. C. Van Breugel and R. E. Lloyd (1999). "Cleavage of poly(A)-binding protein by enterovirus proteases concurrent with inhibition of translation in vitro." J Virol **73**(1): 718-727.

Johnson, D. C. and J. D. Baines (2011). "Herpesviruses remodel host membranes for virus egress." Nat Rev Microbiol **9**(5): 382-394.

Johnston, R. F., S. C. Pickett and D. L. Barker (1990). "Autoradiography using storage phosphor technology." Electrophoresis **11**(5): 355-360.

Kamitani, W., C. Huang, K. Narayanan, K. G. Lokugamage and S. Makino (2009). "A two-pronged strategy to suppress host protein synthesis by SARS coronavirus Nsp1 protein." Nat Struct Mol Biol **16**(11): 1134-1140.

Kanangat, S., J. S. Babu, D. M. Knipe and B. T. Rouse (1996). "HSV-1-mediated modulation of cytokine gene expression in a permissive cell line: selective upregulation of IL-6 gene expression." Virology **219**(1): 295-300.

Karr, B. M. and G. S. Read (1999). "The virion host shutoff function of herpes simplex virus degrades the 5' end of a target mRNA before the 3' end." Virology **264**(1): 195-204.

Kawai, T. and S. Akira (2006). "Innate immune recognition of viral infection." Nat Immunol **7**(2): 131-137.

Kim, T., S. Pazhoor, M. Bao, Z. Zhang, S. Hanabuchi, V. Facchinetti, L. Bover, J. Plumas, L. Chaperot, J. Qin and Y. J. Liu (2010). "Aspartate-glutamate-alanine-histidine box motif (DEAH)/RNA helicase A helicases sense microbial DNA in human plasmacytoid dendritic cells." Proc Natl Acad Sci U S A **107**(34): 15181-15186.

Klann, E. and T. E. Dever (2004). "Biochemical mechanisms for translational regulation in synaptic plasticity." Nat Rev Neurosci **5**(12): 931-942.

Knipe, D. M. (2007). Fields Virology.

Kohler, A. and E. Hurt (2007). "Exporting RNA from the nucleus to the cytoplasm." Nat Rev Mol Cell Biol **8**(10): 761-773.

Krausslich, H. G., M. J. Nicklin, H. Toyoda, D. Etchison and E. Wimmer (1987). "Poliovirus proteinase 2A induces cleavage of eucaryotic initiation factor 4F polypeptide p220." J Virol **61**(9): 2711-2718.

Krug, L. T., J. M. Moser, S. M. Dickerson and S. H. Speck (2007). "Inhibition of NF-kappaB activation in vivo impairs establishment of gammaherpesvirus latency." PLoS Pathog **3**(1): e11.

Krummenacher, C., A. Carfi, R. J. Eisenberg and G. H. Cohen (2007). Entry of Herpesviruses into Cells. Viral Entry into Host Cells. S. Pohlmann and G. Simmons.

Kumar, G. R. and B. A. Glaunsinger (2010). "Nuclear import of cytoplasmic poly(A) binding protein restricts gene expression via hyperadenylation and nuclear retention of mRNA." Mol Cell Biol **30**(21): 4996-5008.

Kuyumcu-Martinez, M., G. Belliot, S. V. Sosnovtsev, K. O. Chang, K. Y. Green and R. E. Lloyd (2004a). "Calicivirus 3C-like proteinase inhibits cellular translation by cleavage of poly(A)-binding protein." J Virol **78**(15): 8172-8182.

Kuyumcu-Martinez, N. M., M. E. Van Eden, P. Younan and R. E. Lloyd (2004b). "Cleavage of poly(A)-binding protein by poliovirus 3C protease inhibits host cell translation: a novel mechanism for host translation shutoff." Mol Cell Biol **24**(4): 1779-1790.

Lam, Q., C. A. Smibert, K. E. Koop, C. Lavery, J. P. Capone, S. P. Weinheimer and J. R. Smiley (1996). "Herpes simplex virus VP16 rescues viral mRNA from destruction by the virion host shutoff function." EMBO J **15**(10): 2575-2581.

Lamphear, B. J., R. Yan, F. Yang, D. Waters, H. D. Liebig, H. Klump, E. Kuechler, T. Skern and R. E. Rhoads (1993). "Mapping the cleavage site in protein synthesis initiation factor eIF-4 gamma of the 2A proteases from human Coxsackievirus and rhinovirus." J Biol Chem **268**(26): 19200-19203.

Le May, N., S. Dubaele, L. Proietti De Santis, A. Billecocq, M. Bouloy and J. M. Egly (2004). "TFIIH transcription factor, a target for the Rift Valley hemorrhagic fever virus." Cell **116**(4): 541-550.

Leang, R. S., T. T. Wu, S. Hwang, L. T. Liang, L. Tong, J. T. Truong and R. Sun (2011). "The anti-interferon activity of conserved viral dUTPase ORF54 is essential for an effective MHV-68 infection." PLoS Pathog **7**(10): e1002292.

Lee, Y. J. and B. A. Glaunsinger (2009). "Aberrant herpesvirus-induced polyadenylation correlates with cellular messenger RNA destruction." PLoS Biol **7**(5): e1000107.

Lee, B. S., S. H. Lee, P. Feng, H. Chang, N. H. Cho and J. U. Jung (2005). "Characterization of the Kaposi's sarcoma-associated herpesvirus K1 signalosome." J Virol **79**(19): 12173-12184.

Lee, H. R., M. H. Kim, J. S. Lee, C. Liang and J. U. Jung (2009). "Viral interferon regulatory factors." J Interferon Cytokine Res **29**(9): 621-627.

Lemon, B. R., Tjian (2000). "Orchestrated response: a symphony of transcription factors for gene control." Genes & Dev. **14**: 2551-2569.

Lewin, B. (2004). Genes VIII, Pearson Prentice Hall**:** 25-26.

Lieber, M. R. (1997). "The FEN-1 family of structure-specific nucleases in eukaryotic DNA replication, recombination and repair." Bioessays **19**(3): 233-240.

Lin, H. W., Y. Y. Chang, M. L. Wong, J. W. Lin and T. J. Chang (2004). "Functional analysis of virion host shutoff protein of pseudorabies virus." Virology **324**(2): 412-418.

Liu, F. a. Z., Z. H. (2007). Comparative virion structures of human herpesviruses. Human Herpesviruses. A. e. a. Arvin, Cambridge University Press.

Longnecker, R. and F. Neipel (2007). Introduction to the human gammaherpesviruses. Human Herpesviruses: Biology, Therapy and Immunoprophylaxis. A. Arvin and G. Campadelli-Fiume, Cambridge Uiversity Press.

Lyles, D. S. (2000). "Cytopathogenesis and inhibition of host gene expression by RNA viruses." Microbiol Mol Biol Rev **64**(4): 709-724.

Lyman, M. G. and L. W. Enquist (2009). "Herpesvirus interactions with the host cytoskeleton." J Virol **83**(5): 2058-2066.

Majerciak, V. and Z. M. Zheng (2009). "Kaposi's sarcoma-associated herpesvirus ORF57 in viral RNA processing." Front Biosci **14**: 1516-1528.

Malik, P., D. J. Blackbourn, M. F. Cheng, G. S. Hayward and J. B. Clements (2004). "Functional co-operation between the Kaposi's sarcoma-associated herpesvirus ORF57 and ORF50 regulatory proteins." J Gen Virol **85**(Pt 8): 2155-2166.

Martinez, R., R. T. Sarisky, P. C. Weber and S. K. Weller (1996). "Herpes simplex virus type 1 alkaline nuclease is required for efficient processing of viral DNA replication intermediates." J Virol **70**(4): 2075-2085.

Martinez, R., Sarisky, R. T., Weber, P. C., & Weller, S. K. (1996). "Herpes Simplex Virus Type 1 Alkaline Nuclease Is Required for Efficient Processing of Viral DNA Replication Intermediates." Journal of Virology **70**(4): 2075-2085.

Martinez-Guzman, D., T. Rickabaugh, T. T. Wu, H. Brown, S. Cole, M. J. Song, L. Tong and R. Sun (2003). "Transcription program of murine gammaherpesvirus 68." J Virol **77**(19): 10488-10503.

Maurer, U. E., B. Sodeik and K. Grunewald (2008). "Native 3D intermediates of membrane fusion in herpes simplex virus 1 entry." Proc Natl Acad Sci U S A **105**(30): 10559-10564.

McCormick, C. and D. Ganem (2005). "The kaposin B protein of KSHV activates the p38/MK2 pathway and stabilizes cytokine mRNAs." Science **307**(5710): 739-741.

McGeoch, D. J., D. Gatherer and A. Dolan (2005). "On phylogenetic relationships among major lineages of the Gammaherpesvirinae." J Gen Virol **86**(Pt 2): 307-316.

McGeoch, D. J., F. J. Rixon and A. J. Davison (2006). "Topics in herpesvirus genomics and evolution." Virus Res **117**(1): 90-104.

McInerney, G. M., N. L. Kedersha, R. J. Kaufman, P. Anderson and P. Liljestrom (2005). "Importance of eIF2alpha phosphorylation and stress granule assembly in alphavirus translation regulation." Mol Biol Cell **16**(8): 3753-3763.

Melroe, G. T., L. Silva, P. A. Schaffer and D. M. Knipe (2007). "Recruitment of activated IRF-3 and CBP/p300 to herpes simplex virus ICP0 nuclear foci: Potential role in blocking IFN-beta induction." Virology **360**(2): 305-321.

Mendes Soares, L. M. and J. Valcarcel (2006). "The expanding transcriptome: the genome as the 'Book of Sand'." EMBO J **25**(5): 923-931.

Messerle, M., I. Crnkovic, W. Hammerschmidt, H. Ziegler and U. H. Koszinowski (1997). "Cloning and mutagenesis of a herpesvirus genome as an infectious bacterial artificial chromosome." Proc Natl Acad Sci U S A **94**(26): 14759-14763.

Mettenleiter, T. C. (2002). "Herpesvirus assembly and egress." J Virol **76**(4): 1537-1547.

Mettenleiter, T. C., B. G. Klupp and H. Granzow (2009). "Herpesvirus assembly: an update." Virus Res **143**(2): 222-234.

Milho, R., C. M. Smith, S. Marques, M. Alenquer, J. S. May, L. Gillet, M. Gaspar, S. Efstathiou, J. P. Simas and P. G. Stevenson (2009). "In vivo imaging of murid herpesvirus-4 infection." J Gen Virol **90**(Pt 1): 21-32.

Miller, N. and L. M. Hutt-Fletcher (1992). "Epstein-Barr virus enters B cells and epithelial cells by different routes." J Virol **66**(6): 3409-3414.

Moore, P. S., C. Boshoff, R. A. Weiss and Y. Chang (1996). "Molecular mimicry of human cytokine and cytokine response pathway genes by KSHV." Science **274**(5293): 1739-1744.

Moorman, N. J., C. Y. Lin and S. H. Speck (2004). "Identification of candidate gammaherpesvirus 68 genes required for virus replication by signature-tagged transposon mutagenesis." J Virol **78**(19): 10282-10290.

Morozov, I. Y., M. G. Jones, A. A. Razak, D. J. Rigden and M. X. Caddick (2010). "CUCU modification of mRNA promotes decapping and transcript degradation in Aspergillus nidulans." Mol Cell Biol **30**(2): 460-469.

Muller, U., U. Steinhoff, L. F. Reis, S. Hemmi, J. Pavlovic, R. M. Zinkernagel and M. Aguet (1994). "Functional role of type I and type II interferons in antiviral defense." Science **264**(5167): 1918-1921.

Murphy, J. A., R. J. Duerst, T. J. Smith and L. A. Morrison (2003). "Herpes simplex virus type 2 virion host shutoff protein regulates alpha/beta interferon but not adaptive immune responses during primary infection in vivo." J Virol **77**(17): 9337-9345.

Murray, E. L. and D. R. Schoenberg (2008). "Assays for determining poly(A) tail length and the polarity of mRNA decay in mammalian cells." Methods Enzymol **448**: 483-504.

Naranatt, P. P., H. H. Krishnan, M. S. Smith and B. Chandran (2005). "Kaposi's sarcoma-associated herpesvirus modulates microtubule dynamics via RhoA-GTP-diaphanous 2 signaling and utilizes the dynein motors to deliver its DNA to the nucleus." J Virol **79**(2): 1191-1206.

Nash, A. A., B. M. Dutia, J. P. Stewart and A. J. Davison (2001). "Natural history of murine gamma-herpesvirus infection." Philos Trans R Soc Lond B Biol Sci **356**(1408): 569-579.

Nemeroff, M. E., S. M. Barabino, Y. Li, W. Keller and R. M. Krug (1998). "Influenza virus NS1 protein interacts with the cellular 30 kDa subunit of CPSF and inhibits 3'end formation of cellular pre-mRNAs." Mol Cell **1**(7): 991-1000.

Newbury, S. F. (2006). "Control of mRNA stability in eukaryotes." Biochem Soc Trans **34**(Pt 1): 30-34.

Nishino, T. and K. Morikawa (2002). "Structure and function of nucleases in DNA repair: shape, grip and blade of the DNA scissors." Oncogene **21**(58): 9022-9032.

Nystrom, K., M. Biller, A. Grahn, M. Lindh, G. Larson and S. Olofsson (2004). "Real time PCR for monitoring regulation of host gene expression in herpes simplex virus type 1-infected human diploid cells." J Virol Methods **118**(2): 83-94.

Pasieka, T. J., B. Lu, S. D. Crosby, K. M. Wylie, L. A. Morrison, D. E. Alexander, V. D. Menachery and D. A. Leib (2008). "Herpes simplex virus virion host shutoff attenuates establishment of the antiviral state." J Virol **82**(11): 5527-5535.

Pe'ery, T. and M. B. Mathews (2000). Viral Translational Strategies and Host Defense Mechanisms. Translational Control of Gene Expression. N. Sonenberg, J. W. Hershey and M. B. Mathews.

Penkert, R. R. and R. F. Kalejta (2011). "Tegument protein control of latent herpesvirus establishment and animation." Herpesviridae **2**(1): 3.

Pfaffl, M. W. (2001). "A new mathematical model for relative quantification in real-time RT-PCR." Nucleic Acids Res. 29(9):e45

Phelan, A., M. Carmo-Fonseca, J. McLaughlan, A. I. Lamond and J. B. Clements (1993). "A herpes simplex virus type 1 immediate-early gene product, IE63, regulates small nuclear ribonucleoprotein distribution." Proc Natl Acad Sci U S A **90**(19): 9056-9060.

Pilder, S., M. Moore, J. Logan and T. Shenk (1986). "The adenovirus E1B-55K transforming polypeptide modulates transport or cytoplasmic stabilization of viral and host cell mRNAs." Mol Cell Biol **6**(2): 470-476.

Piron, M., P. Vende, J. Cohen and D. Poncet (1998). "Rotavirus RNA-binding protein NSP3 interacts with eIF4GI and evicts the poly(A) binding protein from eIF4F." EMBO J **17**(19): 5811-5821.

Qiu, Y., M. Nemeroff and R. M. Krug (1995). "The influenza virus NS1 protein binds to a specific region in human U6 snRNA and inhibits U6-U2 and U6-U4 snRNA interactions during splicing." RNA **1**(3): 304-316.

Raaben, M., M. J. Groot Koerkamp, P. J. Rottier and C. A. de Haan (2007). "Mouse hepatitis coronavirus replication induces host translational shutoff and mRNA decay, with concomitant formation of stress granules and processing bodies." Cell Microbiol **9**(9): 2218-2229.

Randall, R. E. and S. Goodbourn (2008). "Interferons and viruses: an interplay between induction, signalling, antiviral responses and virus countermeasures." J Gen Virol **89**(Pt 1): 1-47.

Read, G. S. and N. Frenkel (1983). "Herpes simplex virus mutants defective in the virion-associated shutoff of host polypeptide synthesis and exhibiting abnormal synthesis of alpha (immediate early) viral polypeptides." J Virol **46**(2): 498-512.

Rezaee, S. A., C. Cunningham, A. J. Davison and D. J. Blackbourn (2006). "Kaposi's sarcoma-associated herpesvirus immune modulation: an overview." J Gen Virol **87**(Pt 7): 1781-1804.

Richner, J. M., K. Clyde, A. C. Pezda, B. Y. Cheng, T. Wang, G. R. Kumar, S. Covarrubias, L. Coscoy and B. Glaunsinger (2011). "Global mRNA degradation during lytic gammaherpesvirus infection contributes to establishment of viral latency." PLoS Pathog **7**(7): e1002150.

Rivas, C., A. E. Thlick, C. Parravicini, P. S. Moore and Y. Chang (2001). "Kaposi's sarcoma-associated herpesvirus LANA2 is a B-cell-specific latent viral protein that inhibits p53." J Virol **75**(1): 429-438.

Roizman, B., G. S. Borman and M. Kamali-Rousta (1965). "Macromolecular synthesis in cells infected with herpes simplex virus." Nat **206**: 1374-1375.

Rowe, M., B. Glaunsinger, D. van Leeuwen, J. Zuo, D. Sweetman, D. Ganem, J. Middeldorp, E. J. Wiertz and M. E. Ressing (2007). "Host shutoff during productive Epstein-Barr virus infection is mediated by BGLF5 and may contribute to immune evasion." Proc Natl Acad Sci U S A **104**(9): 3366-3371.

Ruvolo, V., L. Navarro, C. E. Sample, M. David, S. Sung and S. Swaminathan (2003). "The Epstein-Barr virus SM protein induces STAT1 and interferon-stimulated gene expression." J Virol **77**(6): 3690-3701.

Ruvolo, V., E. Wang, S. Boyle and S. Swaminathan (1998). "The Epstein-Barr virus nuclear protein SM is both a post-transcriptional inhibitor and activator of gene expression." Proc Natl Acad Sci U S A **95**(15): 8852-8857.

Samady, L., E. Costigliola, L. MacCormac, Y. McGrath, S. Cleverley, C. E. Lilley, J. Smith, D. S. Latchman, B. Chain and R. S. Coffin (2003). "Deletion of the virion host shutoff protein (vhs) from herpes simplex virus (HSV) relieves the viral block to dendritic cell activation: potential of vhs- HSV vectors for dendritic cell-mediated immunotherapy." J Virol **77**(6): 3768-3776.

Sandri-Goldin, R. M. (2011). "The many roles of the highly interactive HSV protein ICP27, a key regulator of infection." Future Microbiol **6**(11): 1261-1277.

Sathish, N., X. Wang and Y. Yuan (2012). "Tegument Proteins of Kaposi's Sarcoma-Associated Herpesvirus and Related Gamma-Herpesviruses." Front Microbiol **3**: 98.

Sathish, N. and Y. Yuan (2011). "Evasion and subversion of interferon-mediated antiviral immunity by Kaposi's sarcoma-associated herpesvirus: an overview." J Virol **85**(21): 10934-10944.

Sato, H., L. D. Callanan, L. Pesnicak, T. Krogmann and J. I. Cohen (2002). "Varicella-zoster virus (VZV) ORF17 protein induces RNA cleavage and is critical for replication of VZV at 37 degrees C but not 33 degrees C." J Virol **76**(21): 11012-11023.

Schek, N. and S. L. Bachenheimer (1985). "Degradation of cellular mRNAs induced by a virion-associated factor during herpes simplex virus infection of Vero cells." J Virol **55**(3): 601-610.

Schneider, R. J. (2000). Adenovirus Inhibition of Cellular Protein Synthesis and Preferential Translation of Viral mRNAs. Translational Control of Gene Expression. N. Sonenberg, J. W. Hershey and M. B. Mathews.

Sciabica, K. S., Q. J. Dai and R. M. Sandri-Goldin (2003). "ICP27 interacts with SRPK1 to mediate HSV splicing inhibition by altering SR protein phosphorylation." EMBO J **22**(7): 1608-1619.

Shandilya, J. and S. G. Roberts (2012). "The transcription cycle in eukaryotes: From productive initiation to RNA polymerase II recycling." Biochim Biophys Acta **1819**(5): 391-400.

Sharma, S. and K. A. Fitzgerald (2011). "Innate immune sensing of DNA." PLoS Pathog **7**(4): e1001310.

Sheaffer, A. K., S. P. Weinheimer and D. J. Tenney (1997). "The human cytomegalovirus UL98 gene encodes the conserved herpesvirus alkaline nuclease." J Gen Virol **78 (Pt 11)**: 2953-2961.

Smiley, J. R. (2004). "Herpes Simplex Virus Virion Host Shutoff Protein: Immune Evasion Mediated by a Viral RNase?" Journal of Virology **78**(3): 1063-1068.

Smith, R. W. and N. K. Gray (2010). "Poly(A)-binding protein (PABP): a common viral target." Biochem J **426**(1): 1-12.

Snow, A. L. and O. M. Martinez (2007). "Epstein-Barr virus: evasive maneuvers in the development of PTLD." Am J Transplant **7**(2): 271-277.

Sodeik, B., M. W. Ebersold and A. Helenius (1997). "Microtubule-mediated transport of incoming herpes simplex virus 1 capsids to the nucleus." J Cell Biol **136**(5): 1007-1021.

Song, M. J., S. Hwang, W. H. Wong, T. T. Wu, S. Lee, H. I. Liao and R. Sun (2005). "Identification of viral genes essential for replication of murine gamma-herpesvirus 68 using signature-tagged mutagenesis." Proc Natl Acad Sci U S A **102**(10): 3805-3810.

Spear, P. G. and R. Longnecker (2003). "Herpesvirus entry: an update." J Virol **77**(19): 10179-10185.

Speck, S. H. and D. Ganem (2010). "Viral latency and its regulation: lessons from the gamma-herpesviruses." Cell Host Microbe **8**(1): 100-115.

Sternbach, G. and J. Varon (1995). "Moritz Kaposi: idiopathic pigmented sarcoma of the skin." J Emerg Med **13**(5): 671-674.

Stevenson, P. G. and S. Efstathiou (2005). "Immune mechanisms in murine gammaherpesvirus-68 infection." Viral Immunol **18**(3): 445-456.

Stevenson, P. G., S. Efstathiou, P. C. Doherty and P. J. Lehner (2000). "Inhibition of MHC class I-restricted antigen presentation by gamma 2-herpesviruses." Proc Natl Acad Sci U S A **97**(15): 8455-8460.

Stevenson, P. G., J. S. May, X. G. Smith, S. Marques, H. Adler, U. H. Koszinowski, J. P. Simas and S. Efstathiou (2002). "K3-mediated evasion of CD8(+) T cells aids amplification of a latent gamma-herpesvirus." Nat Immunol **3**(8): 733-740.

Stewart, J. P., E. J. Usherwood, B. M. Dutia and A. A. Nash (1998a). Immunobiology of Murine Gamma Herpesvirus-68. Herpesviruses and Immunity.

Stewart, J. P., E. J. Usherwood, A. Ross, H. Dyson and T. Nash (1998b). "Lung epithelial cells are a major site of murine gammaherpesvirus persistence." J Exp Med **187**(12): 1941-1951.

Stewart, M. (2007). "Ratcheting mRNA out of the nucleus." Mol Cell **25**(3): 327-330.

Strelow, L. I. and D. A. Leib (1995). "Role of the virion host shutoff (vhs) of herpes simplex virus type 1 in latency and pathogenesis." J Virol **69**(11): 6779-6786.

Strand, S. S. and D. A. Leib (2004). "Role of the VP16-binding domain of vhs in viral growth, host shutoff activity, and pathogenesis." J Virol **78**(24): 13562-13572.

Stylianou, J., K. Maringer, R. Cook, E. Bernard and G. Elliott (2009). "Virion incorporation of the herpes simplex virus type 1 tegument protein VP22 occurs via glycoprotein E-specific recruitment to the late secretory pathway." J Virol **83**(10): 5204-5218.

Su, M. J. and R. Bablanian (1990). "Polyadenylated RNA sequences from vaccinia virus-infected cells selectively inhibit translation in a cell-free system: structural properties and mechanism of inhibition." Virology **179**(2): 679-693.

Sunil-Chandra, N. P., S. Efstathiou, J. Arno and A. A. Nash (1992). "Virological and pathological features of mice infected with murine gamma-herpesvirus 68." J Gen Virol **73 (Pt 9)**: 2347-2356.

Suzutani, T., M. Nagamine, T. Shibaki, M. Ogasawara, I. Yoshida, T. Daikoku, Y. Nishiyama and M. Azuma (2000). "The role of the UL41 gene of herpes simplex virus type 1 in evasion of non-specific host defence mechanisms during primary infection." J Gen Virol **81**(Pt 7): 1763-1771.

Svejstrup, J. Q. (2004). "The RNA polymerase II transcription cycle: cycling through chromatin." Biochim Biophys Acta **1677**(1-3): 64-73.

Swaminathan, S. (2005). "Post-transcriptional gene regulation by gamma herpesviruses." J Cell Biochem **95**(4): 698-711.

Szutorisz, H., Dillon. N. & Tora. L. (2005). "The role of enhancers as centres for general transcription factor recruitment." Trends in Biochemical Sciences **30**(11): 593-599.

Taddeo, B., A. Esclatine, W. Zhang and B. Roizman (2003). "The stress-inducible immediate-early responsive gene IEX-1 is activated in cells infected with herpes simplex virus 1, but several viral mechanisms, including 3' degradation of its RNA, preclude expression of the gene." J Virol **77**(11): 6178-6187.

Taddeo, B., M. T. Sciortino, W. Zhang and B. Roizman (2007). "Interaction of herpes simplex virus RNase with VP16 and VP22 is required for the accumulation of the protein but not for accumulation of mRNA." Proc Natl Acad Sci U S A **104**(29): 12163-12168.

Taddeo, B., W. Zhang and B. Roizman (2009). "The virion-packaged endoribonuclease of herpes simplex virus 1 cleaves mRNA in polyribosomes." Proc Natl Acad Sci U S A **106**(29): 12139-12144.

Taddeo, B., W. Zhang and B. Roizman (2010). "Role of herpes simplex virus ICP27 in the degradation of mRNA by virion host shutoff RNase." J Virol **84**(19): 10182-10190.

Tarun, S. Z., Jr. and A. B. Sachs (1995). "A common function for mRNA 5' and 3' ends in translation initiation in yeast." Genes Dev **9**(23): 2997-3007.

Tavalai, N. and T. Stamminger (2009). "Interplay between Herpesvirus Infection and Host Defense by PML Nuclear Bodies." Viruses **1**(3): 1240-1264.

Temme, C., S. Zaessinger, S. Meyer, M. Simonelig and E. Wahle (2004). "A complex containing the CCR4 and CAF1 proteins is involved in mRNA deadenylation in Drosophila." EMBO J **23**(14): 2862-2871.

Thompson, S. R. and P. Sarnow (2000). "Regulation of host cell translation by viruses and effects on cell function." Curr Opin Microbiol **3**(4): 366-370.

Thorley-Lawson, D. A. (2001). "Epstein-Barr virus: exploiting the immune system." Nat Rev Immunol **1**(1): 75-82.

Tigges, M. A., S. Leng, D. C. Johnson and R. L. Burke (1996). "Human herpes simplex virus (HSV)-specific CD8+ CTL clones recognize HSV-2-infected fibroblasts after treatment with IFN-gamma or when virion host shutoff functions are disabled." J Immunol **156**(10): 3901-3910.

Tomlinson, C. G., J. M. Atack, B. Chapados, J. A. Tainer and J. A. Grasby (2010). "Substrate recognition and catalysis by flap endonucleases and related enzymes." Biochem Soc Trans **38**(2): 433-437.

Trgovcich, J., D. Johnson and B. Roizman (2002). "Cell surface major histocompatibility complex class II proteins are regulated by the products of the gamma(1)34.5 and U(L)41 genes of herpes simplex virus 1." J Virol **76**(14): 6974-6986.

Turcotte, S., J. Letellier and R. Lippe (2005). "Herpes simplex virus type 1 capsids transit by the trans-Golgi network, where viral glycoproteins accumulate independently of capsid egress." J Virol **79**(14): 8847-8860.

Turner, P. C., A.G. McLennan, A.D. Bates & M.R.H. White (2000). Molecular Biology, BIOS Scientific Publishers Ltd.

Unterholzner, L., S. E. Keating, M. Baran, K. A. Horan, S. B. Jensen, S. Sharma, C. M. Sirois, T. Jin, E. Latz, T. S. Xiao, K. A. Fitzgerald, S. R. Paludan and A. G. Bowie (2010). "IFI16 is an innate immune sensor for intracellular DNA." Nat Immunol **11**(11): 997-1004.

Ventoso, I., R. Blanco, C. Perales and L. Carrasco (2001). "HIV-1 protease cleaves eukaryotic initiation factor 4G and inhibits cap-dependent translation." Proc Natl Acad Sci U S A **98**(23): 12966-12971.

Viejo-Borbolla, A. and T. F. Schulz (2003). "Kaposi's sarcoma-associated herpesvirus (KSHV/HHV8): key aspects of epidemiology and pathogenesis." AIDS Rev **5**(4): 222-229.

Virgin, H. W. t., P. Latreille, P. Wamsley, K. Hallsworth, K. E. Weck, A. J. Dal Canto and S. H. Speck (1997). "Complete sequence and genomic analysis of murine gammaherpesvirus 68." J Virol **71**(8): 5894-5904.

von Kobbe, C., J. M. van Deursen, J. P. Rodrigues, D. Sitterlin, A. Bachi, X. Wu, M. Wilm, M. Carmo-Fonseca and E. Izaurralde (2000). "Vesicular stomatitis virus matrix protein inhibits host cell gene expression by targeting the nucleoporin Nup98." Mol Cell **6**(5): 1243-1252.

von Schwedler, U. K., M. Stuchell, B. Muller, D. M. Ward, H. Y. Chung, E. Morita, H. E. Wang, T. Davis, G. P. He, D. M. Cimbora, A. Scott, H. G. Krausslich, J. Kaplan, S. G. Morham and W. I. Sundquist (2003). "The protein network of HIV budding." Cell **114**(6): 701-713.

Wang, N. *e. a.* (2007). "Phylogenetic analysis, genome evolution and the rate of gene gain in the *Herpesviridae*." Molecular Phylogenetics and Evolution **43**: 1066-1075.

Weller, S. K., M. R. Seghatoleslami, L. Shao, D. Rowse and E. P. Carmichael (1990). "The herpes simplex virus type 1 alkaline nuclease is not essential for viral DNA synthesis: isolation and characterization of a lacZ insertion mutant." J Gen Virol **71 (Pt 12)**: 2941-2952.

Wilkinson, D. E. and S. K. Weller (2003). "The role of DNA recombination in herpes simplex virus DNA replication." IUBMB Life **55**(8): 451-458.

Wu, T. T., E. J. Usherwood, J. P. Stewart, A. A. Nash and R. Sun (2000). "Rta of murine gammaherpesvirus 68 reactivates the complete lytic cycle from latency." J Virol **74**(8): 3659-3667.

Yalamanchili, P., R. Banerjee and A. Dasgupta (1997). "Poliovirus-encoded protease 2APro cleaves the TATA-binding protein but does not inhibit host cell RNA polymerase II transcription in vitro." J Virol **71**(9): 6881-6886.

Yalamanchili, P., K. Harris, E. Wimmer and A. Dasgupta (1996). "Inhibition of basal transcription by poliovirus: a virus- encoded protease (3Cpro) inhibits formation of TBP-TATA box complex in vitro." J Virol **70**(5): 2922-2929.

Young, L. S. and A. B. Rickinson (2004). "Epstein-Barr virus: 40 years on." Nat Rev Cancer **4**(10): 757-768.

Yueh, A. and R. J. Schneider (1996). "Selective translation initiation by ribosome jumping in adenovirus-infected and heat-shocked cells." Genes Dev **10**(12): 1557-1567.

Zachar, Z., J. Kramer, I. P. Mims and P. M. Bingham (1993). "Evidence for channeled diffusion of pre-mRNAs during nuclear RNA transport in metazoans." J Cell Biol **121**(4): 729-742.

Zelus, B. D., R. S. Stewart and J. Ross (1996). "The virion host shutoff protein of herpes simplex virus type 1: messenger ribonucleolytic activity in vitro." J Virol **70**(4): 2411-2419.

Zhou, Z. H., D. H. Chen, J. Jakana, F. J. Rixon and W. Chiu (1999). "Visualization of tegument-capsid interactions and DNA in intact herpes simplex virus type 1 virions." J Virol **73**(4): 3210-3218.

Zuo, J., W. Thomas, D. van Leeuwen, J. M. Middeldorp, E. J. Wiertz, M. E. Ressing and M. Rowe (2008). "The DNase of gammaherpesviruses impairs recognition by virus-specific CD8+ T cells through an additional host shutoff function." J Virol **82**(5): 2385-2393.

Appendix A

Vector maps

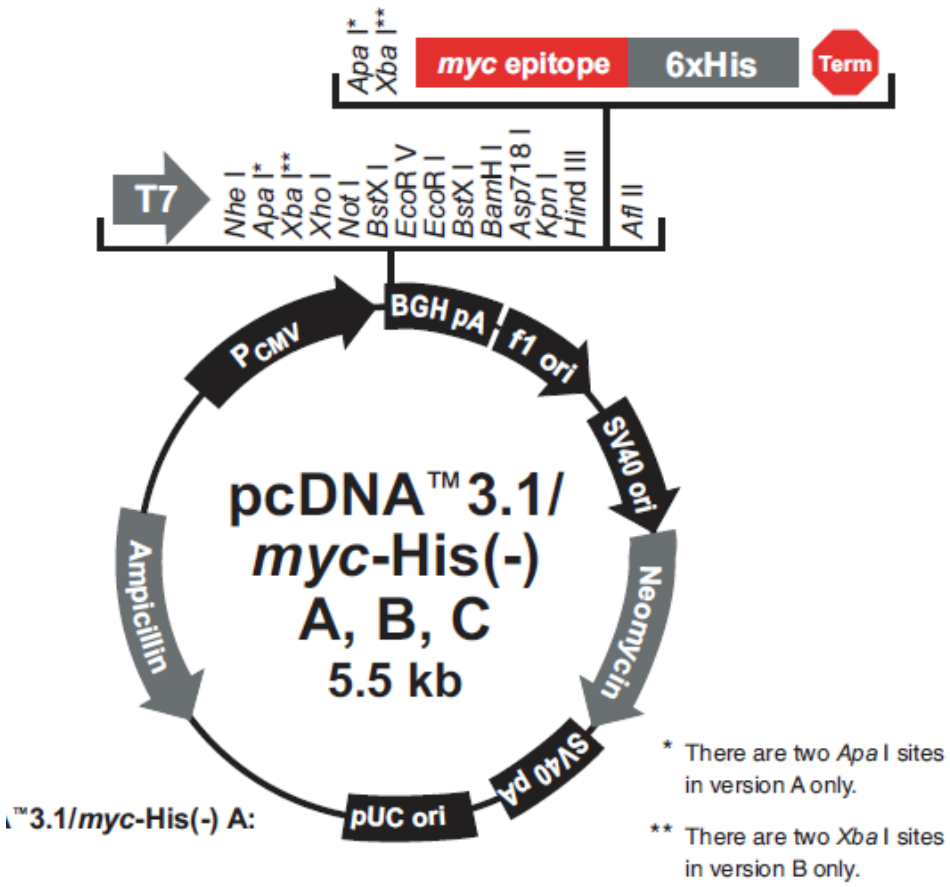

pcDNA3.1 with myc and His-tagged epitope vector circle map.

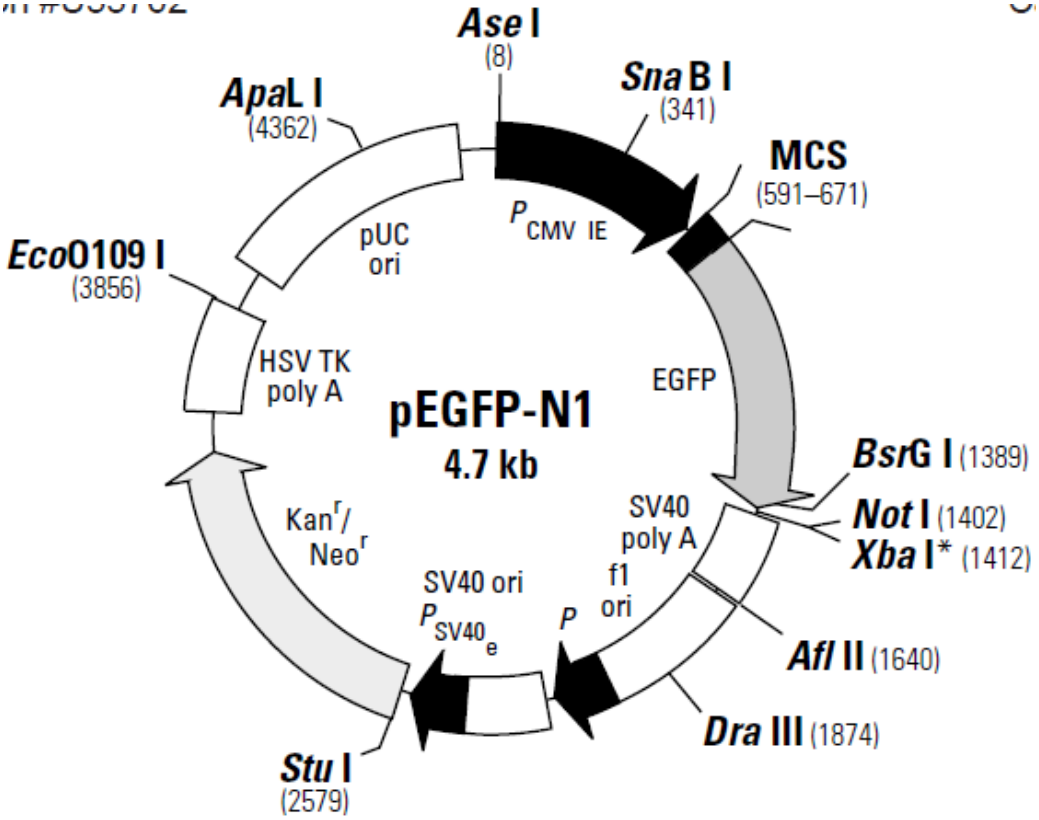

pEGFP-N1 vector circle map.

Appendix B

Molecular biology kits, reagents and chemicals

Kits	Manufacturer	Cat. No.
ABC (Vectastain) kit	Vector labs	AK-5000
BCIP/NBT kit	Vector labs	SK-5400
Qiagen Endofree Maxi Prep kit	Qiagen	12362
Qiashredders	Qiagen	79656
Qiaquick Gel extraction kit	Qiagen	28704
Ready-to-go DNA labelling beads	Amersham	27-9240-01
RNase-free DNase kit	Qiagen	79254
RNeasy mini kit	Qiagen	74104

Biological Reagent	Manufacturer	Cat. No.
10X SuRE/Cut Buffer A	Roche	11417959001
10X SuRE/Cut Buffer H	Roche	11417991001
α-^{32}P dATP	Perkin-Elmer	BLU012H250uc
α-^{32}P dCTP	Perkin-Elmer	BLU013A250uc
Anti-mouse biotin conjugate	Sigma-Aldrich	BA8520
Anti-mouse-HP-linked	GE Healthcare	NA9310
Biotin-anti-rabbit	Vector labs	BA-1000
Bovine serum	Gibco	26170-026
DMEM	Sigma-Aldrich	D6546
dNTP set (dATP, dCTP, dGTP, dTTP)	Invitrogen	10297-018
ECL anti-rabbit	GE Healthcare	NA934
EcoR I	Roche	10703737001
Fungizone-ampotericin B	Gibco	15290-018
Generuler DNA ladder	Fermentas	SM0333
*Hpa*I	Roche	10567647001
Immobilon Western HRP substrate	Millipore	WBKLSO500
L-Glutamine	Sigma-Aldrich	G7513
Lipofectamine	Invitrogen	2000 11668
Low-molecular weight DNA ladder	NEB	N3233L

Opti-MEM	Gibco	51985-026
Penicillin-Streptomycin	Gibco	15140-122
Phosphate buffered saline (10x)	Q biogene	PBS10X02
Platinum *Taq* DNA Polymerase	Invitrogen	10966
Precision plus Dual colour marker	Bio-Rad	161-0374
Protease inhibitor cocktail	Sigma-Aldrich	P2714
Rabbit anti-βactin	Abcam	Ab8227
RNase cocktail	Ambion	AM2286
Strevtavidin-AP conjugate	Roche	11-089-161-001
Superscript II	Invitrogen	18064-014
Trypsin	Gibco	25300-054
Versene-EDTA	Gibco	15040-033
XL-10 Gold supercompetent cells	Agilent	200159
Yeast poly(A) polymerase	Affymetrix	742252

Chemical	**Manufacturer**	**Cat. No.**
6X loading dye	Fermentas	R0611
Acetic acid	BDH	100015N
Acrylamide	Geneflow	EC-890
Agar	Sigma-Aldrich	05040
Agarose	Sigma-Aldrich	A9539
Ammonium acetate (7.5M)	Sigma-Aldrich	A2706
β-mercaptoethanol	Sigma-Aldrich	M7154
Bradford reagent	Bio-Rad	500-0006
Cell extraction buffer	Invitrogen	FNN0011
Chloroform	Sigma-Aldrich	C2432
Coomassie blue (R250)	Geneflow	H8-604
Dithiothreitol (DTT)	Melford	MB1015
EDTA	Sigma-Aldrich	E9884
Ethanol	Sigma-Aldrich	E7023
Ethidium bromide	Sigma-Aldrich	E1510
Gel loading buffer II	Ambion	AM8547
Luria Broth	Sigma-Aldrich	L3022

Methanol	Sigma-Aldrich	322415
Microsieve low melt agarose	Flowgen	G25LM-SVE
PAGE/urea (6%)	Ambion	AM9030
Phenol	Sigma-Aldrich	P1037
PMSF	FLUKA	GA19056
Sigmacoat	Sigma-Aldrich	SL2
Sodium acetate	Sigma-Aldrich	S-7899
Sodium Chloride	Fisher Scientific	S/3160/65
Sodium Citrate	BDM	27833-294
Sodium Hydroxide	Sigma-Aldrich	S8045
SYBR green	Molecular probes	S-7563
TEMED	Bio-Rad	161-0800
Toluidine blue	Sigma-Aldrich	T3260
Transfer buffer (10x)	Bio-Rad	161-0734
Triton X-100	Sigma	T-8787
Trypan blue (0.4%)	Gibco	15250-061
Tween 20	Sigma-Aldrich	P9416
Ultrahyb	Ambion	AM8670

Consumable	**Manufacturer**	**Cat. No.**
Amersham hyperfilm ECL	GE healthcare	28-9068-40
Hybond ECL membrane	GE healthcare	8549057
Hybond-P	GE Healthcare	RPN2020F
Nunc multidish six-well plate	Fisher Scientific	140675
Hybond-N	GE Healthcare	RPN119N

Appendix C

Buffers and reagents

General buffers and biological reagents

Ethanol 70%: 7ml of ethanol and 3ml of Sigma water were mixed thoroughly.

Luria Broth medium / LB agar: consisted of the following, 1l deionised H_2O, 10g tryptone, 5g yeast, 10g NaCl, 1% agar.

50X TAE Buffer : 242g Tris (hydroxymethyl) methylamine, 100ml 0.5M EDTA and 57.1ml acetic acid in a total volume of litre. The buffer was diluted 1/50 to give 1x TAE working solution.

Southern blot buffers

Lysis buffer: 20mM Tris HCl pH 7.5; 2mM EDTA; 1.2% SDS containing proteinase-K to a final concentration of 1mg/ml

Denaturing solution: 1.5M NaCl, 0.5M NaOH

Neutralisation solution: 1.5M NaCl, 1M Tris-HCl (pH 7)

20X SSC: solution was made which consisted of 1.5M NaCl together with 150mM Na3citrate.2H20 (the pH of the solution was brought to pH7 using 1N HCL). 20x SSC buffer was diluted with Millipore water to give lower SSC concentrations.

Wash buffer 1: 2xSSC, 0.1% SDS

Wash buffer 2: 0.1xSSC, 0.1% SDS

Western blot buffers and gels

APS 10%: Ammonium Persulphate 10% (w/v), 1g APS in 10ml Sigma water. Aliquoted 500µl volumes into microfuge tubes and stored at -20^{o}C.

Resolving gel: Gel mix was prepared in a glass universal by adding 5.9ml RO water, 5ml 30% acrylamide, 3.8ml 1.5M Tris (pH8.8), 150µl 10% SDS, 150µl 10% APS and finally 6µl Temed.

Stacking gel: Gel mix was prepared in a glass universal by adding 4.1ml RO water, 1ml 30% acrylamide, 750µl 1M Tris (pH6.8), 60µl 10% SDS, 60µl 10% APS and finally 6µl Temed.

Sample buffer 2x: 100mM Tris-HCL (pH6.8), 4% SDS, 20% glycerol, 0.05% bromophenol blue and 100mM DTT.

SDS-PAGE running buffer 1x: 25mM Tris, 250 mM glycine, and 0.1% SDS (pH 8.3), (50ml 10x Tris-Glycine buffer, 5ml 10% SDS solution in a total volume of 500ml RO water).

Transfer buffer: 140ml RO water, plus 20ml 10x transfer buffer, plus 40ml methanol.

Blocking buffer: 100ml of 1 x TBS plus 5g milk powder, plus 100µl of Tween 20.

Antibody dilution buffer: 100ml 1 x TBS, plus 3g dried milk, plus 100µl of Tween 20.

Wash buffer: 200ml 1x TBS plus 200µl of Tween 20.

Coomasie blue: 1.25g Coomasie blue (R250), 250 ml methanol, 200ml RO water plus 50ml of glacial acetic acid. Solution was mixed well and then filtered through Whatman filter paper.

Destain: 250 ml methanol, 200ml RO water plus 50ml of glacial acetic acid.

Poly(A) tail gel electrophoresis

Gel: Gel mix was prepared in a volumetric flask by adding 64ml 6% PAGE/urea acrylamide to 16ml 0.5x TBE buffer plus 500µl 10% APS.

5x TBE buffer: 54g Tris base, 27.5g boric acid along with 20ml of 0.5M EDTA (pH 8.0) made up to 1L with RO water. The buffer was diluted 1/10 to make a 0.5X solution.

Stop solution: 200mM Tris–HCl (pH 7.9), 300mM NaCl, 25mM EDTA, 2% SDS containing 20 µg proteinase K, 1 µg rRNA and 1 µg glycogen.